Functional organization of the circadian timing system

Functional organization of the circadian timing system

A dissertation presented

by

Nina Vujovic

to

The Division of Medical Sciences

in partial fulfillment of the requirements for the degree of

Doctor of Philosophy

in the subject of

Neurobiology

Harvard University

Cambridge, Massachusetts

October, 2013

Clifford B. Saper Nina Vujovic

Functional organization of the circadian timing system

Abstract

The circadian timing system establishes daily rhythms in behavior and physiology throughout the body, ensuring that functions like activity, sleep and hormone release are appropriately timed. Research suggests that his temporal synchrony within the body is quite important for health and survival. In mammals, the central circadian pacemaker in the suprachiasmatic nucleus (SCN) drives rhythms in behavior and physiology in large part by stimulating or inhibiting other brain regions responsible for these functions at the appropriate times of day. This timed signal is often indirect, i.e. relayed or possibly processed through a series of neurons in different brain regions before reaching the effector site. The subparaventricular zone (SPZ), a region adjacent to the SCN which is the main recipient of direct neuronal inputs from the SCN, is thought to be a critical relay for SCN signals, since loss of the SPZ results in loss of circadian rhythms in body temperature, activity and sleep/wakefulness. Another important relay site, the dorsomedial hypothalamic nucleus (DMH) gets direct input from both the SCN and SPZ and is critical for normal expression of various circadian rhythms.

Both the SPZ and DMH have different subpopulations of neurons which may perform different functions with respect to circadian modulation of physiology and behavior, and which have not been well studied. Chapter 2 of this dissertation focuses on the anatomical connectivity of four spatially defined subpopulations of cells in the SPZ, showing for the first time that they differ in density of their inputs to certain hypothalamic targets and that they project to each other as well as to the SCN. This chapter also reports several novel SPZ targets which may be important for the regulation of wakefulness. Chapter 3 examines the role of an excitatory subpopulation of DMH neurons by deleting a critical exon in the gene for a vesicular glutamate transporter, rendering these neurons unable to synaptically release glutamate. This manipulation blunts circadian rhythms in activity and urinary corticosterone, and decreases average body temperature and activity levels throughout the day, implicating excitatory DMH neurons in regulation of the above parameters.

Table of Contents

Acknowledgments……...……...vi

List of anatomical abbreviations…….……ix

Chapter 1: Introduction and background……..1

The Circadian timing system and its significance for human health

Circadian clocks and the suprachiasmatic nucleus

SCN outflow pathways

Neural outputs of the SCN

How does the circadian timing system communicate with brain regions regulating wakefulness and activity?

How does the circadian timing system communicate with brain regions regulating thermogenesis and heat loss mechanisms?

How does the circadian timing system communicate with brain regions regulating autonomic and neuroendocrine functions?

Neurotransmitters of the SCN, SPZ and DMH

Rationale for experimental work presented in Chapter 2 and 3

References

Chapter 2: Efferent projections of the subparaventricular zone: does the circadian timing system have a four channel output?.....29

Abstract

Introduction

Methods

Results

Discussion

References

Chapter 3: Role of glutamatergic neurons in the dorsomedial hypothalamus.....68

Abstract

Introduction

Methods

Results

Discussion

References

Chapter 4: Conclusions and future directions.....104

Acknowledgements

This work would not be possible without the mentorship, encouragement and support I received from my thesis advisor, Dr. Clifford Saper. I am especially grateful to him for his patience, willingness to share his extensive knowledge, and truly constructive feedback at all stages of this research.

Many individuals in the Neurology and Endocrinology departments contributed to this research, as well as to my sanity and development as a scientist during the process, and deserve thanks. Dr. Patrick Fuller, who took me under his wing from my first day as a rotation student in the Saper lab, has been an informal mentor, great friend and exceptional source of positivity and empowerment. Dr. Vetrivelan Ramalingam has been a bottomless well of creative suggestions for data analysis and troubleshooting, and a great source of humor and inspiration, especially when experiments didn't go as planned. Quan Ha has provided superb technical assistance with many different aspects of this research, has generously shared her time and expertise in neuroanatomical techniques with me, and has always faithfully pointed me to free food in times of need. Dr. Kimberly Rapp acted as my comrade and co-pilot in the development of techniques to measure hormone rhythms in mice. She has shared with me many interesting stories, fun adventures, and (not as unpleasant as they would have been without her) 24-hour data collection shifts. Dr. William Todd has been a great colleague, valuable sounding board and resource on all things related to circadian biology, and has shared with me the joys of data collection at anomalous times. Brian Ellison, the first undergraduate I mentored for an honors thesis, has become as much a friend and teacher as he ever was a student, assisting a great deal in 24-hour data collection and automation of data analysis. Lindsay Agostinelli, who had the pleasure of being my roommate while I had many data collections at anomalous times, has been a very supportive friend and source of helpful advice on everything from immunohistochemistry to the meaning of life. Many thanks also go to Josh Wang, Peagan Lin, and Ashley Schomer for their help with neuroanatomical experiments. Sofia Iqbal and Sarah Keating have been great colleagues and friends, providers of technical support and many a morale boost. I am grateful to Sathyajit Bandaru for care of the mouse colony and providing transgenic animals required for this work, and for his good humor in response to my fickle mouse-needs timelines. I would also like to acknowledge Dr. Satvinder Kaur, Dr. Chloe Alexandre, Dr. Christian Burgess, Dr. Christelle Anaclet, and

Dr. Nigel Pedersen for teaching me how to set up, perform, and interpret sleep recordings. Thanks go to Dr. Ningshan Wang, Dr. Irma Rukadze, and Dr. Ishmael Syed for providing guidance to me on confocal microscopy, in situ hybridization, and ELISA assays, respectively. I also owe a debt of gratitude to Dr. Janet Mullington and Dr. Monika Haack for their expert guidance on statistical analysis. Dr. Thomas Scammell, Dr. Veornique Vanderhorst, Dr. Nancy Chamberlin and Dr. Elda Arrigoni have provided valuable and much appreciated advice and perspective over the years. I have been fortunate to work in a department with so many talented and congenial scientists – there are more than I can name here who contributed to my graduate school experience in smaller ways, and to whom I am appreciative.

I would like to thank our collaborators Dr. Bradford Lowell, Dr. Qingchun Tong, and Dr. Linh Vong, for not only providing several of the transgenic mouse models used in my research, but also for constantly inviting us to think about our research from a new perspective. I am also appreciative to Dr. Linda Lieberman and Dr. George Tsokos who generously shared their equipment and knowledge in order to enable us to measure hormone rhythms in mice. Thanks also go to Dr. Gregory Holmes and Emily Creekmore-Qualls, for going to great lengths to help us study circadian regulation of body temperature. I am also deeply grateful to Dr. Charles Allen and Dr. Nathaniel Klett for their gift which enabled my neuroanatomical characterization of the subparaventricular zone.

. I have also been fortunate to receive great support from the Program in Neuroscience and Division of Medical Sciences throughout my time as a graduate student. I thank Dr. Richard Born for his time, consistent encouragement and down-to-earth advice over our many meetings. Dr. Gary Yellen made difficult concepts simple from day one and made a valuable suggestion when I needed it most. I am also deeply appreciative to Leah Simons for providing help at the critical moment on two occasions and to Gina Conquest and Karen Harmin for always having the time to share the right piece of information or words of wisdom/encouragement. Sincere thanks also go to Alex Shimada-Brand, who single-handedly transformed NIH fellowship applications from a daunting challenge into a perfectly attainable goal. Many thanks are also due to the members of my dissertation advisory committee: Dr. Joseph Majzoub, Dr. Bradford Lowell, and Dr. Charles Czeisler, for their invaluable input and guidance over the years, and in particular to Dr. Majzoub for acting as my dissertation examination chair.

In addition to teaching me a great deal, Dr. Charles Czeisler and Dr. Woodland Hastings deserve thanks for giving me the opportunity to share my knowledge with undergraduate students as a teaching fellow. Relatedly, I would like to thank my past teachers and mentors for training, inspiring and empowering me to pursue neuroscience research. Particular thanks go to Dr. Paul Cammer, Dr. Lisa Goehler, Dr. Ruth Stornetta, Dr. Patrice Guyenet, Dr. Alec Davidson and Dr. Michael Menaker.

Finally, I would like to thank my family and friends for supporting me in my decision to pursue a Ph.D., seeing me through both the peaks and valleys, and also for occasionally bragging to their friends and families about me. Special thanks go to Dr. Dina Eliezer and Dr. Yogesh Surrendranath for striking the perfect balance between cynical humor and pep-talk when I needed them to, to Dr. Robert McConnell for managing to strike the above balance while cheering me on through the part that felt like the end of an unexpectedly steep uphill marathon, and to my mother for being there every step of the journey and teaching me (by example) how to be persistent and resilient.

Table of Neuroanatomical Abbreviations

3 – nucleus of the oculomotor nerve (cranial nerve III)
3PC – parvocellular oculomotor nucleus
AA – anterior amygdaloid area
ac – anterior commissure
ACo – anterior cortical amygdaloid nucleus
AHA – anterior hypothalamic area
AHiAL – amygdalohippocamal area, anterolateral part
APT – anterior pretectal nucleus
ARC – arcuate nucleus of the hypothalamus
AVPe – anteroventral periventricular nucleus
Bar – Barrington's nucleus
BF – basal forebrain
BLA – basolateral nucleus of the amygdala, anterior part
BMA – basomedial nucleus of the amygdala, anterior part
BST – bed nucleus of the stria terminalis
CeA – central nucleus of the amygdala
CG – central gray
CLi – caudal linear nucleus of the raphe
CnF – cuneiform nucleus
CoA – anterior cortical amygdaloid nucleus
CoAl – anterolateral cortical amygdaloid nucleus
CoApl – posterolateral cortical amygdaloid nucleus
CoApm – posteromedial cortical amygdaloid nucleus
CP – cerebral peduncle
CPu – caudate putamen
CST – corticospinal tract
DBB – diagonal band of Broca
DHA – dorsal hypothalamic area
Dk – nucleus of Darkschewitsch
DMH – dorsomedial nucleus of the hypothalamus
dSPZ – dorsal subparaventricular zone
dlSPZ – dorsolateral subparaventricular zone
dmSPZ – dorsomedial subparaventricular zone
EW – Edinger-Westphal nucleus
fr – fasciculus retroflexus

f – fornix
GP – globus pallidus
HDB – horizontal limb of the diagonal band
IC – internal capsule
IMLF – interstitial nucleus of the medial longitudinal fasciculus
InC – interstitial nucleus of Cajal
IPAC – interstitial nucleus of posterior limb of anterior commissure
IPN – interpeduncular nucleus
LA – lateral nucleus of the amygdala
LC – locus coeruleus
LDT – laterodorsal tegmental nucleus
LHA – lateral hypothalamic area
LHb – lateral habenular nucleus
LM – lateral mammillary nucleus
LPB – lateral parabrachial nucleus
LPBel – lateral parabrachial nucleus, externolateral subdivision
LPBS – lateral parabrachial nucleus, superior subdivision
LS – lateral septal nucleus
LSv – lateral septal nucleus, ventral part
ME – median eminence
MeA – medial nucleus of the amygdala, anterior part
Me5 – mesencephalic nucleus of the trigeminal nerve (cranial nerve V)
MCPO – magnocellular preoptic nucleus
MGN – medial geniculate nucleus
MHb – medial habenular nucleus
MLF – medial longitudinal fasciculus
MM – medial mammillary nucleus
MnPO – median pre-optic area
MPB – medial parabrachial nucleus
MPO – medial preoptic area
Me5 – motor nucleus of the trigeminal nerve (cranial nerve V)
MR – median raphe nucleus
MS – medial septal nucleus
mt – mammillothalamic tract
NLOT – nucleus of the lateral olfactory tract
NPC – nucleus of the posterior commissure
OLT – olfactory tubercle

OPT – olivary pretectal nucleus
OT – optic tract
OX – optic chiasm
PAG - periacqueductal gray
PBG – parabigeminal nucleus
PC – posterior commissure
Pe – periventricular hypothalamic nucleus
PIL – posterior intralaminar thalamic nucleus
PMD – premamillary nucleus, dorsal part
PMV – premamillary nucleus, ventral part
Po – posterior thalamic nuclear group
PP – peripeduncular nucleus
Pr5 – principal sensory nucleus of the trigeminal nerve (cranial nerve V)
PS – parastrial nucleus
PTA – pretectal area
PVH – paraventricular nucleus of the hypothalamus
PVT – paraventricular nucleus of the thalamus
RCh – retrochiasmatic area
Re – nucleus reuniens of the thalamus
Red Nuc. – red nucleus
SCN – suprachiasmatic nucleus
SCol – superior colliculus
SCP – superior cerebellar peduncle
SFI – septofimbrial nucleus
SI – substantia innominata
SLD – sublateral dorsal nucleus
sm – stria medullaris
SN – substantia nigra
SNc – substantia nigra pars compacta
SNr – substantia nigra pars reticulata
STN – subthalamic nucleus
SO – supraoptic nucleus
SOC – superior olivary complex
SUM – supramammillary nucleus
ST – stria terminalis
TMN – tuberomammilary nucleus
vSPZ – ventral subparaventricular zone

vlSPZ – ventrolateral subparaventricular zone
vmSPZ – ventromedial subparaventricular zone
VDB – vertical limb of the diagonal band
VLPO – ventrolateral pre-optic area
VMPO – ventromedial pre-optic area
VMH – ventromedial hypothalamic nucleus
VP – ventral pallidum
VPL – ventral posterolateral thalamic nucleus
VPM – ventral posteromedial thalamic nucleus
VTA – ventral tegmental area
ZI – zona incerta

Chapter 1: Introduction and Background

The Circadian timing system and its significance for human health

The circadian timing system (CTS) is an evolutionarily ubiquitous physiological system that regulates daily patterns in gene expression, metabolism, and a wide array of behaviors and physiological functions, and synchronizes these daily rhythms to each other and to external time cues (such as daylight or food availability). The CTS is among few convergent features evolved by plants, fungi, animals and even some prokaryotes, all of which have circadian timing systems built upon molecular feedback loops of approximately 24 hours duration, but based in different groups of organisms on different genes (Ouyang et al., 1998; Foster and Kreitzman, 2004). The ability of an organism to predict regular changes in its environment and time its functions and behaviors accordingly is clearly highly adaptive and selected for. The circadian timing system powerfully regulates our physiology and behavior and thus influences our health (Moore-Ede et al., 1983).

Chronic phase shifting (e.g. jet-lag or shift work, which forces the body to go against intrinsic schedules driven by the CTS), has been linked to a number of illnesses in both humans and animals. These include increased risk of breast cancer (Hansen, 2001), of hypertension (Kawachi et al., 1995) and increased mortality rate in aged animals (Davidson et al., 2006). Prolonged lack of synchrony to external time cues can disrupt function of homeostatic systems in monkeys (Fuller et al., 1978) perhaps via gradual uncoupling of the many oscillating functions throughout the body.

In humans there is evidence that the quality and duration of sleep depends on the circadian phase of its onset and its synchrony with the circadian rhythm in T_b (Czeisler et al., 1980a; Czeisler et al., 1980b). Sleep loss or disruption, in turn has numerous short and long-term consequences. The increased blood levels of pro-inflammatory cytokines associated with sleep loss contribute to a decrease in neurobehavioral function and adversely affect cardiovascular function (Zheng et al., 2006). In particular chronic sleep loss may contribute to the development of atherosclerosis, as indicated by sleep loss-dependent elevations in plasma C-reactive protein (Libby and Ridker, 2004)

Mouse models with mutations in key genes necessary for the CTS exhibit a variety of health deficits including progressive arthropathy (Bunger et al., 2005), severely compromised reproductive health (Miller et al., 2004; Alvarez et al., 2008), increased cancer risk (Rosbash and Takahashi, 2002),

obesity and a metabolic syndrome related to early stage diabetes (Rudic et al., 2004; Turek et al., 2005; Buxton et al., 2012). Both humans (Czeisler et al., 1999; Toh et al., 2001) and mice (Laposky et al., 2005) with mutations in clock genes have abnormal sleep wake cycles and may suffer from secondary consequences of chronic sleep disturbances (see footnote[1]).

The above findings suggest that circadian organization of molecular and system-wide processes throughout an organism are of immense importance to overall health. The now established connection between CTS disruption and cancer could be based on circadian gating of mitosis, endocrine disturbance or both (Okamura, 2004). Disruption in normal levels of estrogen and its circadian and monthly rhythms have been linked to both cancer and reproductive compromise. Likewise, there is evidence that temporal dysregulation of the hormones leptin and ghrelin may underlie the connection between chronic sleep loss and diabetes (Knutson et al., 2007; Van Cauter et al., 2007). Both the CTS and sleep itself exert important regulatory effects on hormone secretion profiles (Czeisler and Klerman, 1999), offering one possible pathway linking circadian disruption and adverse health consequences. Another set of possible pathways come from potent circadian regulation of sympathetic outflow to peripheral organs (Kalsbeek et al., 2006b; Kalsbeek et al., 2006a).

Whatever the pathway, loss of the adaptive temporal organization which normally exists within and between tissues can compromise health and fitness of the whole organism (Hastings et al., 2003). Understanding the neural circuitry underlying temporal synchronization of physiology and behavior may reveal new risk factors and mechanisms for prevention and treatment of some of the diseases and disorders that our society is most afflicted by in this era, including heart disease, diabetes and cancer.

Circadian clocks and the suprachiasmatic nucleus

The CTS is composed of circadian biological clocks (endogenous oscillators with a period of near

---

[1] Do genes driving the circadian timing system also affect other functions?

It bears mention that some genes which drive the CTS are transcription factors for unrelated genes as well, and may have other functions in the body that contribute to or account for some of the phenotypes above. However, more recent studies which disrupt expression of these genes in a tissue-specific manner (Sadacca et al., 2011) or do so in select brain regions of normally developed adult animals (who did not lack these genes during development) (Fuller et al., 2008) (Ramalingam et al., unpublished data), are beginning to tease apart this question. The similarity in problems caused by external schedule disruption vs. clock gene disruption suggest that many of the health consequences seen as a result of knocking out circadian clock genes are in fact secondary to disruption of 24h oscillations in the body.

24 hours), built upon a molecular feedback loop. In mammals, these molecular clocks are present in each cell of most peripheral tissues and within several structures inside the brain. However, the site most important for driving systemic (behavioral and physiological) rhythms is the clock in the suprachiasmatic nucleus (SCN) of the hypothalamus.

Complete bilateral ablation of the SCN has been shown to abolish circadian rhythms of locomotor activity, wakefulness, heart rate, feeding and drinking behavior, plasma levels of glucose, corticosteroids, and melatonin, and core body temperature (T_b) (however, see footnote[2] concerning Tb rhythm) (Moore and Eichler, 1972; Raisman and Brown-Grant, 1977; Stephan and Nunez, 1977; Abe et al., 1979; Refinetti and Menaker, 1992; Warren et al., 1994; Moore, 1996; La Fleur et al., 1999). The above results imply that the clock in the SCN is necessary for driving these rhythms. That said, the majority of these lesions in the above studies likely also damaged adjacent structures or fibers of passage due to limitations of the techniques used (Saper, 2013), but there are numerous other lines of evidence

---

[2]Are circadian rhythms in T_b generated/driven by the molecular clock in the SCN?

Various studies document that large bilateral SCN lesions eliminate circadian variation in T_b (Eastman et al., 1984; Honma et al., 1988; Ruby et al., 1989; Scheer et al., 2005). However several studies in which bilateral SCN lesions were made failed to confirm that finding. Though SCN lesions in these studies abolished rhythms in locomotor activity (Fuller et al., 1981; Satinoff and Prosser, 1988) or were presumed to (Halberg et al., 1979) a significant rhythm in T_b remained, though perhaps with diminished amplitude. Although technical considerations surrounding electrolytic SCN lesions might explain the discrepancy, for years the lesion data was interpreted as controversial and inconclusive.

Since the discovery of the molecular clock driving circadian oscillations, we have also been able to ask whether animals bearing mutations in various clock genes have normal T_b rhythms. So far, this has been studied in a few mouse knock-outs that lack critical clock genes: the Bmal1 -/- mouse, the Clock -/- mouse and the Cryptochrome 1 and 2 (Cry1-/- Cry2 -/-) double knock out mouse. All of these animals show a complete loss of circadian rhythms in locomotor activity in constant dark (DD), but exhibit diurnal patterns of running-wheel activity in light:dark cycles (12:12 L:D), due to light masking. Cry1-/- Cry2 -/- mice show no T_b rhythm in DD but rhythmic oscillations in T_b can be induced in LD or with a special feeding schedule (Nagashima et al., 2005). Similarly Clock -/- and Bmal1 -/- mice have no T_b rhythm in DD and show very low amplitude (Clock -/-) or severely disrupted (Bmal1 -/-) T_b rhythms in LD (Fuller et al., 1981; Tokizawa et al., 2009). Clearly, a functional molecular clock is critical for the generation of intrinsic circadian rhythms in T_b. However, because this clock is expressed in most cells and tissues throughout the body, the question has been raised as to whether it is necessarily the molecular clock in the SCN that drives these rhythms.

Findings from our lab show that the pacemaker in the SCN is at least sufficient (if not necessary) to drive rhythms in T_b, since rescue of the expression of BMAL1 in only the SCN of total body BMAL1 knock-out mice can rescue the full amplitude of T_b rhythms (Fuller et al., 2008). Recent experiments in conditional knock-out (i.e. floxed) BMAL1 mice using stereotaxic injections of an adeno-associated viral vector expressing cre-recombinase, to selectively delete BMAL1 expression in only the SCN from our lab (Ramalingam et al., in preparation) indicate that deletion of BMAL1 in only the SCN severely disrupts circadian rhythms in T_b, even though the molecular clock is intact in every other region that would normally express it in these mice. It appears that the molecular clock in the SCN is both necessary and sufficient for driving circadian rhythms in T_b.

Moreover, lesions of the main target of SCN efferent projections, the subparaventricular zone (SPZ), diminish the amplitude of T_b rhythms by 80-90% (Lu et al., 2001), further supporting the idea that the clock in the SCN drives this rhythm, and suggesting that it does so via neural efferent outputs.

suggesting that the clock in the SCN drives rhythms throughout the body.

In the case of locomotor activity, SCN transplant experiments have conclusively demonstrated the clock in the SCN determines the period and phase of these rhythms (Ralph et al., 1990; Sujino et al., 2003). More recently, selective re-expression of a critical clock gene in the SCN of otherwise arrhythmic knock-out animals demonstrated that the molecular clock in the SCN is sufficient for driving circadian rhythms of locomotor activity and T_b (Fuller et al., 2008).

The SCN clock is also critical for entrainment of systemic rhythms to certain external time cues, the 24-hour light cycle being the best studied and most effective entrainment cue. Moreover, lesions of the SCN result in uncoupling of the phases of other endogenous molecular clocks (Yoo et al., 2004), and synchronous clock gene expression rhythms in these tissues can be restored via fetal SCN transplantation (Guo et al., 2006). It is also worth noting that the loss of endocrine rhythms in SCN-lesioned animals occurs despite the fact that local molecular clocks in all their glands and peripheral tissues remain fully functional (Yoo et al., 2004). Hence, a peripheral organ's local molecular clock appears insufficient to drive its secretion rhythms.

The above evidence strongly argues that the clock in the SCN drives circadian rhythms of behavior and physiology, synchronizes these rhythms with each other and with other endogenous molecular rhythms and further, synchronizes all these rhythms with external light cycles. While much is known about how the SCN receives light cycle information from specialized photoreceptors via the retino-hypothalamic tract (Freedman et al., 1999; Gooley et al., 2001; Gooley et al., 2003), less is understood on how outflow from the SCN drives or synchronizes systemic and cellular rhythms, respectively.

SCN outflow pathways

Neurons of the SCN convey temporal information to other organ systems through both neural and humoral outputs. The SCN has efferent neural connections to a wide array of central and peripheral structures and disruption of these efferents can alter or eliminate a wide array of circadian rhythms (Bartness et al., 2001). However, when transplantation of fetal SCN tissue into the third ventricle of SCN-lesioned hamsters was shown to restore rest-activity rhythms within a few days post-operatively (Ralph et al., 1990; Sujino et al., 2003) the question arose regarding the importance of synaptic signaling from the

SCN for regulation of rhythms in locomotion. Since SCN grafts could restore some degree of rhythmicity in locomotor activity presumably without enough time to innervate the SCN's normal hypothalamic targets, it was proposed that diffusible factors may be the means by which the SCN drives and synchronizes this rhythm. Though a subsequent study found evidence of connections between graft and host tissue in SCN transplant recipients with restored rhythms (Aguilar-Roblero et al., 1994), polymer encapsulated SCN transplants that prevented neuronal communication between host and donor tissue were still able to restore low amplitude rhythms of locomotor activity (Silver et al., 1996; LeSauter et al., 1997) with the amplitude increasing as the graft implant site approaches the normal location of the SCN near the third ventricle. Taken together, these results suggest that rhythmic paracrine signaling from the SCN contributes to locomotor activity rhythms, though it alone cannot account for their full amplitude.

To date, three SCN-secreted molecules have been proposed as candidates for the activity rhythm-regulating paracrine signal: prokinectin-2 (PK2) (Cheng et al., 2002), cardiotropin like cytokine (CLC) (Kraves and Weitz, 2006), and transforming growth factor-α (TGF-α) (Kramer et al., 2001), although it is unclear whether the latter is produced by neurons or astrocytes in the SCN. All three show clock-controlled expression, peaking during subjective day in rodents, i.e. the quiescent portion of their activity cycle. Infusion of TGF-α, PK2 or CLC into the third ventricle disrupts normal rhythms of locomotor activity and, in the case of TGF-α, rhythms of T_b as well. TGF-α and CLC produce these effects without affecting the underlying phase of the clock in the SCN. All three of these molecules appear to inhibit locomotor activity via receptors expressed in the vicinity of the third ventricle (including the periventricular nucleus). Mice with a hypomorhphic mutation of the receptor for TGF-α have abnormal circadian activity profiles and fail to show the normal suppression of activity in response to light (Kramer et al., 2001).

More recent parabiosis and SCN transplant experiments have also indicated that diffusible factors from may underlie the coupling of certain peripheral molecular clocks to each other and the light cycle (Guo et al., 2005). However, such a signal needn't necessarily be a secreted factor released directly by the SCN. It appears more likely to be a hormone whose release is regulated by neural outputs of the SCN or perhaps a consequence of rhythmic food intake, since all known factors released directly by the SCN act in a paracrine rather than endocrine fashion.

One important methodological consideration regarding the studies suggesting that SCN-secreted factors can drive rhythms is age of the animal in which they are performed. SCN transplants have only been successful in restoring activity rhythms in very young animals, and newer studies suggest that the influence of SCN secreted factors on sleep/wake rhythms declines during development, coincident with the formation of neural connections that drive these rhythms in adults (Gall et al., 2012).

While the above summarizes the role for diffusible SCN outputs in coordination of system-wide rhythms, the sections that follow can only partially cover the considerably more extensive literature on neural efferents of the SCN and how they act to relay entrainment cues and drive rhythms throughout the body. We know that neural outputs of the SCN are responsible for entrainment of hormonal and physiological rhythms as SCN transplantation does nothing to restore them (Lehman et al., 1987; Meyer-Bernstein et al., 1999) and lesions of specific synaptic targets of the SCN destroys them (Bartness et al., 2001; Lu et al., 2001; Chou et al., 2003). The fact that the left and right SCN can be de coupled and produce antiphase rhythms in their targets on each side of the brain with high temporal precision (de la Iglesia et al., 2003) also implicates neural as opposed to humoral outflow (however, see footnote[3]). The important role these efferent connections play in regulation of behavioral rhythms and arousal states is best illustrated by the dramatic decrease in amplitude of these rhythms following lesions of certain SCN projection targets and will be the subject of the passages below. In addition, synaptic signaling is much faster than paracrine, and may be required to explain the high level of temporal precision with which the circadian system responds to environmental cues and organizes rhythms throughout the organism. Finally, since receptors for diffusible factors released by the SCN are expressed in hypothalamic regions near the third ventricle, they may well be acting on neurons which synapse onto targets of the SCN and thus ultimately drive outflow through some of the same circuitry.

---

[3] Can diffusible factor produce ipsilateral effects?

Although there are rare examples where diffusible factors appear to produce effects only ipsilaterally, e.g. gonadal digenesis during development, these occur over a longer time scale in a developing organism, where strong gradients of diffusible factors are often present to guide tissue and organ formation and developing tissues may exhibit differential sensitivity to signaling factors present (Houle and Taketo, 1992). Diffusible factors are considerably less likely to produce ipsilateral effects on the order of minutes and in a regular, cyclic fashion in fully formed adult animals with symmetrical sensitivity to the factors in question.

Neural outputs of the SCN

Most studies tracing neural SCN outputs have been carried out in rat (Swanson and Cowan, 1975; Watts and Swanson, 1987; Watts et al., 1987) or golden hamster (Kalsbeek et al., 1993; Morin et al., 1994), although these outputs have also been mapped in mice and in certain primates (Moore, 1993). Primary efferent projections from the SCN for the most part target midline structures within the hypothalamus although a few of them terminate in the forebrain, thalamus or midbrain. The majority of these projections appear to be ipsilateral although there are exceptions. By far the most dense projection is a bundle of fibers arching dorsally and caudally out of the SCN. Most of these terminate in the subparaventricular zone (SPZ) though a few fibers continue dorsally to synapse on neurons in the PVH. Another group of fibers continues caudally to terminate in the dorsomedial nucleus of the hypothalamus (DMH), in the area surrounding the ventromedial nucleus of the hypothalamus (VMH), and in the posterior hypothalamus (PH), with a few terminals falling within the boundaries of the lateral hypothalamic area (LHA). Compared to the above dorso-caudally bound collection of fibers, all other projections from the SCN are significantly more sparse. Their targets include certain pre-optic hypothalamic regions including the median pre-optic nucleus (MNPO) and, in some tracing studies, a weak projection to the ventrolateral pre-optic region (VLPO). Other targets include the lateral septum, bed nucleus of the stria terminalis (BSTL), retrochiasmatic area (RCA), paraventricular thalamus (PVT), paratenial thalamus, the intergeniculate leaflet (IGL) within the lateral geniculate thalamus (LGN), olivary pretectal nucleus (OPT), and part of the periacqueductal gray (PAG) area in the midbrain.

Given the importance of the circadian timing system in regulation of sleep-wake cycle timing and behavior, it is surprising how few primary SCN efferents directly target structures known to regulate sleep and arousal, such as the VLPO, LHA and PAG. These areas are not even consistently identified as SCN output targets across tracing studies, and when reported, projections to them are characterized as extremely sparse. While the tracing of primary SCN efferents revealed circuitry likely to underlie circadian control of endocrine rhythms (e.g. projections to the PVH which can drive pituitary secretion and sympathetic outflow), it generated new questions about circuitry underlying circadian regulation of behavior and arousal state. As described below, it is the second and third order projections from targets

of the SCN's primary efferents that have enabled us to propose a circuit diagram connecting the two systems.

How does the circadian timing system communicate with brain regions regulating wakefulness and activity?

For the better part of the 20th century, the study of neural circuits and formal properties regulating sleep, arousal and related physiological parameters constituted an area separate from the study of the circadian timing system (or its properties and underlying anatomy). Here, I provide a brief overview of some of the central pathways driving sleep and waking and then discuss several proposed regulators of behavioral state transition

Arousal states can be divided into three main categories based on electroencephalogram (EEG) wave patterns: (1) waking; (2) rapid eye movement (REM) sleep (characterized by fast eye movements, atonia in muscles throughout the body except those driving eye movements and breathing, and high cortical activity); and (3) slow-wave or non-REM (NREM) sleep (characterized by low levels of cortical activity appearing as slow waves on the EEG). A wide array of nuclei in the brainstem, midbrain and caudal hypothalamus, together drive or contribute to arousal via ascending projections to the cortex and structures in the forebrain, thalamus and hypothalamus. This system has historically been divided into two groups:

(1) the cholinergic pedunculopontine and laterodorsal tegmental nuclei which project to thalamic relay neurons and help activate cortical neurons in waking and REM sleep. These cholinergic tegmental neurons fire most rapidly in wake and REM stages and are silent during NREM.

(2) the monoaminergic nuclei dispersed through the brainstem, midbrain and caudal hypothalamus, including the serotonergic dorsal and median raphe nuclei, noradrenergic locus coeruleus, dopaminergic ventral periaqueductal grey matter and histaminergic tuberomammilary nucleus, which all drive activity in neurons of the cerebral cortex, basal forebrain (BF) and lateral hypothalamus during waking. Neurons in these monoaminergic nuclei fire at the highest rates during wakefulness, more slowly during NREM and are silent during REM.

Neurons in the LHA and BF contribute to cortical activation during wakefulness (and also REM) through their own projections. The aforementioned neurons from the LHA release either the peptide orexin or melanin concentrating hormone (MCH) while those from the BF release acetylcholine (ACh) and GABA. In the LHA, separate populations drive the cortex in wake vs. REM; orexin neurons fire most rapidly during wakefulness and MCH neurons during REM sleep. Many neurons on the BF fire rapidly in both wake and REM, so it's not as easy to tease apart which population does what.

All the above structures (except MCH-ergic LHA neurons and some cells in the BF) drive arousal. What then, drives sleep? Much of it seems to come from an anterior hypothalamic region called the ventrolateral preoptic area (VLPO). Evidence that VLPO promotes sleep: VLPO lesions or degeneration with age both cause insomnia and VLPO neurons are most active during sleep and send direct inhibitory GABAergic and galaninergic projections to monoaminergic ARAS nuclei (Sherin et al., 1996). The VLPO in turn receives direct projections from each of the monoaminergic nuclei of the ascending arousal system (Chou et al., 2002) and is inhibited by them (Gallopin et al., 2000). This mutual inhibition may enable more rapid state transitions, minimizing the amount of time animals spend not fully awake or asleep, for review see (Saper et al., 2005b; Saper et al., 2005a). Orexin neurons in the LHA seem to help consolidate the waking state; though these neurons are not critical for arousal, loss of them leads to many rapid and uncontrolled state transitions throughout the day and is in fact an animal model for narcolepsy (Mochizuki et al., 2004). More recent work also implicates LHA neurons expressing melanin concentrating hormone (MCH) in the regulation of sleep and wakefulness (Adamantidis et al., 2008; Jego et al., 2013), as well as neurons in the parabrachial nucleus and pre-coeruleus region (Fuller et al., 2011; Kaur et al., 2013), basal ganglia (Qiu et al., 2010), and parafacial zone (Anaclet et al., 2012).

Connections to the circadian system

Of the many structures important in arousal/sleep described above, the SCN only sends very sparse projections to the VLPO, LHA and PAG. The SPZ, however innervates many of the same targets as the SCN only more densely (Watts and Swanson, 1987), which has led to the idea that it may be an "amplifier" of SCN signals. One of the major targets of the SPZ, the DMH sends two very strong projections to arousal system structures: an inhibitory, GABA-ergic projection to the VLPO and an

excitatory, glutamatergic (and TRH) projection to the orexinergic cells of the LHA, having a net effect of driving arousal.

Several lines of evidence support the idea that these SPZ and DMH projections are functionally important, and will be discussed in Chapter 2 and 3, respectively. Among the most compelling are the consequences of lesions to these areas. Cell-specific lesions of the SPZ disrupt circadian rhythms of activity, temperature and sleep/wake (Lu et al., 2001). Moreover, lesioning different parts of the SPZ disrupted different outputs. Ibotenic acid lesions of the dorsal region of SPZ (dSPZ) greatly reduced the amplitude of rhythms in body temperature (T_b) but had little effect on rhythms in activity and sleep-wake. Meanwhile, lesions of the ventral SPZ (vSPZ) resulted in dramatic blunting of circadian rhythms in locomotor activity, sleep and wakefulness with minimal effects on temperature. Lesions of the DMH, which receives neural inputs mostly from the vSPZ, diminished circadian variation in locomotor activity, corticosteroid secretion and sleep-wake EEG patterns (Chou et al., 2003). So in summary, the SCN projects to the SPZ, which amplifies its signal and targets the DMH, which stimulates arousal by exciting wake-promoting neurons in the LHA and silencing sleep-promoting ones in the VLPO (Figure 1.1).

Homeostatic vs. circadian regulation of sleep

Daily rhythms of behavior and arousal state are not only regulated by the circadian timing system but also by a separate system mediating homeostatic drive for sleep (Achermann and Borbely, 2003). Though the circadian and homeostatic drives for rest constitute two distinct systems, it is not easy to functionally separate them in experimental measurements of behavioral output, for review see (Gooley, 2005;). Temporal organization of behavior is one of the most important contributions of the CTS to survival and evolutionary fitness. Likewise, homeostatic systems regulating sleep duration and consolidations are absolutely critical for maintenance of normal performance and metabolism. In order for an animal to perform at its full potential during the temporal niche which is most adaptive for them (e.g. when daylight helps them detect food or when their predators are asleep), the circadian and homeostatic control of sleep have had to evolve ways of communicating with each other so as to not send conflicting output signals to the rest of the body.

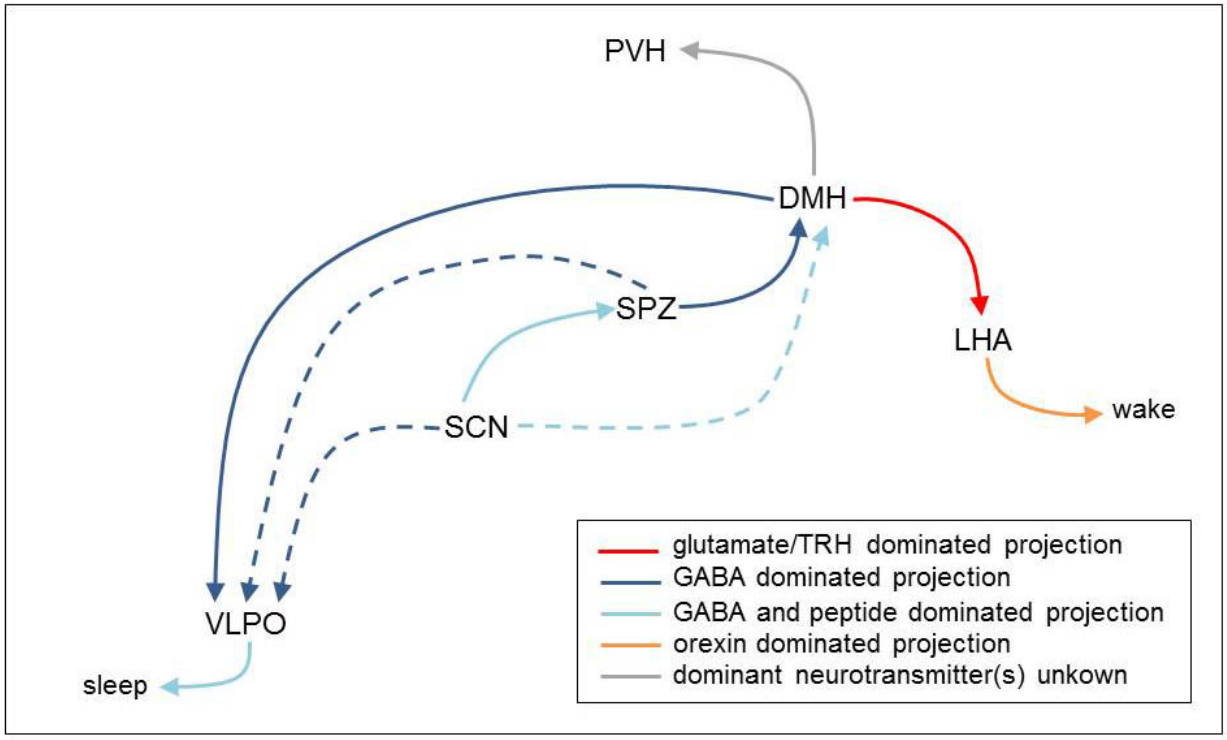

Figure1.1: Schematic diagram of circadian regulation of sleep and wakefulness based on previous literature.

Current hypotheses about mechanism of action for the "sleep homeostat" propose that energy expenditure in certain brain regions during prolonged wakefulness leads to sequential de-phosphorylations of ATP and through them an accumulation of adenosine. Accumulation (or experimental injection) of adenosine in the BF, adjacent to the VLPO, induces sleep and increased immediate early gene expression in the VLPO (Porkka-Heiskanen et al., 2000; Scammell et al., 2001). Thus, while neurons of the VLPO are inhibited by the monoaminergic arousal system and GABAergic DMH inputs in order to promote arousal, after many hours of wakefulness they appear to be disinhibited, either by adenosine itself, inputs of adenosine-sensing neurons elsewhere in the brain, or perhaps some combination thereof. Our current model of homeostatic regulatory mechanisms of arousal would suggest that the homeostat acts on the system only by driving sleep (after a high enough sleep pressure has built up). Meanwhile, it would appear that the circadian system exerts its input on sleep both by neurally driving arousal/activity at the appropriate times (via excitation of orexinergic LHA neurons and inhibition of the VLPO) and by inhibiting it during the other half of the day (via diffusible factors).

How does the circadian timing system communicate with brain regions regulating thermogenesis and heat loss mechanisms?

In homeotherms, body temperature is sensed by both peripheral and central neurons (Boulant, 2006; Romanovsky, 2007; Nakamura and Morrison, 2008), integrated (compared to a "set-point") at a series of hierarchically organized central regions in the hypothalamus, midbrain, brainstem and even spinal cord (Satinoff, 1978) and maintained within a narrow range close to 37°C via autonomic effector outputs triggering either heat production or loss. Critical central structures for maintenance of core T_b include the pre-optic hypothalamus (median, medial and dorsolateral pre-optic areas (MnPO) and (MPA), the dorsal hypothalamic area adjacent to the DMH (DH), the periaqueductal gray (PAG), and raphe pallidus (RPa) (Yoshida et al., 2005; Benarroch, 2007; Dimicco and Zaretsky, 2007; Nakamura and Morrison, 2007; Yoshida et al., 2009). Ultimate effector pathways for heat production include sympathetically controlled cutaneous vasoconstriction, shivering, piloerection, secretion of thyroid hormones and, in many mammals, activation of brown adipose tissue. Cooling mechanisms conversely involve cutaneous vasodilation, evaporation of water from the respiratory tract and increased autonomic tone to sweat glands in furless animals like humans and salivary glands in furry animals like rats and dogs, which spread the fluid on their coat to promote heat loss by evaporation.

Although T_b in homeotherms is maintained within a rather narrow range, typically 36.5 ± 1.0°C, it shows a very predictable circadian oscillation throughout the day peaking during the active period (night for rodents) and reaching its minimum near the middle of the quiescent period. This rhythm has been characterized in at least 28 different animal species including avian, rodent, ovine, bovine and primate groups, and though there are differences in the waveform and amplitude of T_b rhythms in these groups, the phase angle between peak activity and temperature is relatively consistent (Refinetti and Menaker, 1992). Because of this correlation in the two rhythms, some have proposed that T_b rhythm is (at least in part) secondary to heat generated as a consequence of activity. However, since the increase in T_b typically precedes the start of activity and always persists in experiments where activity levels are kept constant over 24 hours in humans (either via chair or bed restriction),where, its amplitude often is not even significantly diminished (Fuller et al., 1981; Marotte and Timbal, 1981; Czeisler et al., 1986; Gander et al., 1986), it is widely accepted that the T_b rhythm is generated autonomously and does not depend on

activity rhythms. Because Tb is affected by many other factors including feeding, sleep, light exposure, hormone rhythms and acute stressors, it is important to note that experiments controlling for all of these have also found a persisting near-24-hour oscillation in T_b. The primary example of such an experiment is T_b measurement during constant routine in humans, where sleep and feeding are controlled and evenly distributed into many short episodes over the circadian day, the subject remains seated or reclined for the duration of the experiment and all external factors (such as light level and ambient temperature) are kept as constant as possible (Dunlap et al., 2004)-see their chapter 9). While this cannot be done in rodents, fortuitously, there are lesions that can achieve the same end. Ablation of the dorsomedial nucleus of the hypothalamus (DMH) severely disrupts rhythms in locomotor activity, sleep and wakefulness, feeding and corticosteroid secretion, but barely reduces the amplitude of circadian rhythms in T_b in constant darkness (Chou et al., 2003). Thus in both humans and rodents, we know that Tb rhythms are not dependent on any other physiological rhythms or external time cues, although they may be affected, enhanced or perturbed by these factors.

In fact, not only is the Tb rhythm not a mere consequence of other rhythms in the body, it likely acts to synchronize molecular clocks throughout the body and ensure they are in phase with the SCN clock (see Buhr et al., 2010, Saper et al. 2013). The clock in the SCN drives circadian rhythms in body temperature (Fuller et al., 2008, Ramalingam et al., unpublished data), and likely does so via efferent projections to the dSPZ (Lu et al., 2001), however, the downstream effectors in the neural circuit for rhythms in body temperature are not yet known (see footnote[4]).

---

[4]The unknown pathway driving circadian oscillation in Tb:

At present, there is not a good hypothesis for where the anatomical connection between the dSPZ and effector sites in the brain known to maintain core T_b homeostasis lies. Large pre-optic Satinoff et al. (1982); (Szymusiak et al., 1985), DMH (Chou et al., 2003) and RPa (Fuller and Lu, personal communication) lesions do not reduce the amplitude of T_b rhythms. In fact, MnPO and RPa lesions may even increase the amplitude of this rhythm. The potential role of the PAG as an integrator has not been investigated, in part because its anatomical connections to the CTS are relatively weak. Though its role in thermoregulation is less clear, the PVH, a major autonomic relay and neuroendocrine interface, receives both direct and indirect projections from the SCN. Lesions of this region also do not diminish the amplitude of T_b rhythms at all (Moore and Danchenko, 2002).

Preliminary studies from our lab show that T_b rhythms in hypophysectomized rats are completely intact and have, if anything, slightly higher amplitude than sham controls, likely due to lower body weight. (Vujovic, unpublished data). Normal amplitude circadian oscillations in T_b also persist in rats with full chemical sympathectomy or spinal transections at the T2/T3 level, even during a 24 hour fast, which accounts for potential effects of rhythmic diet induced thermogenesis (Vujovic, unpublished data).

It is possible that parasympathetic or non-pituitary humoral signals are the most important signals driving circadian oscillations in T_b, or that this rhythm is the product of several redundant outflow pathways.

How does the circadian timing system communicate with brain regions regulating autonomic and neuroendocrine functions?

Retrograde transneuronal tract tracing shows that the SCN is connected (presumably through indirect, multisynaptic pathways) to many peripheral tissues via the sympathetic and parasympathetic branches of the autonomic nervous system (Ueyama et al., 1999). One important junction at which primary (or higher order) efferents from the SCN connect to neurons of the autonomic nervous system is the PVH (Teclemariam-Mesbah et al., 1997). The PVH sends direct projections to sympathetic pre-ganglionic neurons in the spinal cord, to pre-parasympatheitc targets in the brainstem, and drives pituitary hormone release via both synaptic and paracrine outputs. Through these pathways, the PVH can regulate rhythms and control the phases of many endocrine outputs (Perreau-Lenz et al., 2004).

Adrenergic signals from the sympathetic nervous system have been shown to underlie certain physiological responses to light, including diurnal entrainment of important rhythms. The most thoroughly studied of these are rhythms of pineal melatonin synthesis (Moore, 1996; Perreau-Lenz et al., 2005) and adrenal corticosteroid release (Jasper and Engeland, 1994). There are also many examples of light stimuli more acutely affecting sympathetically controlled or regulated functions, presumably via sympathetic nerve activity [*e.g.* ambulatory heart rate (Scheer et al., 1999; Scheer et al., 2001), adrenal corticosterone secretion (Buijs et al., 1999; Ishida et al., 2005; Mohawk et al., 2007), pineal melatonin release (Kalsbeek et al., 1996; Kalsbeek et al., 1999; Kalsbeek et al., 2000), and salivary secretion (Bellavia and Gallara, 2000)]. These findings suggest that both normal photic entrainment of the clock and intermittent light exposure (whether at appropriate or inappropriate circadian times) may affect the temporal organization of physiological and endocrine function through sympathetic outflow.

Circadian rhythms in plasma glucose are thought to be dependent on GABAergic SCN projections to the PVH and sympathetic outflow from the PVH to preganglionic neurons that control the liver (Kalsbeek et al., 2004; Cailotto et al., 2005). Rhythmic synthesis and secretion of pineal melatonin also depends on SCN projections to the PVH and its projections to sympathetic preganlionic neurons that regulate the pineal gland (Moore, 1996).

Of most relevance for the experimental work discussed in subsequent chapters, indirect SCN connections to the DMH and PVH are thought to be important for driving rhythms in plasma

corticosteroids. Lesions of the DMH have been shown to diminish the amplitude of corticosteroid rhythms (Chou et al., 2003) and the PVH (which receives input from the SCN, SPZ and DMH) regulates adrenal corticosteroid release both via sympathetic projections to the adrenal cortex and through the hypothalamo-pituitary-adrenal axis. Both these connections from the PVH to the adrenal gland are well characterized. For the latter, release of corticotrophin-releasing hormone (CRH) from parvicellular hypophysiotropic neurons in the PVH drives the release of adrenocorticotropic hormone (ACTH) from the anterior pituitary. For the former, projections from the PVH stimulate sympathetic pre-ganglionic neurons in the intermediolateral column of the thoracic spinal cord which in turn drive splanchnic nerve activity, which can modulate adrenal function. Further complicating matters, the molecular clock in the adrenal gland itself is shown to drive circadian oscillation in the expression and intracellular levels of enzymes responsible for corticosterone synthesis (Son et al., 2011; Ota et al., 2012). This clock is likely sensitive to perturbation and, in the absence of an intact SCN is clearly not able to drive full-amplitude corticosterone rhythms (Moore and Eichler, 1972; Abe et al., 1979). Furthermore, studies showing that CRH-knockout mice lack normal diurnal corticosteroid rhythms, and that these can be restored via constant infusion of exogenous CRH, suggest that a functional hypothalamo-pituitary adrenal axis is necessary for normal expression of these rhythms (Muglia et al., 1997). The circadian timing system may regulate corticosterone rhythms via the hypothalamo-pituitary adrenal axis, by neural modulation of splanchnic nerve activity, via (direct or indirect) modulation humoral factors which could affect the phase or amplitude of local adrenal gland molecular clocks, or, most likely by some combination of the above factors. It is not yet understood which neurotransmitter(s) are released by the SCN, vSPZ and DMH in the circuit connecting the circadian timing system to these neuroendocrine and autonomic interfaces.

Neurotransmitters of the SCN, SPZ and DMH

Figure 1.1 (see page 11) includes some of the known neurotransmitters in the circuits underlying circadian influence on arousal. However, the identity of neurotransmitter(s) used by several key neurons in this circuit remains to be ascertained. With particular relevance to this proposal, it is still not known which transmitters are used by projections of the SCN and SPZ and certain projections from the DMH in the regulation of circadian rhythms of locomotor activity, sleep, corticosteroid and T_b. Below we describe

some of the candidate classic transmitters and peptides acting at these sites; this is also summarized in Table 1.1.

Table 1.1: Neurotransmitters expressed in the SCN, SPZ and DMH.

SCN	SPZ	DMH
GABA core/ventrolateral: vasoactive intestinal polypeptide(VIP) gastrin releasing peptide (GRP) neurotensin (NT) peptide histidine isoleucine (PHI) shell/dorsomedial: arginine vasopressin (AVP) angiotensin II enkephalin boundary: somatostatin (SOM) substance P (SP)	GABA dopamine	GABA glutamate (*VGlut2* only) thyrotropin releasing hormone (TRH) orexin (ORX) alpha atrial natriuretic peptide (α-ANP) alpha cholecystokinin α-CCK α-MSH (sparse & in caudal region)

Neurons of the SCN express and synaptically release many peptides not commonly found in other portions of the central nervous system, but only one classic neurotransmitter, γ-aminobutyric acid (GABA), the major inhibitory transmitter of the brain. While GABA is expressed throughout the entire SCN, many peptides are expressed only in certain sub-regions of this nucleus. The SCN is often divided into two main regions, the ventrolateral "core" and dorsomedial "shell" (Moore, 1983). In the core the most abundantly expressed peptide transmitter is vasoactive intestinal polypeptide (VIP) but many core neurons also contain gastrin releasing peptide, neurotensin or peptide histidine isoleucine (PHI), a peptide made from same precursor as VIP and thus often co-expressed with VIP within individual neurons. By contrast, the shell of the SCN can be anatomically defined by immunostaining for arginine vasopressin (AVP) but also stains with antisera for the hormones angiotensin II and enkephalin. Two other peptides, somatostatin and substance P are expressed by SCN neurons along the core-shell border.

Of the above transmitters AVP, VIP and GABA are considered to be three of the most important. Expression of each of these transmitters in the SCN has been experimentally disrupted, with varying

results. AVP-deficient Brattleboro rats appear to have normal behavioral rhythms, (Peterson et al., 1980; Groblewski et al., 1981), however AVP receptor V1a knockout mice show a lowered amplitude circadian rhythm in locomotor activity and eventually become arrhythmic after a few weeks in constant darkness, (Li et al., 2009). VIP and PHI knock-out mice exhibit a reduction in the amplitude in circadian wheel-running rhythm (Colwell et al., 2003) as do knockouts for the VIP receptor $VPAC_2$ (Kallo et al., 2004). All of these mice still show normal light entrainment and diurnal activity rhythms in a light-dark cycle, however this may be a consequence of light masking (i.e. behavior driven directly by light and instead of a light-entrained endogenous clock). Importantly, several targets of VIP-containing SCN projections express $VPAC_{2,}$ including the SPZ, PVH and lateral septum (Kallo et al., 2004). GABAergic outputs of the SCN appear to drive circadian rhythms of plasma glucose (Kalsbeek et al., 2004) and may be important for entrainment of melatonin (Kalsbeek et al., 1999), locomotor activity and temperature rhythms (Fuller, personal communication).

Not surprisingly, the SPZ, the main target of SCN output fibers, receives input from both the shell and core of the SCN. VIP-ergic fibers from the SCN core tend to project to more lateral portions of the SPZ, while AVP-immunoreactive fibers from the SCN shell target the medial SPZ (Leak and Moore, 2001). It is not clear whether there is any difference in SCN inputs to the functionally distinct dorsal and ventral subdivisions of the SPZ.

Unlike the SCN, the SPZ does not appear to express any known peptide transmitters. Instead, neurons throughout this nucleus express primarily GABA, the major inhibitory neurotransmitter. A few dopaminergic somata may also be seen in medial parts of the SPZ, overlapping with A14, a well-characterized dopaminergic zone in the periventricular nucleus of the hypothalamus.

About equal numbers of neurons in the DMH express markers for GABA or glutamate, and in addition many neurons of the DMH express various peptides (Chou et al., 2003). These include thyrotropin releasing hormone (TRH), orexin (ORX), alpha atrial natriuretic peptide (α-ANP), alpha cholecystokinin α-CCK, and to a lesser extent, melanin concentrating hormone (MCH) in the caudal DMH.

It should be noted that unlike peptidergic neurons, GABAergic and glutamatergic neurons cannot be identified simply by the presence of GABA or glutamate in terminals. Since it is one of the 20 essential amino acids, glutamate is present in all cells and is very difficult to label with a good signal-to-noise ratio

using an antibody. Glutamate is the precursor for GABA, which itself is also not a good target for immunohistochemistry. The enzyme which converts glutamate to GABA, glutamic acid decarboxylase (GAD) is a good marker for neurons which produce GABA. In mammals, it is present in two isoforms, GAD-65 and GAD-67, both detectable through immunohistochemistry and *in situ* hybridization. However, the clearest indicator that a neuron *releases* a given transmitter is the presence of its vesicular transporter (i.e. the protein pump which packages the transmitter into synaptic vesicles). All the GABA-ergic neuronal populations discussed above were confirmed as such through their expression of vesicular GABA transporter (VGAT). Three separate isoforms of vesicular glutamate transporter (VGlut1, *VGlut2* and VGlut3) are present in the mammalian nervous system, each expressed in distinct regions. The glutamatergic neurons of the SPZ and DMH all express *VGlut2*.

Rationale for experimental work presented in Chapter 2 and 3

Tracing efferent projections from the SPZ

As described above, the SPZ is the main recipient of SCN efferents and has been shown to play an important role in relaying information from the SCN clock to other brain regions. Cell-specific lesions of the ventral subdivision of the SPZ cause a profound reduction in the amplitude of locomotor activity and sleep-wake rhythms, while having only modest effects on the amplitude of the circadian rhythm in body temperature. Cell-specific lesions of the dorsal SPZ produce the opposite effect, severely reducing the amplitude of body temperature (but not activity and sleep-wake) rhythms. It would seem that the dorsal and ventral SPZ may have differences in terms of their neural inputs and outputs that underlie this difference in physiological function. However, when inputs to the SPZ are examined, the most striking differences are seen between innervation of the medial vs. lateral SPZ, with the former receiving much more robust input from the SCN shell and the latter from the SCN core and from the retina. This suggests that the medial vs. lateral SPZ may also have differences in function that are not yet understood. To gain a better idea of what roles each subdivision of the SPZ may play, and to test hypotheses about which SPZ efferents could be driving normal rhythms in activity and sleep vs. body temperature, we divided this region into four quadrants (the ventromedial, ventrolateral, dorsomedial, and dorsolateral SPZ) and placed injections of anterograde tracer into each.

Selective disruption of glutamatergic neurotransmission from DMH neurons

The DMH is a major relay and integrator in the circuitry through which circadian patterns in arousal state, behavior and endocrine rhythms are temporally organized, and various homeostatic parameters are regulated. As mentioned, cell-specific lesions of the DMH produce a significant reduction in the amplitude of circadian rhythms of locomotor activity, sleep-wake, corticosteroid secretion and feeding. They also result in lowered overall wakefulness, activity, plasma cortisol and body temperature. Although it is clear that the DMH occupies a prominent role in the neural pathway connecting the circadian timing system to effector circuits driving changes in behavioral state, temperature and endocrine output, it is not known which neurotransmitter(s) it releases to drive downstream targets. It has been proposed that excitatory glutamatergic projections from the DMH to wake-promoting neurons of the LHA and inhibitory GABAergic inputs from the DMH to sleep-promoting neurons in the VLPO may be critical for circadian modulation of activity and feeding rhythms. Circadian regulation of corticosteroid release may depend on an excitatory projection from the DMH to cortictropin releasing hormone-expressing neurons in the paraventricular hypothalamus (PVH). Evidence the above hypothesis comes from neuroanatomical and physiological studies in the rat. We aim to test the extent to which glutamatergic outputs of the DMH drive circadian oscillation in locomotor activity, feeding and corticosteroid release, and absolute levels of body temperature, locomotor activity and corticosterone production.

References

Abe K, Kroning J, Greer MA, Critchlow V (1979) Effects of destruction of the suprachiasmatic nuclei on the circadian rhythms in plasma corticosterone, body temperature, feeding and plasma thyrotropin. Neuroendocrinology 29:119-131.

Achermann P, Borbely AA (2003) Mathematical models of sleep regulation. Front Biosci 8:s683-693.

Adamantidis A, Salvert D, Goutagny R, Lakaye B, Gervasoni D, Grisar T, Luppi PH, Fort P (2008) Sleep architecture of the melanin-concentrating hormone receptor 1-knockout mice. The European journal of neuroscience 27:1793-1800.

Aguilar-Roblero R, Morin LP, Moore RY (1994) Morphological correlates of circadian rhythm restoration induced by transplantation of the suprachiasmatic nucleus in hamsters. Exp Neurol 130:250-260.

Alvarez JD, Hansen A, Ord T, Bebas P, Chappell PE, Giebultowicz JM, Williams C, Moss S, Sehgal A (2008) The circadian clock protein BMAL1 is necessary for fertility and proper testosterone production in mice. J Biol Rhythms 23:26-36.

Anaclet C, Lin JS, Vetrivelan R, Krenzer M, Vong L, Fuller PM, Lu J (2012) Identification and characterization of a sleep-active cell group in the rostral medullary brainstem. The Journal of neuroscience : the official journal of the Society for Neuroscience 32:17970-17976.

Bartness TJ, Song CK, Demas GE (2001) SCN efferents to peripheral tissues: implications for biological rhythms. J Biol Rhythms 16:196-204.

Bellavia S, Gallara R (2000) Effect of photic stimuli on rat salivary glands. Role of sympathetic nervous system. Acta Odontol Latinoam 13:3-19.

Benarroch EE (2007) Thermoregulation: recent concepts and remaining questions. Neurology 69:1293-1297.

Boulant JA (2006) Neuronal basis of Hammel's model for set-point thermoregulation. J Appl Physiol 100:1347-1354.

Buijs RM, Wortel J, Van Heerikhuize JJ, Feenstra MG, Ter Horst GJ, Romijn HJ, Kalsbeek A (1999) Anatomical and functional demonstration of a multisynaptic suprachiasmatic nucleus adrenal (cortex) pathway. Eur J Neurosci 11:1535-1544.

Bunger MK, Walisser JA, Sullivan R, Manley PA, Moran SM, Kalscheur VL, Colman RJ, Bradfield CA (2005) Progressive arthropathy in mice with a targeted disruption of the Mop3/Bmal-1 locus. Genesis 41:122-132.

Buxton OM, Cain SW, O'Connor SP, Porter JH, Duffy JF, Wang W, Czeisler CA, Shea SA (2012) Adverse metabolic consequences in humans of prolonged sleep restriction combined with circadian disruption. Science translational medicine 4:129ra143.

Cailotto C, La Fleur SE, Van Heijningen C, Wortel J, Kalsbeek A, Feenstra M, Pevet P, Buijs RM (2005) The suprachiasmatic nucleus controls the daily variation of plasma glucose via the autonomic output to the liver: are the clock genes involved? Eur J Neurosci 22:2531-2540.

Cheng MY, Bullock CM, Li C, Lee AG, Bermak JC, Belluzzi J, Weaver DR, Leslie FM, Zhou QY (2002) Prokineticin 2 transmits the behavioural circadian rhythm of the suprachiasmatic nucleus. Nature 417:405-410.

Chou TC, Bjorkum AA, Gaus SE, Lu J, Scammell TE, Saper CB (2002) Afferents to the ventrolateral preoptic nucleus. J Neurosci 22:977-990.

Chou TC, Scammell TE, Gooley JJ, Gaus SE, Saper CB, Lu J (2003) Critical role of dorsomedial hypothalamic nucleus in a wide range of behavioral circadian rhythms. The Journal of neuroscience : the official journal of the Society for Neuroscience 23:10691-10702.

Colwell CS, Michel S, Itri J, Rodriguez W, Tam J, Lelievre V, Hu Z, Liu X, Waschek JA (2003) Disrupted circadian rhythms in VIP- and PHI-deficient mice. Am J Physiol Regul Integr Comp Physiol 285:R939-949.

Czeisler CA, Klerman EB (1999) Circadian and sleep-dependent regulation of hormone release in humans. Recent Prog Horm Res 54:97-130; discussion 130-132.

Czeisler CA, Weitzman E, Moore-Ede MC, Zimmerman JC, Knauer RS (1980a) Human sleep: its duration and organization depend on its circadian phase. Science 210:1264-1267.

Czeisler CA, Zimmerman JC, Ronda JM, Moore-Ede MC, Weitzman ED (1980b) Timing of REM sleep is coupled to the circadian rhythm of body temperature in man. Sleep 2:329-346.

Czeisler CA, Allan JS, Strogatz SH, Ronda JM, Sanchez R, Rios CD, Freitag WO, Richardson GS, Kronauer RE (1986) Bright light resets the human circadian pacemaker independent of the timing of the sleep-wake cycle. Science 233:667-671.

Czeisler CA, Duffy JF, Shanahan TL, Brown EN, Mitchell JF, Rimmer DW, Ronda JM, Silva EJ, Allan JS, Emens JS, Dijk DJ, Kronauer RE (1999) Stability, precision, and near-24-hour period of the human circadian pacemaker. Science 284:2177-2181.

Davidson AJ, Sellix MT, Daniel J, Yamazaki S, Menaker M, Block GD (2006) Chronic jet-lag increases mortality in aged mice. Current biology : CB 16:R914-916.

de la Iglesia HO, Meyer J, Schwartz WJ (2003) Lateralization of circadian pacemaker output: Activation of left- and right-sided luteinizing hormone-releasing hormone neurons involves a neural rather than a humoral pathway. The Journal of neuroscience : the official journal of the Society for Neuroscience 23:7412-7414.

Dimicco JA, Zaretsky DV (2007) The dorsomedial hypothalamus: a new player in thermoregulation. American journal of physiology Regulatory, integrative and comparative physiology 292:R47-63.

Dunlap JC, Loros JJ, DeCoursey PJ (2004) Chronobiology : biological timekeeping. Sunderland, Mass.: Sinauer Associates.

Eastman CI, Mistlberger RE, Rechtschaffen A (1984) Suprachiasmatic nuclei lesions eliminate circadian temperature and sleep rhythms in the rat. Physiol Behav 32:357-368.

Foster RG, Kreitzman L (2004) Rhythms of life : the biological clocks that control the daily lives of every living thing. New Haven, CT: Yale University Press.

Freedman MS, Lucas RJ, Soni B, von Schantz M, Munoz M, David-Gray Z, Foster R (1999) Regulation of mammalian circadian behavior by non-rod, non-cone, ocular photoreceptors. Science 284:502-504.

Fuller CA, Sulzman FM, Moore-Ede MC (1978) Thermoregulation is impaired in an environment without circadian time cues. Science 199:794-796.

Fuller CA, Lydic R, Sulzman FM, Albers HE, Tepper B, Moore-Ede MC (1981) Circadian rhythm of body temperature persists after suprachiasmatic lesions in the squirrel monkey. Am J Physiol 241:R385-391.

Fuller PM, Lu J, Saper CB (2008) Differential rescue of light- and food-entrainable circadian rhythms. Science (New York, NY) 320:1074-1077.

Fuller PM, Sherman D, Pedersen NP, Saper CB, Lu J (2011) Reassessment of the structural basis of the ascending arousal system. The Journal of comparative neurology 519:933-956.

Gall AJ, Todd WD, Blumberg MS (2012) Development of SCN connectivity and the circadian control of arousal: a diminishing role for humoral factors? PloS one 7:e45338.

Gallopin T, Fort P, Eggermann E, Cauli B, Luppi PH, Rossier J, Audinat E, Muhlethaler M, Serafin M (2000) Identification of sleep-promoting neurons in vitro. Nature 404:992-995.

Gander PH, Connell LJ, Graeber RC (1986) Masking of the circadian rhythms of heart rate and core temperature by the rest-activity cycle in man. J Biol Rhythms 1:119-135.

Gooley JJ, Lu J, Fischer D, Saper CB (2003) A broad role for melanopsin in nonvisual photoreception. The Journal of neuroscience : the official journal of the Society for Neuroscience 23:7093-7106.

Gooley JJ, Lu J, Chou TC, Scammell TE, Saper CB (2001) Melanopsin in cells of origin of the retinohypothalamic tract. Nat Neurosci 4:1165.

Gooley JJ, Saper C.B. (2005;) Anatomy of the mammalian circadian system. In: Principles and Practice of Sleep Medicine (Kryger R, Dement, eds, ed), pp 351-362.

Groblewski TA, Nunez AA, Gold RM (1981) Circadian rhythms in vasopressin deficient rats. Brain Res Bull 6:125-130.

Guo H, Brewer JM, Lehman MN, Bittman EL (2006) Suprachiasmatic regulation of circadian rhythms of gene expression in hamster peripheral organs: effects of transplanting the pacemaker. J Neurosci 26:6406-6412.

Guo H, Brewer JM, Champhekar A, Harris RB, Bittman EL (2005) Differential control of peripheral circadian rhythms by suprachiasmatic-dependent neural signals. Proceedings of the National Academy of Sciences of the United States of America 102:3111-3116.

Halberg F, Lubanovic WA, Sothern RB, Brockway B, Powell EW, Pasley JN, Scheving LE (1979) Nomifensine chronopharmacology, schedule-shifts and circadian temperature rhythms in di-suprachiasmatically lesioned rats--modeling emotional chronopathology and chronotherapy. Chronobiologia 6:405-424.

Hansen J (2001) Increased breast cancer risk among women who work predominantly at night. Epidemiology 12:74-77.

Hastings MH, Reddy AB, Maywood ES (2003) A clockwork web: circadian timing in brain and periphery, in health and disease. Nat Rev Neurosci 4:649-661.

Honma S, Honma K, Shirakawa T, Hiroshige T (1988) Rhythms in behaviors, body temperature and plasma corticosterone in SCN lesioned rats given methamphetamine. Physiol Behav 44:247-255.

Houle AM, Taketo T (1992) True hermaphrodites: an experimental model in the mouse. The Journal of urology 148:672-676.

Ishida A, Mutoh T, Ueyama T, Bando H, Masubuchi S, Nakahara D, Tsujimoto G, Okamura H (2005) Light activates the adrenal gland: timing of gene expression and glucocorticoid release. Cell metabolism 2:297-307.

Jasper MS, Engeland WC (1994) Splanchnic neural activity modulates ultradian and circadian rhythms in adrenocortical secretion in awake rats. Neuroendocrinology 59:97-109.

Jego S, Glasgow SD, Herrera CG, Ekstrand M, Reed SJ, Boyce R, Friedman J, Burdakov D, Adamantidis AR (2013) Optogenetic identification of a rapid eye movement sleep modulatory circuit in the hypothalamus. Nature neuroscience.

Kallo I, Kalamatianos T, Wiltshire N, Shen S, Sheward WJ, Harmar AJ, Coen CW (2004) Transgenic approach reveals expression of the VPAC2 receptor in phenotypically defined neurons in the mouse suprachiasmatic nucleus and in its efferent target sites. The European journal of neuroscience 19:2201-2211.

Kalsbeek A, Teclemariam-Mesbah R, Pevet P (1993) Efferent projections of the suprachiasmatic nucleus in the golden hamster (Mesocricetus auratus). J Comp Neurol 332:293-314.

Kalsbeek A, Perreau-Lenz S, Buijs RM (2006a) A network of (autonomic) clock outputs. Chronobiol Int 23:201-215.

Kalsbeek A, La Fleur S, Van Heijningen C, Buijs RM (2004) Suprachiasmatic GABAergic inputs to the paraventricular nucleus control plasma glucose concentrations in the rat via sympathetic innervation of the liver. J Neurosci 24:7604-7613.

Kalsbeek A, Cutrera RA, Van Heerikhuize JJ, Van Der Vliet J, Buijs RM (1999) GABA release from suprachiasmatic nucleus terminals is necessary for the light-induced inhibition of nocturnal melatonin release in the rat. Neuroscience 91:453-461.

Kalsbeek A, Drijfhout WJ, Westerink BH, van Heerikhuize JJ, van der Woude TP, van der Vliet J, Buijs RM (1996) GABA receptors in the region of the dorsomedial hypothalamus of rats are implicated in the control of melatonin and corticosterone release. Neuroendocrinology 63:69-78.

Kalsbeek A, Garidou ML, Palm IF, Van Der Vliet J, Simonneaux V, Pevet P, Buijs RM (2000) Melatonin sees the light: blocking GABA-ergic transmission in the paraventricular nucleus induces daytime secretion of melatonin. Eur J Neurosci 12:3146-3154.

Kalsbeek A, Palm IF, La Fleur SE, Scheer FA, Perreau-Lenz S, Ruiter M, Kreier F, Cailotto C, Buijs RM (2006b) SCN outputs and the hypothalamic balance of life. J Biol Rhythms 21:458-469.

Kaur S, Pedersen NP, Yokota S, Hur EE, Fuller PM, Lazarus M, Chamberlin NL, Saper CB (2013) Glutamatergic signaling from the parabrachial nucleus plays a critical role in hypercapnic arousal. The Journal of neuroscience : the official journal of the Society for Neuroscience 33:7627-7640.

Kawachi I, Colditz GA, Stampfer MJ, Willett WC, Manson JE, Speizer FE, Hennekens CH (1995) Prospective study of shift work and risk of coronary heart disease in women. Circulation 92:3178-3182.

Knutson KL, Spiegel K, Penev P, Van Cauter E (2007) The metabolic consequences of sleep deprivation. Sleep Med Rev 11:163-178.

Kramer A, Yang FC, Snodgrass P, Li X, Scammell TE, Davis FC, Weitz CJ (2001) Regulation of daily locomotor activity and sleep by hypothalamic EGF receptor signaling. Science (New York, NY) 294:2511-2515.

Kraves S, Weitz CJ (2006) A role for cardiotrophin-like cytokine in the circadian control of mammalian locomotor activity. Nature neuroscience 9:212-219.

La Fleur SE, Kalsbeek A, Wortel J, Buijs RM (1999) A suprachiasmatic nucleus generated rhythm in basal glucose concentrations. J Neuroendocrinol 11:643-652.

Laposky A, Easton A, Dugovic C, Walisser J, Bradfield C, Turek F (2005) Deletion of the mammalian circadian clock gene BMAL1/Mop3 alters baseline sleep architecture and the response to sleep deprivation. Sleep 28:395-409.

Leak RK, Moore RY (2001) Topographic organization of suprachiasmatic nucleus projection neurons. The Journal of comparative neurology 433:312-334.

Lehman MN, Silver R, Gladstone WR, Kahn RM, Gibson M, Bittman EL (1987) Circadian rhythmicity restored by neural transplant. Immunocytochemical characterization of the graft and its integration with the host brain. The Journal of neuroscience : the official journal of the Society for Neuroscience 7:1626-1638.

LeSauter J, Romero P, Cascio M, Silver R (1997) Attachment site of grafted SCN influences precision of restored circadian rhythm. Journal of biological rhythms 12:327-338.

Li JD, Burton KJ, Zhang C, Hu SB, Zhou QY (2009) Vasopressin receptor V1a regulates circadian rhythms of locomotor activity and expression of clock-controlled genes in the suprachiasmatic nuclei. American journal of physiology Regulatory, integrative and comparative physiology 296:R824-830.

Libby P, Ridker PM (2004) Inflammation and atherosclerosis: role of C-reactive protein in risk assessment. Am J Med 116 Suppl 6A:9S-16S.

Lu J, Zhang YH, Chou TC, Gaus SE, Elmquist JK, Shiromani P, Saper CB (2001) Contrasting effects of ibotenate lesions of the paraventricular nucleus and subparaventricular zone on sleep-wake cycle and temperature regulation. The Journal of neuroscience : the official journal of the Society for Neuroscience 21:4864-4874.

Marotte H, Timbal J (1981) Circadian rhythm of temperature in man. Comparative study with two experiment protocols. Chronobiologia 8:87-100.

Meyer-Bernstein EL, Jetton AE, Matsumoto SI, Markuns JF, Lehman MN, Bittman EL (1999) Effects of suprachiasmatic transplants on circadian rhythms of neuroendocrine function in golden hamsters. Endocrinology 140:207-218.

Miller BH, Olson SL, Turek FW, Levine JE, Horton TH, Takahashi JS (2004) Circadian clock mutation disrupts estrous cyclicity and maintenance of pregnancy. Curr Biol 14:1367-1373.

Mochizuki T, Crocker A, McCormack S, Yanagisawa M, Sakurai T, Scammell TE (2004) Behavioral state instability in orexin knock-out mice. J Neurosci 24:6291-6300.

Mohawk JA, Pargament JM, Lee TM (2007) Circadian dependence of corticosterone release to light exposure in the rat. Physiology & behavior 92:800-806.

Moore-Ede MC, Czeisler CA, Richardson GS (1983) Circadian timekeeping in health and disease. Part 2. Clinical implications of circadian rhythmicity. N Engl J Med 309:530-536.

Moore RY (1983) Organization and function of a central nervous system circadian oscillator: the suprachiasmatic hypothalamic nucleus. Federation proceedings 42:2783-2789.

Moore RY (1993) Organization of the primate circadian system. J Biol Rhythms 8 Suppl:S3-9.

Moore RY (1996) Neural control of the pineal gland. Behav Brain Res 73:125-130.

Moore RY, Eichler VB (1972) Loss of a circadian adrenal corticosterone rhythm following suprachiasmatic lesions in the rat. Brain research 42:201-206.

Moore RY, Danchenko RL (2002) Paraventricular-subparaventricular hypothalamic lesions selectively affect circadian function. Chronobiology international 19:345-360.

Morin LP, Goodless-Sanchez N, Smale L, Moore RY (1994) Projections of the suprachiasmatic nuclei, subparaventricular zone and retrochiasmatic area in the golden hamster. Neuroscience 61:391-410.

Muglia LJ, Jacobson L, Weninger SC, Luedke CE, Bae DS, Jeong KH, Majzoub JA (1997) Impaired diurnal adrenal rhythmicity restored by constant infusion of corticotropin-releasing hormone in corticotropin-releasing hormone-deficient mice. The Journal of clinical investigation 99:2923-2929.

Nagashima K, Matsue K, Konishi M, Iidaka C, Miyazaki K, Ishida N, Kanosue K (2005) The involvement of Cry1 and Cry2 genes in the regulation of the circadian body temperature rhythm in mice. Am J Physiol Regul Integr Comp Physiol 288:R329-335.

Nakamura K, Morrison SF (2007) Central efferent pathways mediating skin cooling-evoked sympathetic thermogenesis in brown adipose tissue. Am J Physiol Regul Integr Comp Physiol 292:R127-136.

Nakamura K, Morrison SF (2008) A thermosensory pathway that controls body temperature. Nat Neurosci 11:62-71.

Okamura H (2004) Clock genes in cell clocks: roles, actions, and mysteries. J Biol Rhythms 19:388-399.

Ota T, Fustin JM, Yamada H, Doi M, Okamura H (2012) Circadian clock signals in the adrenal cortex. Molecular and cellular endocrinology 349:30-37.

Ouyang Y, Andersson CR, Kondo T, Golden SS, Johnson CH (1998) Resonating circadian clocks enhance fitness in cyanobacteria. Proc Natl Acad Sci U S A 95:8660-8664.

Perreau-Lenz S, Kalsbeek A, Van Der Vliet J, Pevet P, Buijs RM (2005) In vivo evidence for a controlled offset of melatonin synthesis at dawn by the suprachiasmatic nucleus in the rat. Neuroscience 130:797-803.

Peterson GM, Watkins WB, Moore RY (1980) The suprachiasmatic hypothalamic nuclei of the rat. VI. Vasopressin neurons and circadian rhythmicity. Behav Neural Biol 29:236-245.

Porkka-Heiskanen T, Strecker RE, McCarley RW (2000) Brain site-specificity of extracellular adenosine concentration changes during sleep deprivation and spontaneous sleep: an in vivo microdialysis study. Neuroscience 99:507-517.

Qiu MH, Vetrivelan R, Fuller PM, Lu J (2010) Basal ganglia control of sleep-wake behavior and cortical activation. The European journal of neuroscience 31:499-507.

Raisman G, Brown-Grant K (1977) The 'suprachiasmatic syndrome': endocrine and behavioural abnormalities following lesions of the suprachiasmatic nuclei in the female rat. Proc R Soc Lond B Biol Sci 198:297-314.

Ralph MR, Foster RG, Davis FC, Menaker M (1990) Transplanted suprachiasmatic nucleus determines circadian period. Science 247:975-978.

Refinetti R, Menaker M (1992) The circadian rhythm of body temperature. Physiol Behav 51:613-637.

Romanovsky AA (2007) Thermoregulation: some concepts have changed. Functional architecture of the thermoregulatory system. Am J Physiol Regul Integr Comp Physiol 292:R37-46.

Rosbash M, Takahashi JS (2002) Circadian rhythms: the cancer connection. Nature 420:373-374.

Ruby NF, Ibuka N, Barnes BM, Zucker I (1989) Suprachiasmatic nuclei influence torpor and circadian temperature rhythms in hamsters. Am J Physiol 257:R210-215.

Rudic RD, McNamara P, Curtis AM, Boston RC, Panda S, Hogenesch JB, Fitzgerald GA (2004) BMAL1 and CLOCK, two essential components of the circadian clock, are involved in glucose homeostasis. PLoS Biol 2:e377.

Sadacca LA, Lamia KA, deLemos AS, Blum B, Weitz CJ (2011) An intrinsic circadian clock of the pancreas is required for normal insulin release and glucose homeostasis in mice. Diabetologia 54:120-124.

Saper CB (2013) The central circadian timing system. Current opinion in neurobiology.

Saper CB, Scammell TE, Lu J (2005a) Hypothalamic regulation of sleep and circadian rhythms. Nature 437:1257-1263.

Saper CB, Lu J, Chou TC, Gooley J (2005b) The hypothalamic integrator for circadian rhythms. Trends in neurosciences 28:152-157.

Satinoff E (1978) Neural organization and evolution of thermal regulation in mammals. Science 201:16-22.

Satinoff E, Prosser RA (1988) Suprachiasmatic nuclear lesions eliminate circadian rhythms of drinking and activity, but not of body temperature, in male rats. J Biol Rhythms 3:1-22.

Satinoff E, Liran J, Clapman R (1982) Aberrations of circadian body temperature rhythms in rats with medial preoptic lesions. Am J Physiol 242:R352-357.

Scammell TE, Gerashchenko DY, Mochizuki T, McCarthy MT, Estabrooke IV, Sears CA, Saper CB, Urade Y, Hayaishi O (2001) An adenosine A2a agonist increases sleep and induces Fos in ventrolateral preoptic neurons. Neuroscience 107:653-663.

Scheer FA, van Doornen LJ, Buijs RM (1999) Light and diurnal cycle affect human heart rate: possible role for the circadian pacemaker. J Biol Rhythms 14:202-212.

Scheer FA, Ter Horst GJ, van Der Vliet J, Buijs RM (2001) Physiological and anatomic evidence for regulation of the heart by suprachiasmatic nucleus in rats. Am J Physiol Heart Circ Physiol 280:H1391-1399.

Scheer FA, Pirovano C, Van Someren EJ, Buijs RM (2005) Environmental light and suprachiasmatic nucleus interact in the regulation of body temperature. Neuroscience 132:465-477.

Sherin JE, Shiromani PJ, McCarley RW, Saper CB (1996) Activation of ventrolateral preoptic neurons during sleep. Science (New York, NY) 271:216-219.

Silver R, LeSauter J, Tresco PA, Lehman MN (1996) A diffusible coupling signal from the transplanted suprachiasmatic nucleus controlling circadian locomotor rhythms. Nature 382:810-813.

Son GH, Chung S, Kim K (2011) The adrenal peripheral clock: glucocorticoid and the circadian timing system. Frontiers in neuroendocrinology 32:451-465.

Stephan FK, Nunez AA (1977) Elimination of circadian rhythms in drinking, activity, sleep, and temperature by isolation of the suprachiasmatic nuclei. Behav Biol 20:1-61.

Sujino M, Masumoto KH, Yamaguchi S, van der Horst GT, Okamura H, Inouye ST (2003) Suprachiasmatic nucleus grafts restore circadian behavioral rhythms of genetically arrhythmic mice. Curr Biol 13:664-668.

Swanson LW, Cowan WM (1975) The efferent connections of the suprachiasmatic nucleus of the hypothalamus. J Comp Neurol 160:1-12.

Szymusiak R, DeMory A, Kittrell EM, Satinoff E (1985) Diurnal changes in thermoregulatory behavior in rats with medial preoptic lesions. Am J Physiol 249:R219-227.

Teclemariam-Mesbah R, Kalsbeek A, Pevet P, Buijs RM (1997) Direct vasoactive intestinal polypeptide-containing projection from the suprachiasmatic nucleus to spinal projecting hypothalamic paraventricular neurons. Brain Res 748:71-76.

Toh KL, Jones CR, He Y, Eide EJ, Hinz WA, Virshup DM, Ptacek LJ, Fu YH (2001) An hPer2 phosphorylation site mutation in familial advanced sleep phase syndrome. Science 291:1040-1043.

Tokizawa K, Uchida Y, Nagashima K (2009) Thermoregulation in the cold changes depending on the time of day and feeding condition: physiological and anatomical analyses of involved circadian mechanisms. Neuroscience 164:1377-1386.

Turek FW, Joshu C, Kohsaka A, Lin E, Ivanova G, McDearmon E, Laposky A, Losee-Olson S, Easton A, Jensen DR, Eckel RH, Takahashi JS, Bass J (2005) Obesity and metabolic syndrome in circadian Clock mutant mice. Science 308:1043-1045.

Ueyama T, Krout KE, Nguyen XV, Karpitskiy V, Kollert A, Mettenleiter TC, Loewy AD (1999) Suprachiasmatic nucleus: a central autonomic clock. Nat Neurosci 2:1051-1053.

Van Cauter E, Holmback U, Knutson K, Leproult R, Miller A, Nedeltcheva A, Pannain S, Penev P, Tasali E, Spiegel K (2007) Impact of sleep and sleep loss on neuroendocrine and metabolic function. Horm Res 67 Suppl 1:2-9.

Warren WS, Champney TH, Cassone VM (1994) The suprachiasmatic nucleus controls the circadian rhythm of heart rate via the sympathetic nervous system. Physiol Behav 55:1091-1099.

Watts AG, Swanson LW (1987) Efferent projections of the suprachiasmatic nucleus: II. Studies using retrograde transport of fluorescent dyes and simultaneous peptide immunohistochemistry in the rat. The Journal of comparative neurology 258:230-252.

Watts AG, Swanson LW, Sanchez-Watts G (1987) Efferent projections of the suprachiasmatic nucleus: I. Studies using anterograde transport of Phaseolus vulgaris leucoagglutinin in the rat. The Journal of comparative neurology 258:204-229.

Yoo SH, Yamazaki S, Lowrey PL, Shimomura K, Ko CH, Buhr ED, Siepka SM, Hong HK, Oh WJ, Yoo OJ, Menaker M, Takahashi JS (2004) PERIOD2::LUCIFERASE real-time reporting of circadian

dynamics reveals persistent circadian oscillations in mouse peripheral tissues. Proc Natl Acad Sci U S A 101:5339-5346.

Yoshida K, Konishi M, Nagashima K, Saper CB, Kanosue K (2005) Fos activation in hypothalamic neurons during cold or warm exposure: projections to periaqueductal gray matter. Neuroscience 133:1039-1046.

Yoshida K, Li X, Cano G, Lazarus M, Saper CB (2009) Parallel preoptic pathways for thermoregulation. The Journal of neuroscience : the official journal of the Society for Neuroscience 29:11954-11964.

Zheng H, Patel M, Hryniewicz K, Katz SD (2006) Association of extended work shifts, vascular function, and inflammatory markers in internal medicine residents: a randomized crossover trial. Jama 296:1049-1050.

Chapter 2: Efferent projections of the subparaventricular zone: does the circadian timing system have a four-channel output?

Abstract

The subparaventricular zone of the hypothalamus (SPZ) is the main efferent target of neural projections from the suprachiasmatic nucleus (SCN) and an important relay for the circadian timing system. Although the SPZ is fairly homogeneous cytoarchitecturally and neurochemically, it has been divided into distinct functional and connectional subdivisions. The dorsal subdivision of the SPZ (dSPZ) plays an important role in relaying signals from the SCN controlling body temperature rhythms while the ventral subdivision (vSPZ) is critical for rhythms of sleep and locomotor activity (Lu et al., 2001). On the other hand, the medial part of the SPZ receives input mainly from the SCN shell, whereas the lateral SPZ receives input from the SCN core and the retinohypothalamic tract (Leak and Moore, 2001). We have therefore investigated whether there are corresponding differences in efferent outputs from these four quadrants of the SPZ (dorsolateral, ventrolateral, dorsomedial and ventromedial) by a combination of anterograde and retrograde tracing. We found that while all four subdivisions of the SPZ share a similar backbone of projections to the septal region, thalamus, hypothalamus, and brainstem, each segment of the SPZ has a specific set of targets where its projections dominate. Furthermore, we observe intra-SPZ projections of varying densities between the four subdivisions. Taken together, this pattern of organization suggests that the circadian timing system may have several parallel neural outflow pathways that provide a road map for understanding how they subserve different functions.

Introduction

In mammals, daily rhythms in physiology and behavior are driven by rhythmic outputs from the pacemaker in the suprachiasmatic nucleus (SCN). The adjacent subparaventricular zone (SPZ), which receives the majority of neural efferent fibers from the SCN (Watts et al., 1987; Leak and Moore, 2001), is thought to be a critical relay for driving rhythms. Lesions of the SPZ (Lu et al., 2001; Schwartz et al., 2009) or knife cuts through it (Inouye and Kawamura, 1979) can dramatically attenuate circadian rhythms of sleep, locomotor activity, body temperature, and multiunit activity of neurons in several other brain regions. Studies showing that multiunit activity in the SPZ has a consistent phase relationship to that in the SCN and to locomotor activity rhythms (Inouye and Kawamura, 1979; Kubota et al., 1981; Sato and Kawamura, 1984; Nakamura et al., 2008) further support the notion that it is involved in SCN outflow circuitry. Differences in the timing of rhythms of immediate early gene expression in the SPZ of rodents active at different times of day suggest that the SPZ may also modify the SCN signal, and perhaps play a role in establishing the diurnality or nocturnality of an animal (Smale et al., 2001; Schwartz et al., 2004; Todd et al., 2012).

Though the SPZ is fairly homogeneous morphologically, it may have different functional subdivisions. Cell-specific lesions in the more dorsal and caudal half of the SPZ (dSPZ) dramatically reduce the amplitude of body temperature rhythms, but not locomotor activity and sleep rhythms, while lesions in the more ventral and rostral portion (vSPZ) significantly blunt rhythms in activity and sleep/wakefulness, largely sparing temperature rhythms (Lu et al., 2001). On the other hand, anatomical data suggests that the SPZ may be organized into medial vs. lateral subdivisions. Outputs of the SCN core (also called the ventrolateral or retinorecipient region of the SCN), which is chiefly responsible for circadian entrainment to light, preferentially innervate the lateral portion of the SPZ, while the SCN shell (or dorsomedial SCN), thought to be more involved in pacemaking and output, projects more to the medial portion of the SPZ (Leak et al., 1999; Leak and Moore, 2001; Moore et al., 2002; Aton and Herzog, 2005). The lateral SPZ also receives far more robust direct retinal input, (Johnson et al., 1988;

Levine et al., 1991; Costa et al., 1999; Gooley et al., 2003; Canteras et al., 2011), suggesting it may be more closely tied to functions that are sensitive to light levels.

The above observations suggest that the SPZ may have four distinct subregions (dorsal vs. ventral, medial vs. lateral), which we hypothesize should underlie regional differences in function. Although previous studies have examined SPZ efferents using anterograde tracing in rats (Watts et al., 1987; Deurveilher et al., 2002; Chou et al., 2003; Deurveilher and Semba, 2003, 2005; Canteras et al., 2011) and other rodents (Morin et al., 1994; Kriegsfeld et al., 2004; Schwartz et al., 2011), none of these have explored differences in projections from these different SPZ subdivisions. We have used a combination of anterograde and retrograde tracing to identify distinct projections from each of the SPZ subregions that provide a map for exploring their functional specificity.

Materials and Methods

Animals and surgery

All protocols used in this study were approved by the Harvard University and Beth Israel Deaconess Medical Center Animal Care and Use Committees and conform to the regulations detailed in the National Institutes of Health *Guide for the Care and Use of Laboratory Animals*. Adult male Sprague-Dawley rats weighing 350-400g were obtained from Harlan, and housed individually in a 12:12hour light dark cycle with *ad libitum* access to water and food (Purina rodent chow). Surgeries to inject tracer were performed as described previously (Chamberlin et al., 1998). Briefly, rats were anesthetized with an intraperitoneal injection of either chloral hydrate (350 mg/kg) or ketamine-xylazine (80mg/kg ketamine, 8mg/kg xylazine) and placed in a stereotaxic apparatus (David Kopf Instruments, Tujunga, CA). Under aseptic conditions the brain was exposed and an injection of tracer delivered through a fine (20 μm tip diameter) glass micropipette by using a compressed air puff system. The skin was then closed with wound clips and the animals given subcutaneous injections of the analgesic meloxicam (1 mg, daily for two days) or flunixin (1 mg/kg, every 12 hours for two days).

Tracers and coordinates

Retrograde tracing was accomplished using 3-10nl injections of Cholera toxin subunit B (CTb) (10 µg/µl saline, List Biological, Campbell, CA), whereas anterograde tracing was done using either 3-15 nl injections of biotinylated dextran amine (BDA) (125 µg/µl saline, Molecular Probes, Eugene, OR) or 7-20nl of a solution containing adeno-associated viral vectors (either serotype 2 or 8) bearing a gene for green fluorescent protein (AAV-GFP), prepared by the Harvard Gene Therapy Initiative Virus Production Core as described previously (Chamberlin et al., 1998). This vector selectively transduces neurons near the injection site, which then produce GFP that fills the entire cytoplasmic compartment (including fibers and terminals), without causing inflammatory astrocytic or microglial responses in the surrounding tissue, and with minimal retrograde transport. Animals injected with CTb or BDA were perfused one to two weeks following surgery, but we allowed five to nine weeks between injection of AAV-GFP and perfusion, to ensure adequate filling of the terminals of transduced neurons. All injection coordinates were based on the atlas of Paxinos and Watson (Paxinos and Watson, 2005) (1986) and were as follows: VMH (AP -2.2; DV -8.8; RL +0.3), DMH (AP -3.5; DV -8.5; RL +0.5), VLPO (AP +0.4; DV -8.4; RL +0.9), SPZ/SCN (injections placed at 16° angle AP -1.75; DV -8.6; RL +2.6). We also examined brain tissue from rats which received intraocular injections of 4µl AAV-GFP in a previous study (Gooley et al., 2003).

Tissue Preparation

One to nine weeks following the injection, rats were deeply anesthetized with chloral hydrate (500 mg/kg) and transcardially perfused with 0.9% saline followed by 10% neutral buffered formalin (Sigma). Brains were removed and postfixed for approximately 3 hours in formalin then allowed to equilibrate for at least 12 hours in a 20% sucrose solution in phosphate buffered saline with 0.01% sodium azide. Brains were subsequently sectioned at 40 µm on a freezing microtome into five series.

Immunohistochemistry

Immunohistochemistry was performed on floating sections following a protocol described in previous publications (Bruinstroop et al., 2011). Sections were rinsed at least three times for 5-10 minutes in 0.1M phosphate buffered saline (PBS), pH 7.4, for 1 hour, then were incubated in 0.3%

hydrogen peroxide to block endogenous peroxidase activity. Following at least three more rinses in PBS, sections were incubated for at least 10 hours in a solution containing the appropriate primary antibody (see below) in PBS containing 0.3% Triton X-100 and 0.01% sodium azide. Sections were then rinsed at least three more times in PBS before a one-hour incubation in a corresponding secondary antibody (see below for specific information), rinsed three more times in PBS, and then incubated for 60-90 minutes in an avidin-biotin complex solution (Elite ABC, Vector Laboratories). After three more PBS rinses, the tissue was moved to a solution containing 1% 3,3'-diaminobenzidine (DAB) and reacted with 0.01% hydrogen peroxide to visualize the sites containing antigen in the tissue. Once the desired staining intensity was reached, this reaction was quenched with several rinses of the tissue in a PBS solution containing 0.01% sodium azide. Sections were then mounted onto gelatin coated glass slides and allowed to dry overnight at room temperature. This was followed in some cases by silver-gold enhancement and/or counterstaining with thionin. Silver-gold enhancement consisted of a 30 - 45 minute incubation of desalinated slides in 1% silver nitrate solution at 56 °C, followed by three rinses with water, a 10-20 minute incubation in 0.1% gold chloride, three more rinses and a brief treatment with 5% sodium thiosulfate solution until the tissue reaches the desired background level. All slides were rinsed in distilled water before they were dehydrated in graded alcohols then cleared in xylene for at least 2 hours and cover-slipped with Permaslip medium (Alban Scientific, St. Louis, MO). Counterstained sections were incubated briefly in thionin solution and differentiated in acid alcohol prior to dehydration.

Neurons labeled with the AAV-GFP vector were visualized with a primary antibody against GFP raised in rabbit raised against Aquaphora GFP protein (Molecular probes/Invitrogen ca# A6455 Lot# 771568), used at a concentration of 1:20,000 followed by biotinylated donkey anti-rabbit secondary (Jackson Immunoresearch Laboratories) used at a 1:1,000 dilution. This GFP antibody does not stain anything in tissue from uninjected animals. Tissue from cases injected with BDA underwent the same steps in the avidin-biotin staining protocol, except did not require primary or secondary antibodies. For retrograde tracing cases, immunohistochemistry was done with a primary antibody against CTb raised in goat against CTb protein, used at a 1:25,000 dilution, followed by a biotinylated donkey anti-goat secondary (Jackson Immunoresearch Laboratories) used at a 1:1,000 dilution. This antibody does not stain anything above background level in tissue from uninjected animals.

For AVP/VIP double fluorescent immunolabeling, brains from a transgenic line of AVP-GFP reporter rats (Ueta et al., 2008), a generous gift from the laboratory of Dr. Charles Allen, were stained for VIP, and GFP signal in AVPergic cells was amplified immunohistochemically. Tissue was incubated for two nights with a polyclonal primary antibody raised in rabbit against synthetic VIP coupled to bovine thyroglobulin with a carbodiimide linker (ImmunoStar, cat# 20077, lot: 722001) at a concentration of 1:1,000 and a monoclonal primary antibody raised in mouse against Aquaphora GFP protein (Molecular probes/Invitrogen ca# A11120 Lot# 71C1-1), used at a concentration of 1:500. VIP antibody specificity was validated by preadsorption with VIP (which abolished staining) vs. related peptides (which did not), as described in the manufacturer's technical information. Patterns of VIP labeling in the SCN and proximal areas also matched that reported in previous publications (Hattar et al., 2006; Belenky et al., 2008). The GFP antibody did not stain anything in wildtype rat brains. After incubation with primary antibodies, tissue was taken through six 3-minute long PBS rinses, prior to incubation with a pre-adsorbed biotinylated donkey anti-rabbit secondary (Jackson Immunoresearch Laboratories). This secondary antibody, at a 1:100 concentration, was pre-adsorbed for 1 hour with a solution of rat brain powder to decrease non-specific background labeling. The solution was then centrifuged, and only the supernatant was incubated with tissue for immunolabeling. Following this 1-hour incubation, tissue was rinsed five times for three minutes, then incubated for 30 minutes in a solution containing an Alexa 488-tagged donkey anti-mouse secondary antibody (Invitrogen), used at 1:500, and biotinylated Cy-3 used at 1:500. Rinsed tissue was mounted onto slides and allowed to dry in a darkened chamber before it was cover-slipped with Dako fluorescent mounting medium (Dako, Carpinteria, CA).

Illustration and photography

Slides were examined and brightfield/darkfield photomicrographs were acquired with a Zeiss Axioplan 2 microscope with a 1.5 megapixel color Evolution MP camera (MediaCybernetics, Bethesda, MD) using Axiovision software. Dual labeling immunofluorescence images were acquired using a Zeiss LSM 510 confocal microscope and processed using ImageJ software. All images were then processed with Adobe Photoshop software to optimize the brightness/contrast. Red fluorescence was shifted to magenta in some images to make the difference from green visible to viewers with red-green color-

blindness (Fig. 2.1A-C) and in images of DAB-stained injection sites, red, orange, and yellow hues were partially desaturated to distinguish between the injection site and fibers radiating at high density from it (Fig. 2.1D-I, 2.4). Illustrations of injection sites and anterogradely labeled fibers were made using a Leitz Wetzlar camera lucida attachment on a Letiz LaborluxS microscope (Germany). These drawings were digitized using a Wacom Intuos PTK-1240 tablet and Adobe Illustrator Software.

Results

SCN and retinal afferents to the SPZ define its medial and lateral subdivisions

The SPZ is defined by the dense terminal area occupied by axons from the SCN rather than by any characteristic cytological pattern. In Nissl sections it is not possible to divide the SPZ into regions, or even to differentiate it from the rest of the periventricular nucleus or anterior hypothalamic area. For these reasons we have used the inputs to the SPZ from the retina and the SCN to clarify its medial vs. lateral organization and to designate the regions we will refer to as the dmSPZ, dlSPZ, vmSPZ and vlSPZ throughout subsequent analysis.

To visualize SPZ inputs from both major SCN subregions, we took tissue from rats in which cells containing arginine vasopressin (AVP), a marker for many neurons in the SCN shell, natively express green fluorescent protein and labeled it with an antiserum against vasoactive intestinal polypeptide (VIP) a marker for many neurons in the SCN core (Leak and Moore, 2001, Moore et al. 2002) (see Fig. 2.1A-C). AVP and VIP positive fibers course dorsally and caudally from the SCN, with the densest region of immunoreactive fibers and terminals defining the SPZ. VIP-immunoreactive fibers and terminals in the SPZ are densest in the more lateral aspects of the SPZ, and rarely are found in the 100 μm or so along the edge of the third ventricle. AVP-immunoreactive fibers, on the other hand, course through the more medial aspect of the SPZ, closer to the wall of the third ventricle, but are rarely found in the most lateral 150 μm or so of the territory marked by the VIP axons. The two fiber groups overlap in the middle 150 μm or so of the SPZ. The source of these VIP fibers is unambiguous, as there are no other major VIP-expressing cell groups or fiber pathways in the hypothalamus. However, AVP-immunoreactive cell bodies in the paraventricular and periventricular hypothalamic nuclei make the origin of the AVP-

Figure 2.1 A series of photomicrographs to illustrate topographic specificity of afferent inputs to the subparaventricular zone from (A, B, C) neurons (in the SCN) expressing arginine vasopressin (green) vs. neurons labeled for vasoactive intestinal polypeptide (magenta), (D, E, F) retinal ganglion cells transduced with AAV-GFP (with immunohistochemical enhancement of GFP signal), and (G, H, I) SCN shell neurons transduced with AAV-GFP (with immunohistochemical enhancement of GFP signal), photographed at (A, D, G) the level of the SCN, (B, E, H) the level of the rostral/ventral SPZ, and (C, F, I) the level of the caudal/dorsal SPZ.

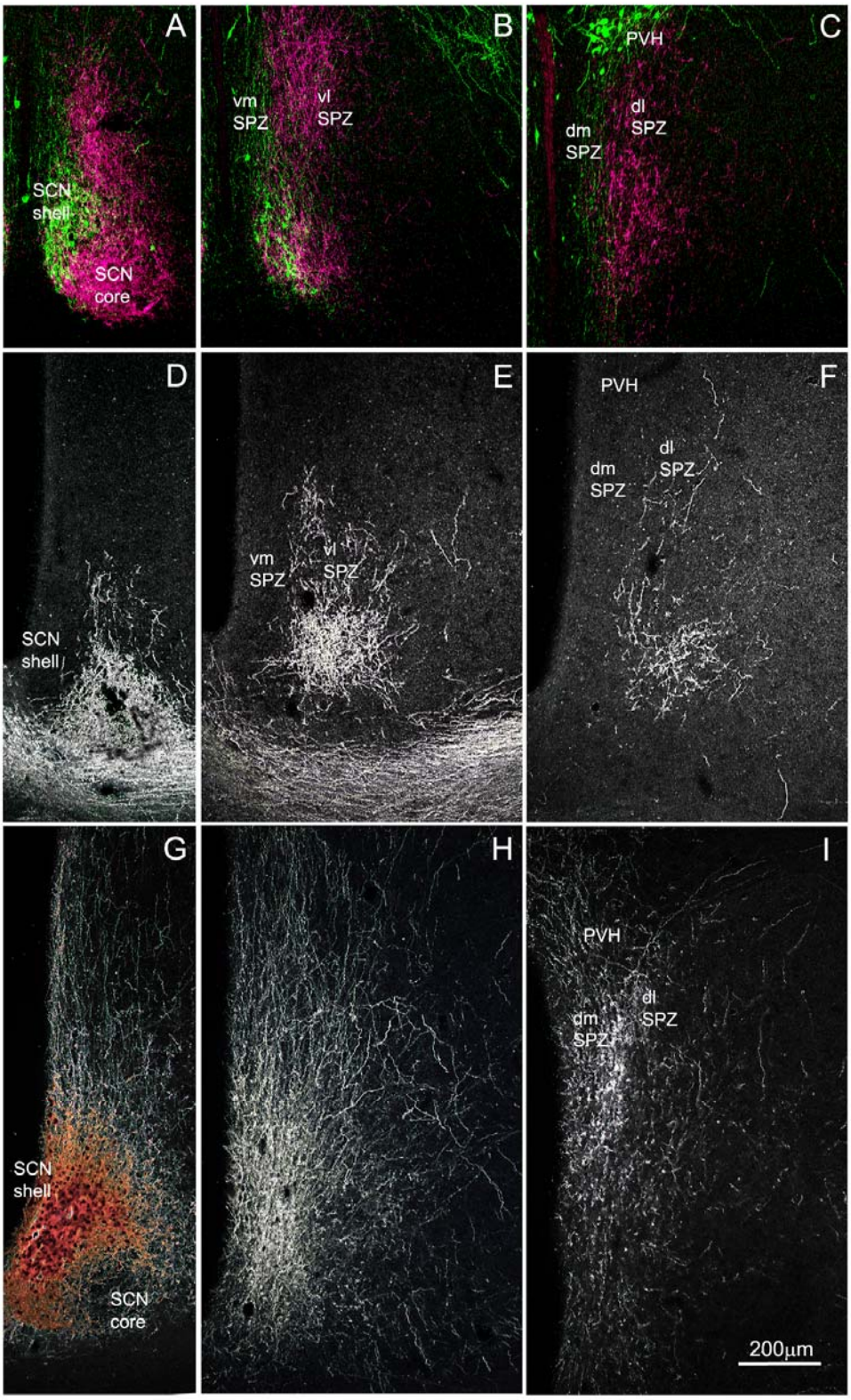

Figure 2.1 (continued)

immunoreactive fibers in the SPZ less clear. To address this, we also placed an injection of AAV-GFP selectively into the SCN shell (Fig. 2.1G-I). Fibers and terminals originating in the SCN shell were present medially along the third ventricle extending out laterally to cover all of the medial SPZ and a fraction of the lateral, avoiding approximately the most lateral one-fourth of the SPZ. More axonal ramification was seen laterally at intermediate levels of the SPZ (Fig. 2.1H) than at the most rostral/ventral or caudal/dorsal. In a case in which AAV-GFP had been injected into the eye (as described in (Gooley et al., 2003)), the labeled retinal axons mainly occupied the lateral part of the ventral SPZ (see Fig. 2.1 D-F). Based on the above findings, we therefore identify the SPZ in rats as a zone about 400μm wide extending dorsally and caudally from the SCN along the third ventricle, in which the medial half is dominated by SCN shell input and the lateral half by SCN core and retinal input. Furthermore, there is an exclusive area, about 100 μm wide on the medial, and 150 μm wide on the lateral side of the SPZ that receives input from only the medial or lateral pathway, respectively, with a zone of overlap of about 150 μm in the center of the SPZ. We further divided the SPZ, based upon earlier physiological findings and the extent of retinal input, into a ventral zone extending about 600μm dorsally and caudally from the border of the SCN and a dorsal zone, extending about 600μm ventrally and rostrally from the border of the paraventricular nucleus.

Injections of anterograde tracer into the subparaventricular zone

Twenty-four cases had injections that included at least some part of the SPZ. We selected ten AAV-GFP injections and two BDA injections placed most focally within the SPZ for analysis of SPZ subregion targets (Fig. 2.2).

In case 2569 (Fig. 2.2A), the injection was placed in the vlSPZ. This injection filled most of the vlSPZ and involved little else, although a few neurons along the dorsal margin of the SCN were included. In case NVA84 (Fig. 2.2A), the injection was placed into the vmSPZ, extending to laterally to include a part of the vlSPZ and just a few cells along the dorsal surface of the SCN shell, but not the most dorsal aspect of the vmSPZ. In cases NVA36 and NVA37 (Fig. 2.2A), the injections predominantly involved vmSPZ neurons, but extended considerably further into adjacent areas than NVA84. However, they did confirm the projection pattern from the vmSPZ as identified in NVA84.

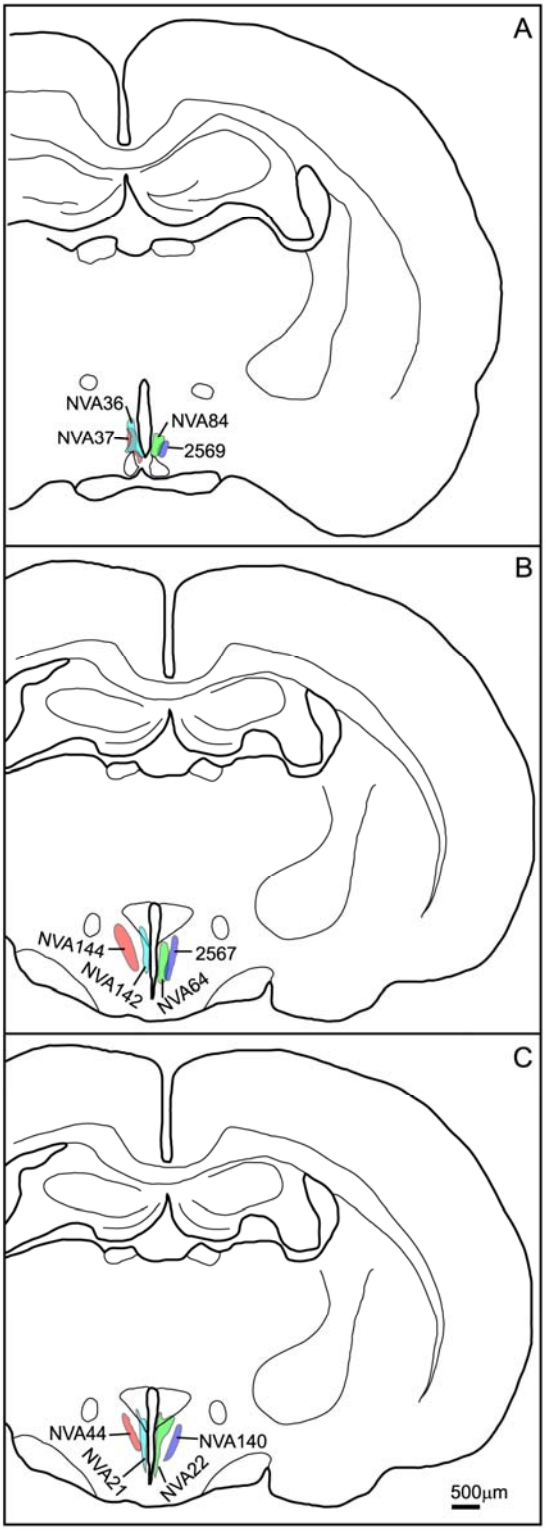

Figure 2.2 Camera lucida plots illustrating placement of SPZ injection sites in cases used for comparative analysis across the four SPZ subdivisions at (A) the level of the rostral/ventral SPZ and (B, C) the level of the caudal/dorsal SPZ

In cases 2567 (Fig.2.2B) and NVA140 (Fig. 2.2C), the injections were confined to the dlSPZ, while the injection sites in cases NVA44 (Fig. 2.2C) and NVA144 (Fig. 2.2B) include both dlSPZ as well as some adjacent cells in parts of the anterior hypothalamic area that receive few direct SCN efferents. In case NVA64 (Fig. 2.2B), the injection was placed selectively in the dmSPZ, whereas in cases NVA22, NVA21 (Fig. 2.2C) and NVA142 (Fig. 2.2C) the injections included dmSPZ neurons as well as a few neurons in the PVH. We found no major differences in projections labeled by comparable injections using AAV-GFP (e.g., NVA140) vs. BDA (Case 2567) except that AAV-GFP often provided better filling of axons innervating the most distal targets.

Efferent projections from the subparaventricular zone

We found that although the backbone of major output pathways was similar after injections in each quadrant of the SPZ, there were substantial differences in the patterns of terminal areas that were innervated. Most of these projections were similar to earlier descriptions (Watts and Swanson, 1987; Morin et al., 1994; Kriegsfeld et al., 2004; Deurveilher and Semba, 2005), but a few of the longer projections (e.g., to the amygdala and brainstem) had not been previously reported. To put these into perspective and to provide a background for considering the specific origins of particular projections, we first provide an overall description of the backbone pathways from which the terminal fields emerge with the aid of case NVA36. Although the injection in this case was centered in the vmSPZ, it also included parts of the adjacent vlSPZ and dmSPZ. More importantly, all of the common major pathways that were labeled in the other experiments were seen in this example (Fig. 2.3). We will then focus on the differences between the most densely labeled terminal areas after injections in specific quadrants of the SPZ.

It is convenient to describe the projections labeled in case NVA36 based on the four major directions of outflow, rostral, dorsal, caudal and lateral. Most projections were predominantly on the ipsilateral side of the brain, with a much smaller number of axons forming a similar pattern on the other side of the brain, although a few sites identified below had more extensive contralateral projections. These appeared to cross the midline mainly as part of the ventral supraoptic commissure.

Figure 2.3 A series of camera lucida drawings illustrating the pattern of axonal labeling in case NV36. Note presence of fibers in the dorsal raphe, lateral parabrachial nucleus, pre-coeruleus region, locus coeruleus and Barrington's nucleus

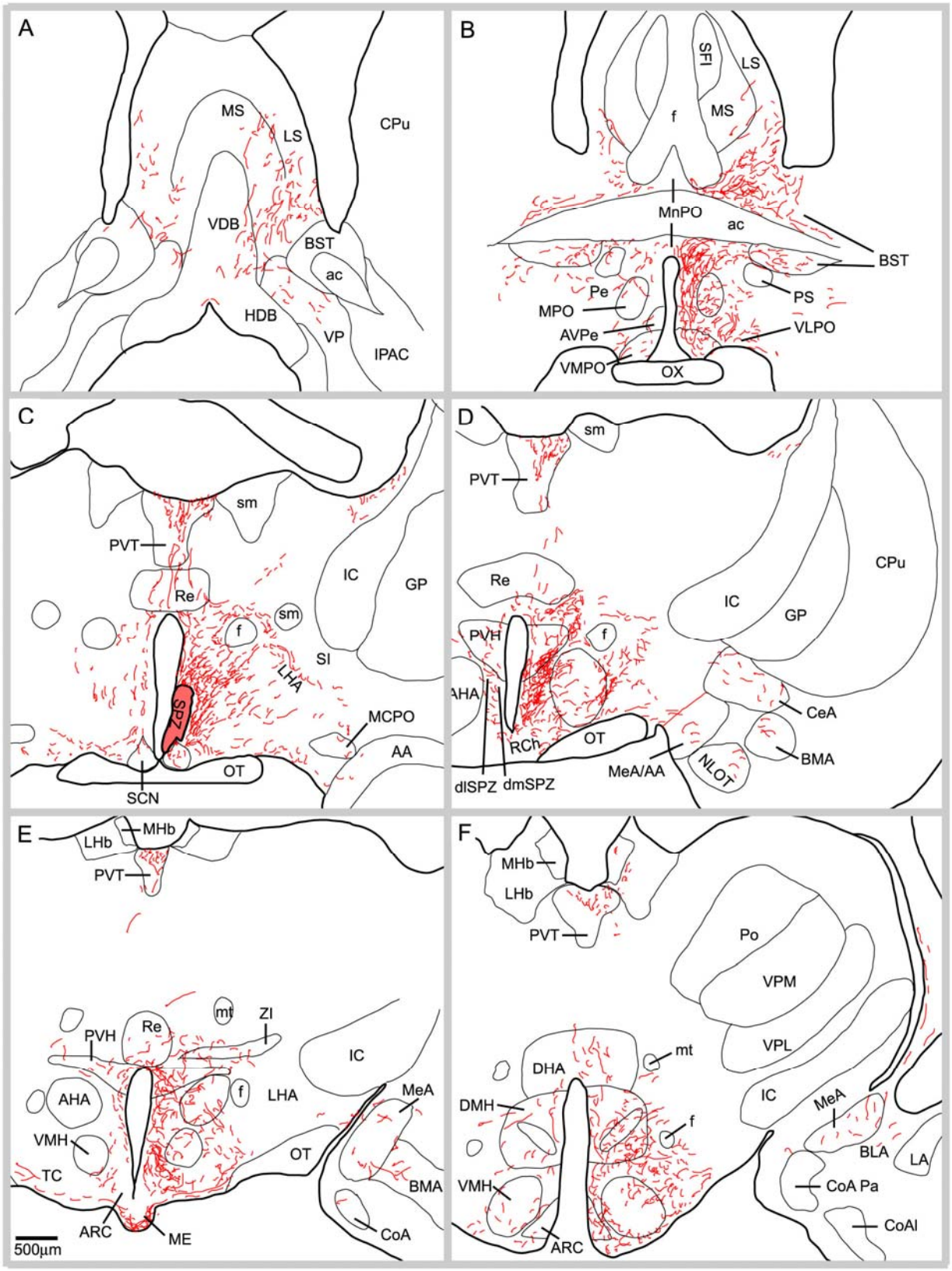

Figure 2.3 (continued)

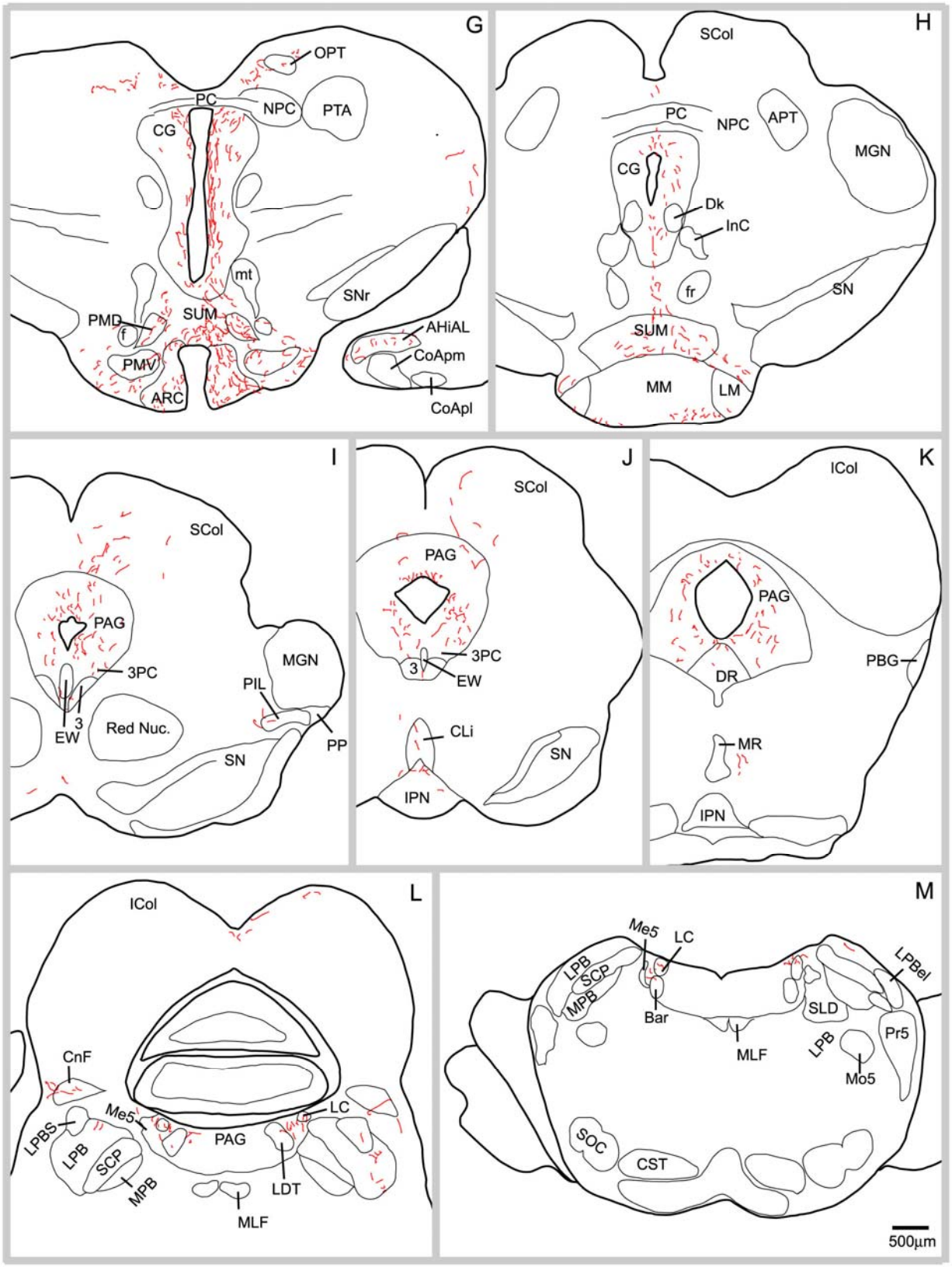

Figure 2.3 (continued)

Rostral projections

This group of axons richly innervated the rostral periventricular nucleus, medial and median pre-optic nuclei and to a lesser extent, the anterior hypothalamic area. Fibers continued rostrally to provide a dense terminal field in the anteroventral periventricular nucleus and the ventromedial preoptic nucleus. Slightly less dense innervation was present in the adjacent ventrolateral preoptic nucleus and relatively few fibers are seen further laterally in the nucleus of the horizontal limb of the diagonal band, the ventral pallidum, and the substantia innominata. A considerably heavier group of fibers coursed anterodorsally, many of them hugging the ventral boundary of the anterior commissure, with some terminating in the parastrial nucleus. Many fibers from this trajectory continued anterodorsally to terminate in the bed nucleus of the stria terminalis, the lateral septal nucleus (chiefly in the ventral subdivision of this nucleus), and a few in the medial septal nucleus.

A clearly distinct subpopulation of fibers in the rostral pathway diverged from the rest at approximately the level of the optic chiasm and coursed dorsolaterally in a diagonal path to merge with the stria terminalis. These fibers terminated in the medial nucleus, and to a lesser extent the central nucleus of the amygdala.

Dorsal projections

This outflow pathway from the SPZ was perhaps the most robust. Fibers coursed from the injection site dorsally along the third ventricle to the foramen of Monro, where they turned caudally to innervate the paraventricular nucleus of the thalamus (PVT). At more caudal SPZ levels, smaller numbers of axons penetrated the paraventricular nucleus of the hypothalamus and thalamic reuniens nucleus (which they sparsely innervated), to reach the PVT. Some axons left the PVT laterally to form boutons in the paratenial nucleus of the thalamus or in the lateral habenular nucleus. The PVT was one of the SPZ's most densely innervated targets, receiving SPZ projections along its full rostrocaudal extent, with the densest projection targeting the rostral aspect of this nucleus on the side ipsilateral to the injection site.

Caudal projections

The pathway from the SPZ to more posterior hypothalamic structures and ventromedial midbrain targets was also one of its most robust outputs, and as will be discussed later, axons from different SPZ subregions innervated specific targets. The axons in this pathway coursed caudally along the wall of the third ventricle, providing variable amounts of innervation to the ventromedial (VMH) and dorsomedial (DMH) hypothalamic nuclei. In case NVA36, there was an exceptionally dense cluster of fibers and boutons around the capsule and perimeter of the VMH, and moderate innervation of the central division of the VMH, but comparatively sparser innervation to the dorsomedial or ventrolateral divisions of the VMH. Many fibers coursed along the medial and ventromedial edge of the VMH, filling the internuclear space between it and the DMH, periventricular nucleus, and arcuate nucleus, and innervating these adjacent structures as well. In case NVA36 the DMH received moderate innervation throughout its rostrocaudal extent, which was most dense in the medial portion of this nucleus and tapered toward its lateral edge. Input to the arcuate nucleus was largely confined to its lateral division and was denser at caudal levels of the nucleus. Case NVA36 showed a very rich input to the median eminence, with a dense terminal field in both the internal and external laminae ipsilaterally and a fairly dense plexus of boutons and fibers in only the external lamina contralaterally. Fibers continued caudally to the premamillary, supramammilary, and medial mamillary nuclei with the latter two showing greater bilateral symmetry than other targets. Fibers also extended ventrally to line the ventral edge of the mamillary body itself. At the premammillarly level, a subset of caudal pathway axons projected posterolaterally with a few fibers curving ventrally to terminate in the ventral tuberomamillary nucleus and others coursing laterally through (or just dorsal to) the substantia nigra pars compacta, likely giving rise to the terminal field seen in the thalamic intergeniculate leaflet.

The remainder of the fibers in the caudal pathway flowed dorsomedially through the posterior hypothalamic area into the central gray matter and Edinger-Westphal nucleus. Occasional fibers branched outward from the periaqueductal gray matter to end on nearby caudal targets, such as the dorsal and caudal linear raphe nuclei, and the pretectal area. A small number of fibers traversed the tectum, often passing along the midline between the superior and inferior colliculi. As the cerebral aqueduct opened into the fourth ventricle, the fibers in the periaqueductal gray matter provided modest

innervation of the lateral parabrachial nucleus (bilaterally), the pre-coeruleus area (ipsilaterally) and a few fibers reached the ipsilateral locus coeruleus and Barrington's nucleus as well.

Lateral projections

This outflow from the SPZ was more sparse than the rostral, caudal, or dorsal outflow. Axons exiting the SPZ laterally innervated neurons in the anterior hypothalamic area and lateral hypothalamic area. This projection was bilateral although much more dense ipsilaterally. While innervation patterns in the lateral hypothalamus were fairly similar across injection cases, there was considerably more variability in the anterior hypothalamic area, particularly the subregion flanking the SPZ, which varied depending upon placement of the injection in the SPZ. Other laterally-bound fibers first descended ventrally and then coursed laterally along the optic tract in the supraoptic decussation, forming terminals along the way in the retrochiasmatic area and the supraoptic nucleus. Fibers were present along the optic tract at all levels bilaterally, and a subset of these may give rise to the small terminal field seen in the intergeniculate leaflet.

Subparaventricular zone subregions differ most in their intrahypothalamic efferent projections

Whereas the four SPZ subdivisions share many of the features described for case NVA36, each subdivision has a distinct pattern of terminal innervation, particularly in the preoptic and caudal hypothalamus. These differences are discussed at length below and highlighted in Fig. 2. 4. Table 2.1 contains a comprehensive, semiquantitative listing of terminal strength for efferent outputs of all four subparaventricular zone subregions.

Ventromedial SPZ

Of all four subregions, the vmSPZ showed the strongest outputs in the rostral and dorsal pathways. Ventral preoptic targets near the midline, including the organum vasculosum of the lamina terminalis, anteroventral periventricular nucleus, median preoptic nucleus, and ventromedial and ventrolateral preoptic nuclei were more richly innervated in case NVA84 than any other injection case confined to only one SPZ quadrant (Fig. 2.4E, Table 2.1). Also, while other subregions sent at least as

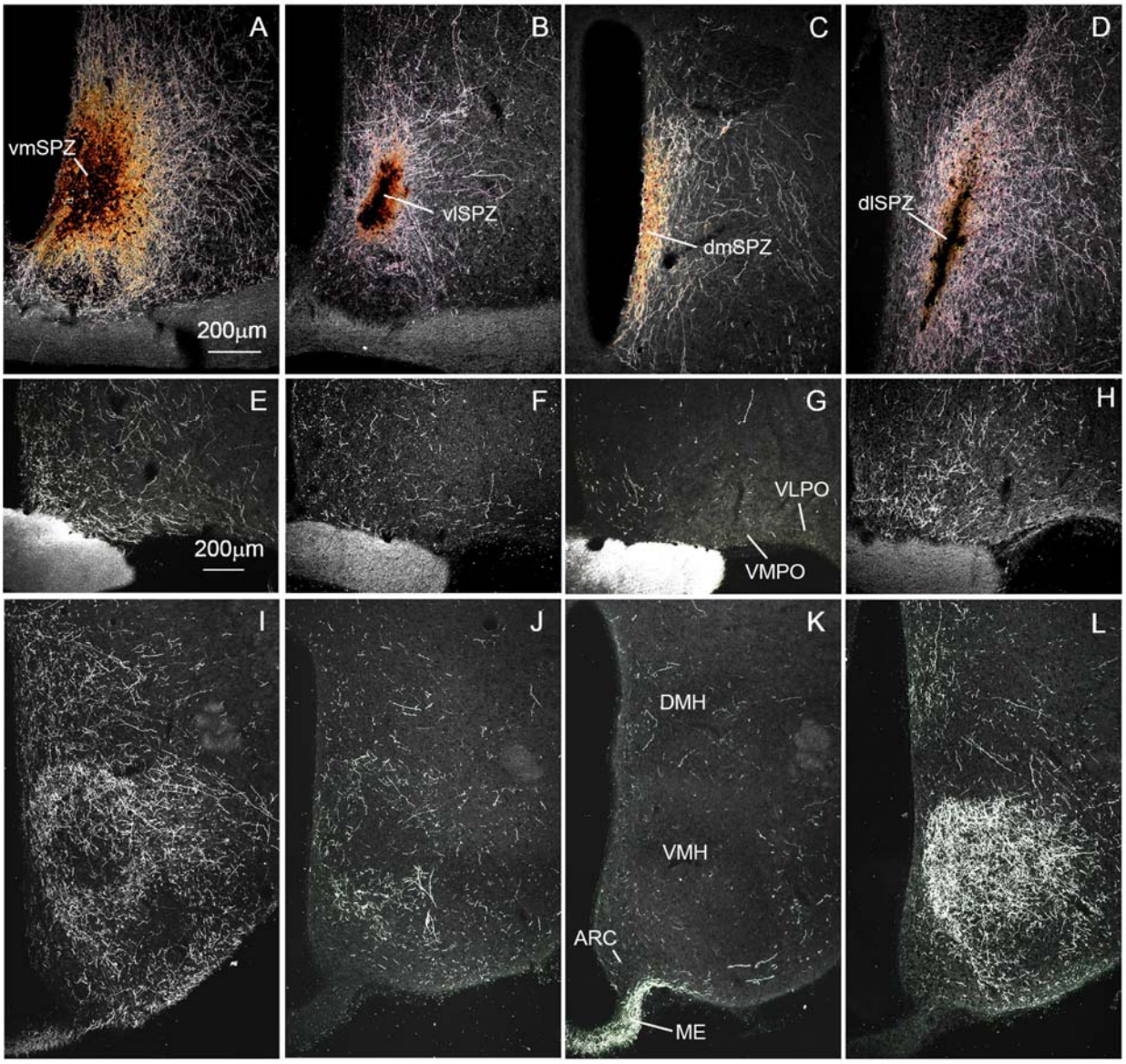

Figure 2.4 Darkfield photomicrographs showing (A-D) injection sites (scalebar in A, 200μm) and (E-L) anterogradely labeled fibers and terminals (scalebar in E, 200μm) in cases of anterograde tracing from (A, E, I) vmSPZ, (B, F, J) vlSPZ, (C, G, K) dmSPZ, and (D, H, L) dlSPZ.

Table 2.1 Semiquantitative analysis of density of efferent projections from the four SPZ subregions

Table 2.1: Projection density from subparaventricular zone subregions

Region	dlSPZ	vlSPZ	dmSPZ	vmSPZ
Basal Forebrain				
Lateral septum (predominantly ventral part)	+++	++	+	+++
Bed nucleus of the stria terminalis	+++(+)	++(+)	+(+)	+++
Parastrial nucleus	+++	++	+	+++
Diagonal band of Broca	++	++	(+)	+
Organum vasculosum of the lamina terminalis	+	0	(+)	+++
Substantia innominata	++	0	0	0
Hypothalamus				
Median pre-optic nucleus (MnPO)	(+)	(+)	(+)	+++
Medial pre-optic nucleus (MPO)	++	+	(+)	++
Ventromedial pre-optic nucleus (VMPO)	++(+)	+	+	++++
Ventrolateral pre-optic area (VLPO)	+(+)	+	+	++
Suprachiasmatic nucleus (SCN)	+	++(+)	+(+)	+++(+)
Ventromedial subparaventricular zone (vmSPZ)	++	++(+)	+++	n/a
Ventrolateral subparaventricular zone (vlSPZ)	++++	n/a	+	++++
Dorsolateral subparaventricular zone (dlSPZ)	n/a	+++	+(+)	+++
Dorsomedial subparaventricular zone (dmSPZ)	+	+	n/a	+++
Anteroventral periventricular nucleus (AVPe)	+	+	(+)	+++
Anterior hypothalamic area (AHA)	++++	+++	+ (+)	+++
Retrochiasmatic area (RCh)	++(+)	++(+)	+++	++(+)
Supraoptic nucleus (SON)	(+)	+	(+)	+
Supraoptic decussation (Sox)	+++	+(+)	++(+)	+++
Supraoptic nucleus, retrochiasmatic part (SOR)	+++	++	++(+)	+++
Paraventricular nucleus of the hypothalamus (PVH) - anterior parvicellular	+++	++	++(+)	+++(+)
Paraventricular nucleus of the hypothalamus (PVH) - middle	+	+	++	++(+)
Paraventricular nucleus of the hypothalamus (PVH) - lateral wing	++	++	++(+)	+++
Dorsomedial nucleus of the hypothalamus (DMH) - anterior	+++(+)	+++	+(+)	++++
Dorsomedial nucleus of the hypothalamus (DMH) - compact and surrounding	++(+)	++	+(+)	++(+)
Dorsomedial nucleus of the hypothalamus (DMH) - posterior	++	++	+(+)	+(+)
Lateral hypothalamic area (LHA)	+(+)	+	++	++(+)
Ventromedial nucleus of the hypothalamus (VMH) – dorsomedial	+++++	+	+	+++
Ventromedial nucleus of the hypothalamus (VMH) - central	+++++	++	(+)	+(+)
Ventromedial nucleus of the hypothalamus (VMH) - ventrolateral	++++	+++	(+)	+(+)
Arcuate nucleus of the hypothalamus – medial	+	(+)	+	++(+)
Arcuate nucleus of the hypothalamus – lateral	+++	++	+(+)	+++(+)
Median eminence (ME)	+	+	++++	+++

Table 2.1 (continued)

Table 2.1 – continued: Projection density from subparaventricular zone subregions				
Region	dlSPZ	vlSPZ	dmSPZ	vmSPZ
Supramamillary	+++	+	(+)	++
Medial mamillary	++	+	(+)	(+)
Mamillary body (edges)	++	++	++	+++
Tuberomamillary nucleus (TMN)	++(+)	++	+	++
Posterior hypothalamus	++(+)	+	(+)	++
Pons and brainstem				
Periacqueductal/central gray (PAG/CG)	+++(+)	+++(+)	(+)	+++
Ventral tegmental area (VTA)	++	+	+	+
Substantia nigra	(+)	(+)	(+)	(+)
Pre-coeruleus	(+)	n/a	(+)	+
Locus coeruleus	0	n/a	0	(+)
Parabrachial nucleus	+	n/a	(+)	+(+)
Thalamus and habenula				
Paraventricular thalamus - anterior	+++	++(+)	+	++++
Paraventricular thalamus - middle	+++	+	(+)	++++
Paraventricular thalamus posterior	++	+	(+)	+++
Habenula	+(+)	+(+)	0	(+)
Paratenial thalamus	++	++	(+)	++
Reuniens thalamus	+	++	(+)	++(+)
Intergeniculate leaflet (IGL)	(+)	+(+)	0	+
Lateral geniculate nucleus of the thalamus (LGN)	(+)	(+)	0	+(+)
Cortical structures				
Medial Amygdala	++	+(+)	++	++
Central Amygdala	+	0	+	+

strong a projection to the medial preoptic area as to the median preoptic nucleus (if not stronger), in case NVA 84 the median preoptic was preferentially innervated.

The vmSPZ also sent the richest projections dorsally into the anterior portion of the periventricular zone, to the rostral paraventricular thalamus and to the PVH, providing a particularly strong input to the anterior parvicellular division of this nucleus. The contralateral input to paraventricular thalamus was remarkably strong, and contralateral innervation of the anterior PVH was also substantial.

The vmSPZ innervated the ipsilateral SCN and dmSPZ more richly than did any other SPZ subdivision (Fig. 2.4A, 2.5C). It also provided fairly strong input to the ipsilateral vlSPZ, and an unusually robust projection to the contralateral vmSPZ, extending somewhat into the contralateral vlSPZ as well. The vmSPZ, more so than other SPZ subdivisions, innervated the adjacent AHA, LHA and DMH (Table 2.1), in particular the DMH at its most rostral level and at the level of the compact subdivision (especially the medial third of these), although the density of boutons tapered off toward the more caudal aspect of the DMH. Its projection to the VMH was not quite as strong as that from the dlSPZ (Fig. 2.4I, L), but showed a very distinct spatial pattern, with terminals preferentially innervating the dorsomedial VMH, dorsal and medial aspects of the VMH capsule, the central portion of the VMH, and the internuclear spaces in between the VMH and the DMH, arcuate nucleus, and periventricular zone (Fig. 2. 4I). The vmSPZ also sent a significantly stronger projection to the median eminence (Fig. 2. 4I) than did the vlSPZ or dlSPZ, although, as described below, not as strong as that of the dmSPZ (Fig. 2.4L).

Ventrolateral SPZ

The vlSPZ had moderate to strong outflow in all four general pathways, and its distinct features were found in a few individual regions along each pathway. In particular, unlike other SPZ subregions, the vlSPZ preferentially innervated the ventrolateral portion of the VMH (Fig.2. 4J), making it the only SPZ region whose VMH terminal field became more and more dense the further caudally it went. However, like most subregions, the vlSPZ provided stronger inputs to the capsule of the VMH (and internuclear spaces surrounding it) than to the body of the VMH. The vlSPZ gave rise to a moderate projection to the rostral DMH with slightly less bias toward its medial aspect than seen with vmSPZ projections. More caudally,

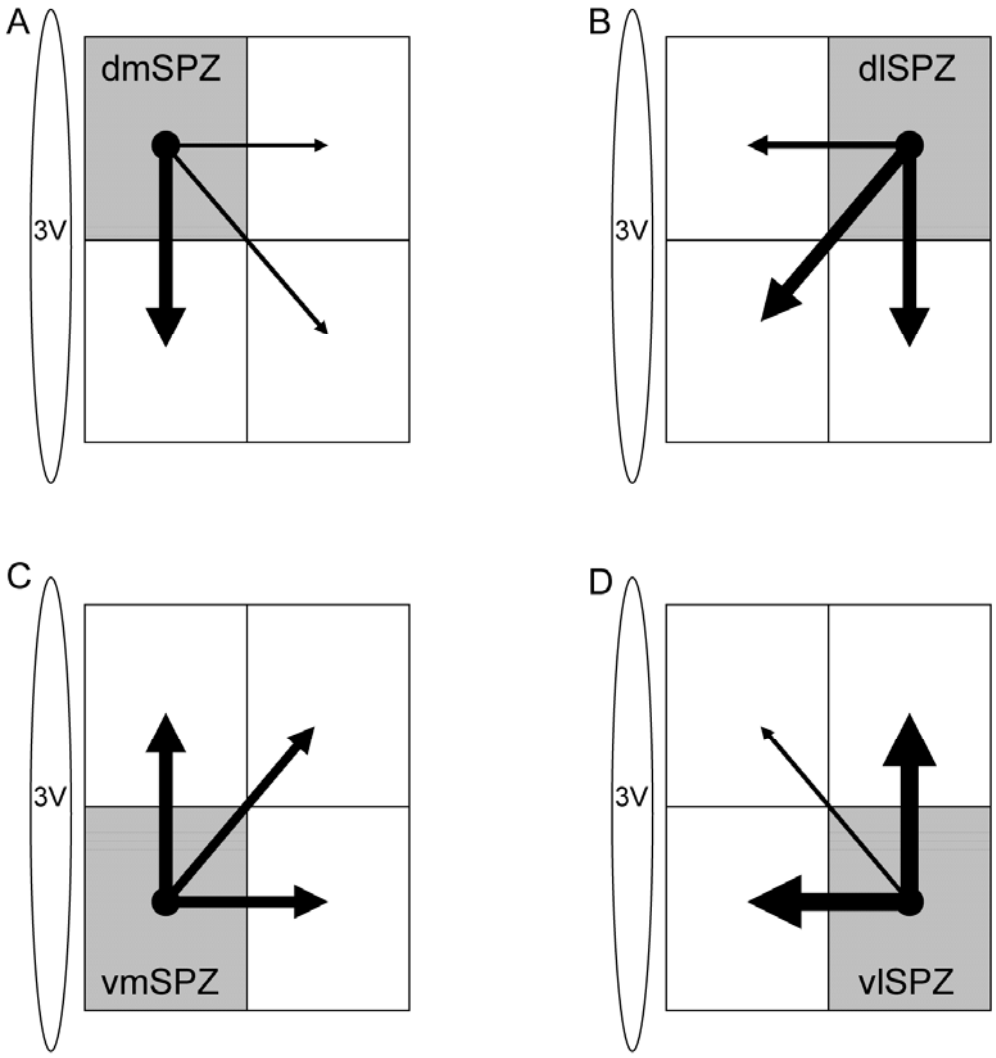

Figure 2.5 Schematic diagram illustrating estimated density of intra-SPZ projections based on anterograde tracing from the (A) dorsomedial, (B) dorsolateral, (C) ventromedial, and (D) ventrolateral SPZ.

the vlSPZ sent a particularly strong input to the central gray matter and ipsilateral premamillary region, but a fairly weak input to the supramamillary nucleus, and the weakest input to the median eminence of all four SPZ subdivisions. The vlSPZ also strongly innervated the SCN, vmSPZ and dlSPZ, but only sparsely innervated the dmSPZ or any of these structures on the contralateral sides of the brain (Table 2.1, Fig. 2.5). Inputs to the amygdala were confined to the ipsilateral medial nucleus, showing no innervation of the central nucleus or the contralateral side.

Dorsomedial SPZ

The dmSPZ includes the portion of the periventricular nucleus which is richly innervated by the shell of the SCN (Fig. 2.1). Thus, it is to be expected that projections from this subregion share certain similarities with outputs from the periventricular zone in general. Our experiments demonstrated that this was indeed the case.

Unlike the other SPZ subregions, the dmSPZ did not have a particularly strong dorsal or caudal outflow. Its caudal projection was for the most part sparse compared to other SPZ subregions, save for an intense input to a series of endocrine structures including the external lamina of the median eminence, a somewhat less intense projection through the internal lamina of the median eminence, and a moderate projection to the arcuate nucleus (Fig. 2.4K), suggesting that this may be a major site for circadian interactions with the endocrine system. Projections to the tuberomamillary, premamillary, supramammilary and medial mamillary nuclei were much less intense, although the subset of fibers terminating along the edges of the mamillary body was as dense after dmSPZ injections as any SPZ subregion. Across all four of our dmSPZ injection cases, the DMH received a more substantial input than the VMH, although neither terminal field was heavy (Fig. 2.4K). Though not intense at any level, the innervation of the DMH by the dmSPZ was more consistent along the rostro-caudal extent of this nucleus than innervation coming from other SPZ domains.

Inputs from the dmSPZ to the paraventricular thalamus were also sparse (especially to the more posterior portions of this nucleus). In three of our four cases, we could not find labeled fibers in the lateral habenula. The fourth case injection included a few labeled neurons in the dlSPZ and PVH, which we believe account for the very sparse habenular innervation seen. More rostrally, there was a moderate

input to the anterior PVT, although not much innervation to the thalamic reuniens nucleus and even less to parataenial nucleus. The parvicellular PVH did receive a substantial projection from the dmSPZ, which preferentially innervated the most rostral and caudal parvicellular subregions of this nucleus (Fig. 2.4C). Axons from the dmSPZ innervated the magnocellular PVH subdivision less intensely than its parvicellular components, but more extensively than did other SPZ subregions.

Anterior projections from the dmSPZ followed a pattern similar to the vlSPZ but with less intensity. Interestingly, the projection curving anterolaterally into the stria terminalis gave rise to a projection to the amygdala which was as intense as that from other SPZ subregions and was more bilaterally robust. Ipsilaterally, we saw a particularly widespread projection to the amygdala with fibers coursing through adjacent structures to terminate predominantly in the medial and central nuclei.

Finally the dmSPZ gave rise to a particularly heavy lateral projection, with many fibers following arcing trajectories into the lateral hypothalamus. Some of these may have been from displaced vasopressin cells belonging to the PVH and sending their axons in this classic arcing trajectory, which turns back along the surface of the optic tract to run into the median eminence. However, some axons innervated the supraoptic nucleus and others apparently entered the ventral supraoptic commissure. Axons in the lateral pathway were also followed back along the optic tract to the intergeniculate leaflet and lateral geniculate nucleus, as with other cases. The dmSPZ sent a sizeable projection down to the vmSPZ and a stronger projection to the retrochiasmatic area than any other SPZ subregion.

Dorsolateral SPZ

The dlSPZ had robust outputs along all four pathways, but preferentially innervated certain structures along each outflow path. Rostrally, the dlSPZ provided the densest input to the bed nucleus of the stria terminalis and substantia innominata (relative to other SPZ subregions). There was also fairly strong input to the diagonal band nuclei and parastrial nucleus. Via the dorsal outflow pathway, it provided a consistently strong input to all rostro-caudal levels of the PVT and a stronger input to the habenula than any other part of the SPZ. Fibers in the lateral pathway gave rise to the most dense terminal field seen in the anterior hypothalamic area with less extension into the lateral hypothalamic area.

Along the caudal pathway, dlSPZ neurons provided an exceptionally dense and uniform terminal field throughout the entire length of the VMH (Fig. 2.4, Table 2.1), most densely innervating the core of the dorsomedial subdivision of the VMH as well as the central subdivision and the internuclear capsular spaces surrounding the VMH. The projection to the DMH was of more modest intensity, distinctly favoring the rostral and medial third of this nucleus. Axons continued caudally through and lateral to the arcuate nucleus, providing moderate numbers of labeled boutons in the median eminence and the caudal arcuate nucleus. Of all subregions, the dlSPZ gave rise to the densest terminal fields in the tuberomammilary nucleus, posterior hypothalamus, and ventral tegmental area, with a strong input to the central gray matter as well.

The dlSPZ also provided local projections to the SCN and other SPZ subdivisions. In particular, a heavy field of terminals and ramifications was seen in the ipsilateral vlSPZ, and vmSPZ. While some terminals were also visible in the dmSPZ and SCN, these were much lower in number.

Retrograde tracing confirms heterogeneity of efferents from different subparaventricular domains

To confirm the validity of differences in anterograde projections to certain targets from the different SPZ subregions, we injected a retrograde tracer (CTb) into four of these target areas: the VLPO, VMH, DMH, and medial ARC (see Fig. 2.6 A, D and G, respectively).

Ventrolateral preoptic afferents

CTb was injected into the VLPO, filling the entire rostro-caudal extent of this nucleus, with densest staining in the ventral VLPO, and extending a bit medially into the ventromedial preoptic area. Retrograde tracing from this site most densely labeled cell bodies in the SCN shell and vmSPZ, but labeled no cells in the vlSPZ (see Fig. 2.6B). A number of cells were labeled in the dorsal SPZ, mostly around the boundary between the dmSPZ and dlSPZ (Fig. 2.6C). This is consistent with our anterograde tracing data suggesting that of the sites we analyzed, the vmSPZ is the largest contributor of projections the VLPO (see Fig. 2.4E, Table 2.1).

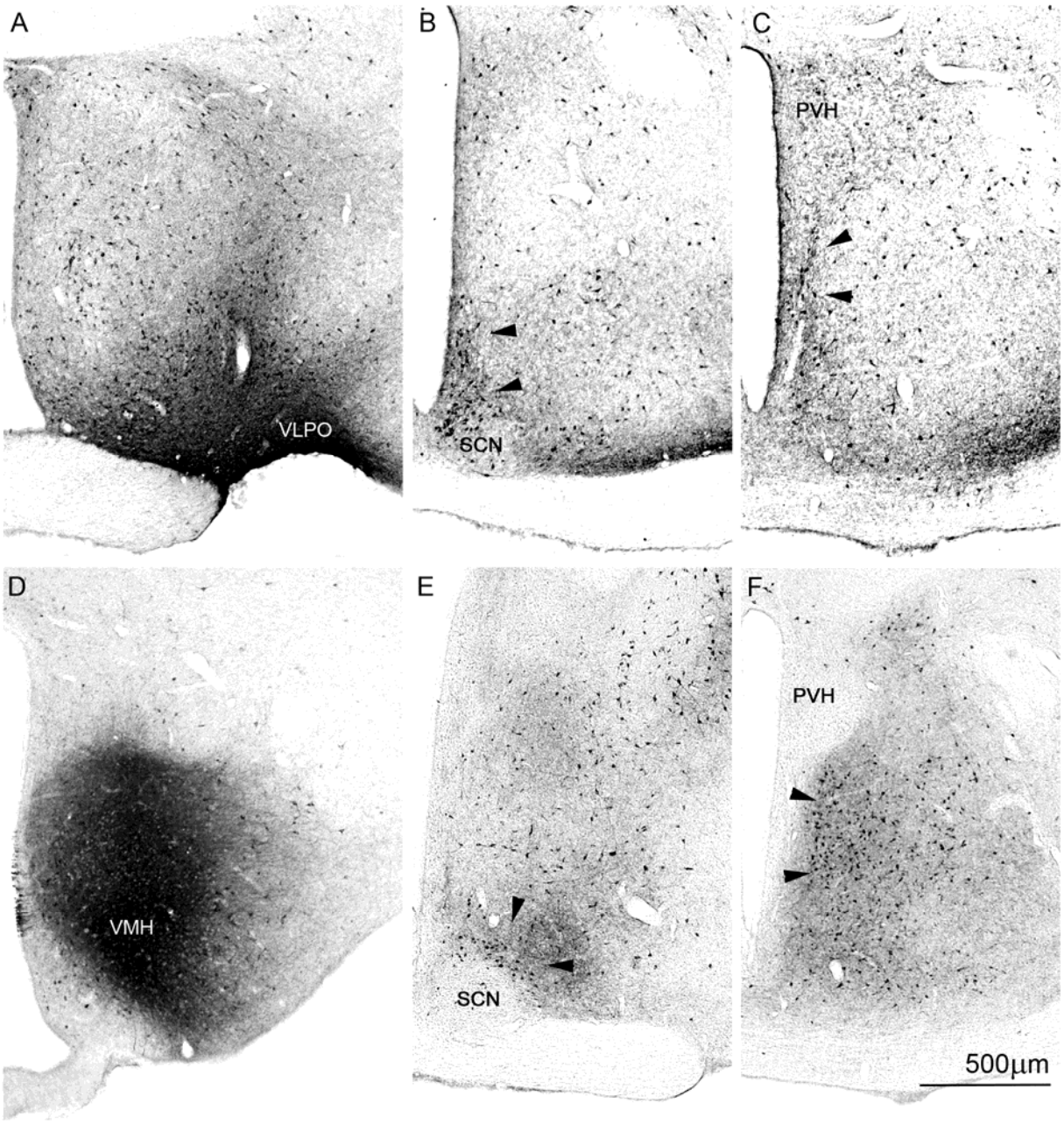

Figure 2.6 Brightfield photomicrographs showing (A, D, G, J) injection sites and retrogradely labeled cells (all middle and left panels) following CTb injection into the (A-C) ventrolateral pre-optic nucleus, (D-F) ventromedial hypothalamic nucleus, (G-I) dorsomedial hypothalamic nucleus, and (J-L) arcuate nucleus

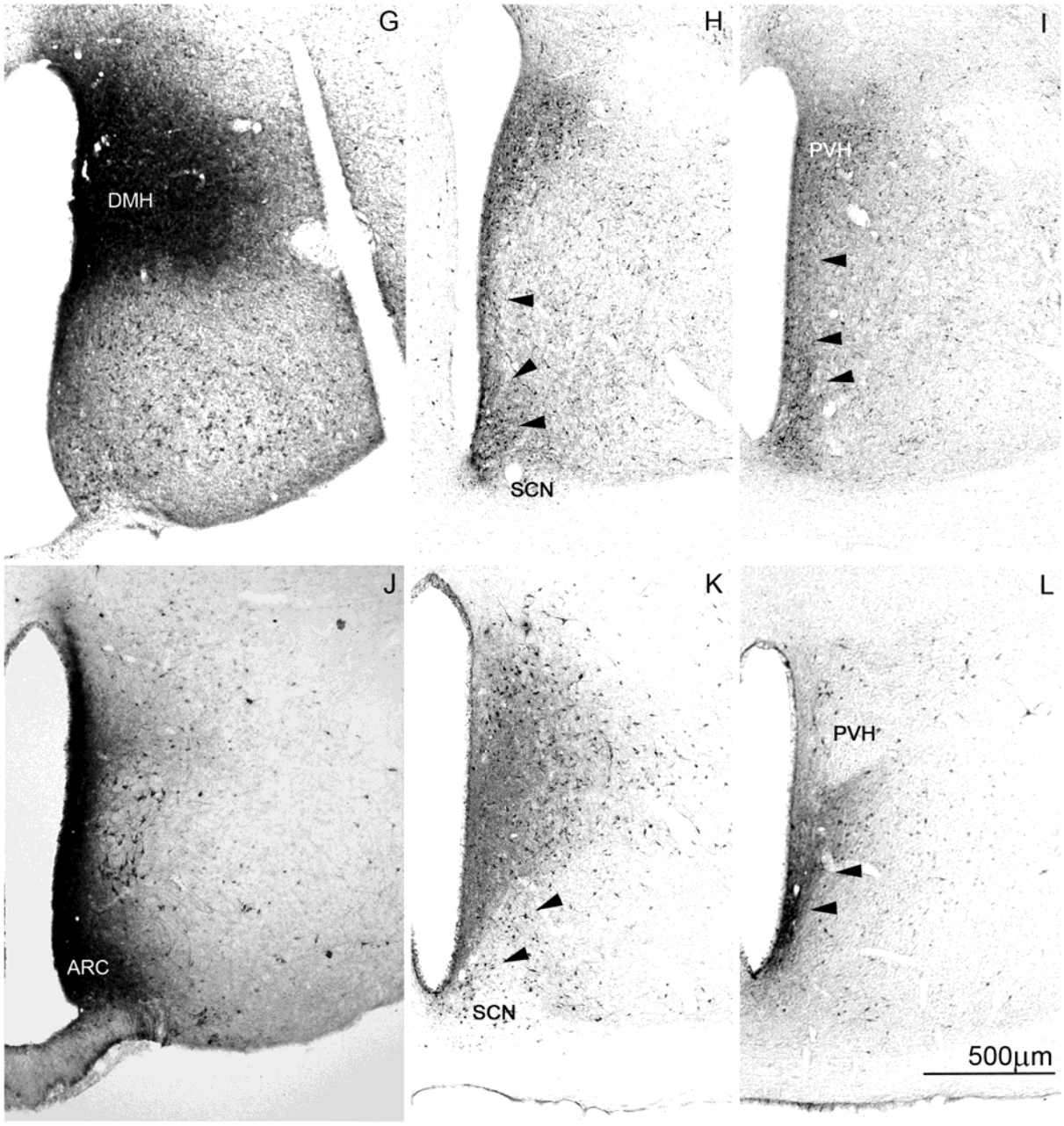

Figure 2.6 (continued)

Ventromedial hypothalamic nucleus afferents

After an injection of CTb into the dorsomedial and central subdivisions of the VMH, but including parts of its capsule and a small amount of the ventrolateral VMH, the pattern of retrograde labeling seen in the SPZ was essentially as predicted by our anterograde tracing experiments (see Fig. 2 4D, L). The dlSPZ, which sends by far the densest projection to the VMH, showed the highest numbers of retrogradely labeled SPZ neuron (Fig. 2.6E, F). The retrogradely labeled neurons spilled over more laterally into other portions of the anterior hypothalamic area, so it may be more accurate to consider this an anterior hypothalamic projection, the medial portion of which is influenced by the SCN. The ventral most (perisuprachiasmatic) portion of the vlSPZ (Fig. 2.6E) also showed a fairly high density of retrogradely labeled cells although a lower number of cells than that seen in the dlSPZ. This pattern is consistent with our anterograde injection data showing that the vlSPZ projects predominantly to the ventral portion of the VMH capsule (Fig. 2.4J). The retrogradely labeled neurons overlap into the midportion of the ventral SPZ (but not the exclusively medial zone), which explains why the projection to the VMH was also labeled in some of our vmSPZ cases (e.g., Fig. 2.4I). There was a striking absence of retrogradely labeled cells in the dmSPZ of this case, much as there is a striking lack of labeled anterograde projections in the VMH from this region (Fig. 2.4K).

Dorsomedial hypothalamic nucleus afferents

An injection of CTb was placed in the DMH (Fig. 2.6G), showing particularly intense filling in the medial third of the rostral DMH but filling the whole rostrocaudal extent of the nucleus. Very light filling was also present in the periventricular zone anterior to the DMH, adjacent LHA at rostral DMH levels, and in small portions of the medial posterior arcuate nucleus that lie just caudal and ventral to the DMH. This injection resulted in labeling of cell bodies along the most medial portion of the SPZ, including mostly cells in the vmSPZ and to some extent in the dmSPZ, with almost no labeling in the vlSPZ (Fig. 2.6H, I). It seems likely, based on this result, that the dlSPZ injection shown in Fig, 2.4D labeled axons in the DMH (Fig. 2.4L) (and which was even heavier in the most caudal portion of the DMH, see Table 2.1) by including some cells in the middle portion of the dorsal SPZ, along the medial edge of that injection. This result is consistent with retrograde labeling previously reported from our lab (Chou et al., 2003).

Arcuate nucleus afferents

In this case (NVA 150) CTb was injected into the medial portion of the arcuate nucleus and continued dorsally to fill part of the adjacent periventricular zone (Fig. 2.6J). The injection extended through the rostral and middle levels of the arcuate nucleus, tapering off at the posterior level (just caudal to the VMH). CTb was seen in the adjacent periventricular zone just dorsal to the arcuate nucleus only at rostral levels of the injection. Extremely faint CTb stain could be observed just rostral to this in the ventral periventricular zone at the level of the retrochiasmatic area. In this case, there was an especially dense cluster of retrogradely labeled cells present in the caudal portion of the vmSPZ (Fig. 2.6K, L), with scattered retrogradely labeled neurons in the remainder of the SPZ, consistent with our anterograde tracing (see Table 2.1).

Discussion

Previous work on inputs to the SPZ (Leak and Moore, 2001) had indicated a medial vs. lateral organization, while physiological evidence from lesion studies (Lu et al., 2001) suggested a dorsal vs. ventral organization. Our systematic analysis of SPZ projections indicates that its outputs are organized along both of these lines, demonstrating that each of the four SPZ quadrants has a distinct set of targets (see below).

In addition, the SPZ innervates several brain regions that have not previously been reported. Using expression of GFP induced by viral-vectors, we observe fibers and terminals from SPZ neurons in the dorsal raphe, locus coeruleus, pre-coeruleus region, lateral parabrachial nucleus and Barrington's nucleus, (see Fig. 2.3, Table 2.1), none of which have been previously reported. In addition to these novel targets in the hindbrain, we also observed a slightly different and more extensive pattern of innervation than previously described in the amygdala, habenula, and median eminence (see Fig. 2.3, Table 2.1). We also observed that the four SPZ subdivisions project to each other and to the suprachiasmatic nucleus. The dl,vl, and dm SPZ all seem to project strongly to vmSPZ, which in turn projects most strongly to the dm SPZ and SCN. The vlSPZ and dlSPZ also project strongly to each other but don't receive much vmSPZ input and get almost no dmSPZ input. This connectivity allows for local

circuits to share information within the SPZ and suggests circadian outflow through it could be considerably more complex than previously described.

Technical considerations

The anterograde tracers used for this study, an adeno-associated viral vector expressing GFP (AAV-GFP) and in a few cases biotinylated dextran amine (BDA) have certain strengths and weaknesses that must be considered when interpreting the data. BDA is an excellent anterograde tracer but carries a risk of retrograde uptake and transport anterogradely down collaterals of those same neurons. This risk is strongly diminished when using an AAV-GFP from the serotype 2 group, as we did here. AAV2-GFP retrogradely labels only one or two neurons per brain, hence collateral transport is unlikely to contribute substantially to the projections seen (Chamberlin et al., 1998).

Although we use a combination of BDA and AAV-GFP injection cases to analyze differences in SPZ subregion projections, we fortunately we have injection cases with AAV-GFP (alone or in addition to BDA) for three out of four SPZ subregions, and are able to compare and verify that injections with the different tracers that are placed in similar sites give rise to extremely similar fiber and terminal fields elsewhere in the brain. The only subregion for which we must rely on BDA anterograde tracing alone is the vlSPZ. Fortunately, this is a subregion whose efferents have previously been reported using another tracer with less risk for retrograde uptake (PHAL), and our findings match the previous reports of vlSPZ efferent targets (Canteras et al., 2011). We also examined our own AAV-GFP cases for labeled neuronal cell bodies more than 1,000 μm from the injection site, and found fewer than one per brain.

An important advantage of tracing with AAV-GFP is that once neurons take up this vector, GFP expression within them persists in the brain indefinitely, (as oppsed to BDA or PHAL which degrade around 4 weeks' time), and this makes it possible to ensure filling of extrememly distal fibers and boutons by allowing many weeks or months for the AAV-GFP to fill the neurons in a long range pathway. This may explain why we were able to visualize distal SPZ targets including the the dorsal raphe, locus coeruleus, pre-coeruleus region, lateral parabrachial nucleus and Barrington's nucleus, when previous tracing studies did not. It is worth noting that injection cases in which we saw labelling in these regions were all cases where eight to nine weeks elapsed between AAV-GFP injection and perfusion, and they

typically involved more than one SPZ subdivision. Even though we focus much of our analysis in this study on assessing which SPZ subdivisions provide the most significant input to certain targets, it bears mention that SPZ fibers and terminals in distal sites like Barrington's nucleus may only be seen after large injections of AAV-GFP covering multiple SPZ subregions, suggesting that in some projections there is no SPZ subregion acting as the dominant relay channel.

Furthermore, though we make an effort to estimate them, it is not possible to make rigorous quantitative comparisons of terminal density across two injection cases given the fact that each injection fills a different number and distribution of neuronal cell bodies. However, semi-quantitative comparison across several different cases of injections placed in adjacent/overlapping regions can still provide information regarding differential innervation of target sites by adjacent SPZ subdivisions. Furthermore, retrograde tracing from targets of the SPZ can resolve the ambiguity in interpretation of anterograde tracing findings. We have relied heavily on case-to-case comparison and complementary retrograde tracing in selected terminal fields to clarify the differences between projections from different SPZ subdivisions.

Functional implications of SPZ connectivity

Many of the novel SPZ targets we observed receive the bulk of their input from the vmSPZ and are thought to play a role in sleep/wake regulation, namely the parabrachial nucleus, locus coeruleus, pre-coeruleus region, and dorsal raphe nuclei (Saper et al., 2010). These observations are consistent with earlier studies showing that the ventral SPZ plays a particularly important role in the circadian modulation of sleep. The vmSPZ also projects to the lateral hypothalamic area, median preoptic nucleus, VLPO and the anterior and compact levels of the DMH (see Table 2.1). In the case of the VLPO and DMH, we have been able to confirm via retrograde tracing that their SPZ afferents come mostly from the ventromedial quadrant (see Fig. 2.6). While all the sites listed above play significant roles in sleep-wake regulation, only lesions of the DMH specifically disrupt the circadian timing of sleep and wake throughout the day (Chou et al., 2003), suggesting the vmSPZ projection to this level of the DMH may carry particular functional relevance in circadian modulation of behavioral state.

Lesions of the DMH have also been shown to disrupt circadian rhythms in adrenal corticosteroid secretion and feeding, which may also depend on intact vmSPZ fibers relaying SCN clock input to this portion of the DMH. We also show both via anterograde and retrograde tracing that the vmSPZ is the main contributor of SPZ inputs to the arcuate nucleus, particularly its medial subdivision (and to the periventricular zone just dorsal to it) (Table 2.1, Fig. 2.6). These sites contain neurons mediating prolactin release (Moore, 1987), as well as feeding behavior and energy expenditure, and their responses to leptin and ghrelin (Cone, 2005; Krashes et al., 2011; Kong et al., 2012).

There is also evidence that SPZ transections disrupt diurnal rhythms in reproductive hormones (Watts et al., 1989). Knife cuts through the SPZ were reported to blunt diurnal rhythms of both prolactin and luteinizing hormone (Watts et al., 1989). Prolactin release is regulated by periventricular and arcuate dopamine neurons, which receive major inputs from the vmSPZ. The anteroventral periventricular nucleus (AVPe) is thought to regulate leutenizing hormone (LH) release (Robertson et al., 2009). Circadian regulation of LH release is dependent on ipsilateral neural outflow from the shell region of the SCN to the AVPe (de la Iglesia et al., 2003; de la Iglesia and Schwartz, 2006; Smarr et al., 2012) , although direct projections from the SCN shell to the AVPe are quite sparse. As the vmSPZ both receives a strong input from the SCN shell and sends a robust projection to AVPe, it is likely to be a critical relay in this pathway. The vmSPZ may affect circadian regulation of other endocrine rhythms together with the dmSPZ. Both of these subregions give rise to an impressively dense terminal field in the external lamina and to a fiber bundle in the internal lamina (dorsal third) of the median eminence bilaterally. This makes the medial SPZ well positioned to modulate the release of pituitary hormones.

It thus seems likely that the medial SPZ may be involved in endocrine rhythm regulation, while the vmSPZ is particularly involved in circadian regulation of sleep and wakefulness. The lateral SPZ subdivisions, on the other hand, may act more as an entry point for non-SCN inputs to these circadian outflow circuits, with more limited roles in outflow.

The dlSPZ has strong reciprocal connections with the VMH, which may have a variety of physiological implications. The dlSPZ both receives a strong input from leptin-sensitive neurons in the dorsomedial VMH (Elmquist et al., 1998) sends a robust projection to that region (Table 2.1, Fig. 2.4). These dmVMH neurons are implicated in energy homeostasis and maintenance of plasma glucose levels

(Tong et al., 2007; Hawke et al., 2009; Xu et al., 2010). The dlSPZ also projects strongly to the vmSPZ and vlSPZ, perhaps relaying satiety/energy balance signals, and has a particularly impressive projection to the ventrolateral VMH, an area implicated in control of aggression and reproductive behavior (Lin et al., 2011).

The vlSPZ receives the largest share of the retinal (see Fig. 2.1, (Gooley et al., 2003; Canteras et al., 2011) and IGL (Moga and Moore, 1997) input to the SPZ, an area implicated in exercise mediated and photic circadian phase resetting (Harrington and Rusak, 1986; Harrington, 1997). The vlSPZ is also the subdivision projecting most strongly to the IGL, vmSPZ, and dlSPZ, making it well positioned to integrate photic and activity-based entrainment cues into circadian outflow circuitry downstream of the SCN. Previous studies have suggested that light masking of various rhythms can still occur following damage to the SCN (Redlin and Mrosovsky, 1999) or knife cuts between the SCN and SPZ (Watts et al., 1989), but not following SCN lesions which extend into the adjacent ventral subparaventricular zone (Li et al., 2005). These findings suggest that light masking of activity could be mediated through direct or relayed retinal inputs to the vlSPZ and its downstream outputs. Studies of nocturnal vs. rodents also indicate that retinal innervation of the vlSPZ (or lack thereof) between postnatal day 8 and 15 coincides with the development of consolidated night-time vs. day time wakefulness, respectively, and may explain how an rodent's (or any mammal's) active phase is determined (Todd et al., 2012).

The configuration and development of neural connections between the SPZ and other brain regions can surely explain much about a mammal's phase angle of entrainment and daily temporal patterns, as well as adaptability to new or alternate schedules. While these neural connections and default schedules are typically formed early in life, e.g. by postnatal day 15 in rats (Blumberg et al., 2005; Gall et al., 2008), it is not uncommon for adult mammals to change their active phase in response to environmental pressures or external incentives (Saper et al., 2005; Gattermann et al., 2008; Cohen et al., 2010). It is likely that changes in the way the SPZ receives, processes and communicates information to other parts of the central nervous system underlie adaptation to new schedules as well as the development of circadian and diurnal rhythms early in life.

Acknowledgments

We are grateful to Quan Ha for superb technical assistance throughout this study and to Dr. Charles Allen (and members of his laboratory at OHSU) for generously providing us with AAV-GFP reporter rat brains. We also thank Dr. Ningshan Wang for assistance with confocal microscopy, Ashley Schomer and Peagan Lin for assistance with histology, and Dr. Veronique Van der Horst for thoughtful input at various stages of this project. This work was supported by USPHS grants NS072337, AG09975 awarded to C. Saper and the F31 NS071890-03 and NSFGRFP fellowships awarded to N. Vujovic.

References

Aton SJ, Herzog ED (2005) Come together, right...now: synchronization of rhythms in a mammalian circadian clock. Neuron 48:531-534.

Belenky MA, Yarom Y, Pickard GE (2008) Heterogeneous expression of gamma-aminobutyric acid and gamma-aminobutyric acid-associated receptors and transporters in the rat suprachiasmatic nucleus. The Journal of comparative neurology 506:708-732.

Blumberg MS, Seelke AM, Lowen SB, Karlsson KA (2005) Dynamics of sleep-wake cyclicity in developing rats. Proceedings of the National Academy of Sciences of the United States of America 102:14860-14864.

Bruinstroop E, Cano G, Vanderhorst VG, Cavalcante JC, Wirth J, Sena-Esteves M, Saper CB (2011) Spinal projections of the A5, A6 (locus coeruleus), and A7 noradrenergic cell groups in rats. The Journal of comparative neurology.

Canteras NS, Ribeiro-Barbosa ER, Goto M, Cipolla-Neto J, Swanson LW (2011) The retinohypothalamic tract: comparison of axonal projection patterns from four major targets. Brain research reviews 65:150-183.

Chamberlin NL, Du B, de Lacalle S, Saper CB (1998) Recombinant adeno-associated virus vector: use for transgene expression and anterograde tract tracing in the CNS. Brain research 793:169-175.

Chou TC, Scammell TE, Gooley JJ, Gaus SE, Saper CB, Lu J (2003) Critical role of dorsomedial hypothalamic nucleus in a wide range of behavioral circadian rhythms. The Journal of neuroscience : the official journal of the Society for Neuroscience 23:10691-10702.

Cohen R, Smale L, Kronfeld-Schor N (2010) Masking and temporal niche switches in spiny mice. Journal of biological rhythms 25:47-52.

Cone RD (2005) Anatomy and regulation of the central melanocortin system. Nature neuroscience 8:571-578.

Costa MS, Santee UR, Cavalcante JS, Moraes PR, Santos NP, Britto LR (1999) Retinohypothalamic projections in the common marmoset (Callithrix jacchus): A study using cholera toxin subunit B. The Journal of comparative neurology 415:393-403.

de la Iglesia HO, Schwartz WJ (2006) Minireview: timely ovulation: circadian regulation of the female hypothalamo-pituitary-gonadal axis. Endocrinology 147:1148-1153.

de la Iglesia HO, Meyer J, Schwartz WJ (2003) Lateralization of circadian pacemaker output: Activation of left- and right-sided luteinizing hormone-releasing hormone neurons involves a neural rather than a humoral pathway. The Journal of neuroscience : the official journal of the Society for Neuroscience 23:7412-7414.

Deurveilher S, Semba K (2003) Indirect projections from the suprachiasmatic nucleus to the median preoptic nucleus in rat. Brain research 987:100-106.

Deurveilher S, Semba K (2005) Indirect projections from the suprachiasmatic nucleus to major arousal-promoting cell groups in rat: implications for the circadian control of behavioural state. Neuroscience 130:165-183.

Deurveilher S, Burns J, Semba K (2002) Indirect projections from the suprachiasmatic nucleus to the ventrolateral preoptic nucleus: a dual tract-tracing study in rat. The European journal of neuroscience 16:1195-1213.

Elmquist JK, Ahima RS, Elias CF, Flier JS, Saper CB (1998) Leptin activates distinct projections from the dorsomedial and ventromedial hypothalamic nuclei. Proceedings of the National Academy of Sciences of the United States of America 95:741-746.

Gall AJ, Todd WD, Ray B, Coleman CM, Blumberg MS (2008) The development of day-night differences in sleep and wakefulness in norway rats and the effect of bilateral enucleation. Journal of biological rhythms 23:232-241.

Gattermann R, Johnston RE, Yigit N, Fritzsche P, Larimer S, Ozkurt S, Neumann K, Song Z, Colak E, Johnston J, McPhee ME (2008) Golden hamsters are nocturnal in captivity but diurnal in nature. Biology letters 4:253-255.

Gooley JJ, Lu J, Fischer D, Saper CB (2003) A broad role for melanopsin in nonvisual photoreception. The Journal of neuroscience : the official journal of the Society for Neuroscience 23:7093-7106.

Harrington ME (1997) The ventral lateral geniculate nucleus and the intergeniculate leaflet: interrelated structures in the visual and circadian systems. Neuroscience and biobehavioral reviews 21:705-727.

Harrington ME, Rusak B (1986) Lesions of the thalamic intergeniculate leaflet alter hamster circadian rhythms. Journal of biological rhythms 1:309-325.

Hattar S, Kumar M, Park A, Tong P, Tung J, Yau KW, Berson DM (2006) Central projections of melanopsin-expressing retinal ganglion cells in the mouse. The Journal of comparative neurology 497:326-349.

Hawke Z, Ivanov TR, Bechtold DA, Dhillon H, Lowell BB, Luckman SM (2009) PACAP neurons in the hypothalamic ventromedial nucleus are targets of central leptin signaling. The Journal of neuroscience : the official journal of the Society for Neuroscience 29:14828-14835.

Inouye ST, Kawamura H (1979) Persistence of circadian rhythmicity in a mammalian hypothalamic "island" containing the suprachiasmatic nucleus. Proceedings of the National Academy of Sciences of the United States of America 76:5962-5966.

Johnson RF, Morin LP, Moore RY (1988) Retinohypothalamic projections in the hamster and rat demonstrated using cholera toxin. Brain research 462:301-312.

Kong D, Tong Q, Ye C, Koda S, Fuller PM, Krashes MJ, Vong L, Ray RS, Olson DP, Lowell BB (2012) GABAergic RIP-Cre neurons in the arcuate nucleus selectively regulate energy expenditure. Cell 151:645-657.

Krashes MJ, Koda S, Ye C, Rogan SC, Adams AC, Cusher DS, Maratos-Flier E, Roth BL, Lowell BB (2011) Rapid, reversible activation of AgRP neurons drives feeding behavior in mice. The Journal of clinical investigation 121:1424-1428.

Kriegsfeld LJ, Leak RK, Yackulic CB, LeSauter J, Silver R (2004) Organization of suprachiasmatic nucleus projections in Syrian hamsters (Mesocricetus auratus): an anterograde and retrograde analysis. The Journal of comparative neurology 468:361-379.

Kubota A, Inouye ST, Kawamura H (1981) Reversal of multiunit activity within and outside the suprachiasmatic nucleus in the rat. Neuroscience letters 27:303-308.

Leak RK, Moore RY (2001) Topographic organization of suprachiasmatic nucleus projection neurons. The Journal of comparative neurology 433:312-334.

Leak RK, Card JP, Moore RY (1999) Suprachiasmatic pacemaker organization analyzed by viral transynaptic transport. Brain research 819:23-32.

Levine JD, Weiss ML, Rosenwasser AM, Miselis RR (1991) Retinohypothalamic tract in the female albino rat: a study using horseradish peroxidase conjugated to cholera toxin. The Journal of comparative neurology 306:344-360.

Li X, Gilbert J, Davis FC (2005) Disruption of masking by hypothalamic lesions in Syrian hamsters. Journal of comparative physiology A, Neuroethology, sensory, neural, and behavioral physiology 191:23-30.

Lin D, Boyle MP, Dollar P, Lee H, Lein ES, Perona P, Anderson DJ (2011) Functional identification of an aggression locus in the mouse hypothalamus. Nature 470:221-226.

Lu J, Zhang YH, Chou TC, Gaus SE, Elmquist JK, Shiromani P, Saper CB (2001) Contrasting effects of ibotenate lesions of the paraventricular nucleus and subparaventricular zone on sleep-wake cycle and temperature regulation. The Journal of neuroscience : the official journal of the Society for Neuroscience 21:4864-4874.

Moga MM, Moore RY (1997) Organization of neural inputs to the suprachiasmatic nucleus in the rat. The Journal of comparative neurology 389:508-534.

Moore KE (1987) Interactions between prolactin and dopaminergic neurons. Biology of reproduction 36:47-58.

Moore RY, Speh JC, Leak RK (2002) Suprachiasmatic nucleus organization. Cell and tissue research 309:89-98.

Morin LP, Goodless-Sanchez N, Smale L, Moore RY (1994) Projections of the suprachiasmatic nuclei, subparaventricular zone and retrochiasmatic area in the golden hamster. Neuroscience 61:391-410.

Nakamura W, Yamazaki S, Nakamura TJ, Shirakawa T, Block GD, Takumi T (2008) In vivo monitoring of circadian timing in freely moving mice. Current biology : CB 18:381-385.

Paxinos G, Watson C (2005) The rat brain in stereotaxic coordinates, 5th Edition. Amsterdam ; Boston: Elsevier Academic Press.

Redlin U, Mrosovsky N (1999) Masking by light in hamsters with SCN lesions. Journal of comparative physiology A, Sensory, neural, and behavioral physiology 184:439-448.

Saper CB, Lu J, Chou TC, Gooley J (2005) The hypothalamic integrator for circadian rhythms. Trends in neurosciences 28:152-157.

Saper CB, Fuller PM, Pedersen NP, Lu J, Scammell TE (2010) Sleep state switching. Neuron 68:1023-1042.

Sato T, Kawamura H (1984) Circadian rhythms in multiple unit activity inside and outside the suprachiasmatic nucleus in the diurnal chipmunk (Eutamias sibiricus). Neuroscience research 1:45-52.

Schwartz MD, Nunez AA, Smale L (2004) Differences in the suprachiasmatic nucleus and lower subparaventricular zone of diurnal and nocturnal rodents. Neuroscience 127:13-23.

Schwartz MD, Nunez AA, Smale L (2009) Rhythmic cFos expression in the ventral subparaventricular zone influences general activity rhythms in the Nile grass rat, Arvicanthis niloticus. Chronobiology international 26:1290-1306.

Schwartz MD, Urbanski HF, Nunez AA, Smale L (2011) Projections of the suprachiasmatic nucleus and ventral subparaventricular zone in the Nile grass rat (Arvicanthis niloticus). Brain research 1367:146-161.

Smale L, Castleberry C, Nunez AA (2001) Fos rhythms in the hypothalamus of Rattus and Arvicanthis that exhibit nocturnal and diurnal patterns of rhythmicity. Brain research 899:101-105.

Smarr BL, Morris E, de la Iglesia HO (2012) The dorsomedial suprachiasmatic nucleus times circadian expression of Kiss1 and the luteinizing hormone surge. Endocrinology 153:2839-2850.

Todd WD, Gall AJ, Weiner JA, Blumberg MS (2012) Distinct retinohypothalamic innervation patterns predict the developmental emergence of species-typical circadian phase preference in nocturnal Norway rats and diurnal nile grass rats. The Journal of comparative neurology 520:3277-3292.

Tong Q, Ye C, McCrimmon RJ, Dhillon H, Choi B, Kramer MD, Yu J, Yang Z, Christiansen LM, Lee CE, Choi CS, Zigman JM, Shulman GI, Sherwin RS, Elmquist JK, Lowell BB (2007) Synaptic glutamate release by ventromedial hypothalamic neurons is part of the neurocircuitry that prevents hypoglycemia. Cell metabolism 5:383-393.

Ueta Y, Fujihara H, Dayanithi G, Kawata M, Murphy D (2008) Specific expression of optically active reporter gene in arginine vasopressin-secreting neurosecretory cells in the hypothalamic-neurohypophyseal system. Journal of neuroendocrinology 20:660-664.

Watts AG, Swanson LW (1987) Efferent projections of the suprachiasmatic nucleus: II. Studies using retrograde transport of fluorescent dyes and simultaneous peptide immunohistochemistry in the rat. The Journal of comparative neurology 258:230-252.

Watts AG, Swanson LW, Sanchez-Watts G (1987) Efferent projections of the suprachiasmatic nucleus: I. Studies using anterograde transport of Phaseolus vulgaris leucoagglutinin in the rat. The Journal of comparative neurology 258:204-229.

Watts AG, Sheward WJ, Whale D, Fink G (1989) The effects of knife cuts in the sub-paraventricular zone of the female rat hypothalamus on oestrogen-induced diurnal surges of plasma prolactin and LH, and circadian wheel-running activity. The Journal of endocrinology 122:593-604.

Xu Y, Hill JW, Fukuda M, Gautron L, Sohn JW, Kim KW, Lee CE, Choi MJ, Lauzon DA, Dhillon H, Lowell BB, Zigman JM, Zhao JJ, Elmquist JK (2010) PI3K signaling in the ventromedial hypothalamic nucleus is required for normal energy homeostasis. Cell metabolism 12:88-95.

Chapter 3: Role of glutamatergic neurons in the dorsomedial hypothalamic nucleus in circadian organization of behavior

Abstract

The dorsomedial nucleus of the hypothalamus (DMH) has been implicated in a wide array of physiological and behavioral regulatory functions, including modulation of endocrine output, activity and wakefulness, ingestive behaviors, thermogenesis, as well as the circadian regulation of many of these functions. Cell-specific DMH lesions lower the amplitude of circadian rhythms in locomotor activity, wake-sleep, food intake and corticosteroid release (but not body temperature), and lead to decreased activity, wakefulness, plasma cortisol and core body temperature over the whole circadian day (Chou et al., 2003). The DMH is a heterogeneous brain region, and it is unclear which neurotransmitters and projections mediate these various functions. Most neurons in the DMH are either glutamatergic or GABAergic. Experimental evidence implicates glutamatergic projections from the dorsal hypothalamic area (DHA) and adjacent DMH to the raphe pallidus in thermoregulation (Yoshida et al., 2009; Morrison et al., 2012) and glutamatergic projections from the DMH to the lateral hypothalamic area, as well as GABAergic projections from the DMH to the ventrolateral preoptic nucleus in modulation of temporal patterns in behavioral state (Chou et al., 2003). To test the importance of glutamatergic efferents of the DMH for shaping circadian rhythms, we employed mice in which the second exon of the vesicular glutamate transporter 2 (*VGlut2*) gene was flanked by loxP sites. After stereotaxically injecting an adeno-associated viral vector expressing Cre recombinase into the DMH, neurons in the DMH expressed Cre and showed loss of *VGlut2*, which is necessary for loading glutamate into their synaptic vesicles. Mice in which the glutamatergic transmission by DMH neurons had been deleted showed many of the same features as rats with cell-specific DMH lesions. The amplitude of the circadian and diurnal rhythm in locomotor activity rhythm in mice with *VGlut2* deletion in the DMH was reduced to roughly 50% that of control animals. Average locomotor activity for the day was reduced to approximately 75% that of controls. Average body temperature was lowered by 0.3 ºC though the amplitude of circadian and diurnal rhythms in body temperature was not significantly affected. As with cell-specific lesions to the DMH, the deletion of *VGlut2* from the DMH significantly lowered the amplitude of circadian rhythms of

corticosteroids. The above findings suggest that glutamatergic neurons in the DMH are critical for normal, healthy rhythms in activity and corticosteroid release and the DMH/DHA is necessary for maintaining normal core body temperature throughout the day. To selectively investigate glutamatergic efferent projections from the DMH that could underlie these effects, we performed a conditional tracing experiment by injecting a viral vector expressing GFP downstream from a loxP-flanked stop codon into the DMH of a *VGlut2*-Cre mouse. We observed fairly robust glutamatergic projections from the DMH to the lateral hypothalamic area and from the DMH/DHA to the raphe pallidus nucleus which may be directly involved in regulation of daily rhythms and levels of locomotor activity, and in maintenance of normal core body temperature, respectively.

Introduction

The dorsomedial nucleus of the hypothalamus (DMH) is involved in regulation of many different autonomic, endocrine and behavioral parameters and plays an important role in relaying information from the circadian clock in the suprachiasmatic nucleus (SCN) to the rest of the brain. It is thought to integrate circadian inputs with signals from other sources (e.g., food availability, stress, etc.) to coordinate daily patterns of behavior and physiology. It receives direct synaptic input from both the SCN (Watts and Swanson, 1987; Watts et al., 1987; Abrahamson and Moore, 2001) and the subparaventricular zone (Watts and Swanson, 1987; Thompson and Swanson, 1998; Chou et al., 2003). It also receives inputs from sites including the median preoptic nucleus, likely relaying information on body or brain temperature; from the parabrachial and arcuate nuclei, likely conveying information about hunger and satiety; and from catecholaminergic groups in the brainstem, which are strongly implicated in stimulation of behavior and endocrine responses to stress, i.e. increased locomotion and a rise in corticosterone release (Thompson and Swanson, 1998). Notably, neurons in the DMH itself are sensitive to hunger and satiety signals; a subpopulation of them expresses leptin receptors and shows immediate early gene activation following leptin infusion (Elmquist et al., 1998; Elmquist et al., 2005; Gautron et al., 2010).

In rats, cell-specific DMH lesions decrease the amplitude of circadian rhythms in wake-sleep, locomotor activity, food intake and corticosteroid release (but not body temperature), and lead to decreased baseline wakefulness, activity, plasma cortisol and core body temperature (Chou et al., 2003). Based on histological evidence available in rat, it has been hypothesized that the effects seen on wakefulness could depend on a predominantly glutamatergic projection to the wake-consolidating lateral hypothalamic area (LHA), and a predominantly GABAergic projection to the sleep-promoting ventrolateral pre-optic nucleus (VLPO), but this has not been tested. Evidence from rat studies also suggests that a glutamatergic projection to the raphe pallidus (RPa) from a very specific subpopulation of dorsal hypothalamic area neurons and adjacent DMH neurons (DMH/DHA) may be responsible for the effects seen on body temperature.

These DMH/DHA neurons, which are implicated in mediating body temperature and heart rate regulation (Dimicco and Zaretsky, 2007), sit along the dorsal border of the DMH at the level where the mammillothalamic tract rises above the dorsal edge of the third ventricle. A number of physiological

studies suggest that this group of neurons drives brown adipose tissue thermogenesis via an excitatory projection to pre-sympathetic neurons in the raphe pallidus (RPa) in the rostral medulla (Morrison et al., 2012). Retrograde tracing from the RPa coupled with cold-induced immediate early gene labeling in rat pinpoints a region in the DMH/DHA at the level of the compact zone of the DMH (Yoshida et al., 2009). No stimulation/inhibition of this region or retrograde tracing from RPA has been reported in mouse.

While histological evidence from the rat model can provide useful hypotheses regarding which DMH projections underlie which physiological function, and what neurotransmitters they release, these questions are much more readily testable by employing genetic manipulations in a mouse model. Here, we employed such a model to specifically study the role of glutamatergic DMH neurons in regulation of basal levels and daily rhythms of locomotor activity, body temperature, corticosterone output and nutrient intake. Since glutamatergic signaling significantly affects synapse and neural circuit formation during brain development (Cline, 2001), we allowed mice to develop normally and introduced viral vectors to disrupt glutamatergic signaling in the DMH only in mice over 9 weeks old.

Because light has been shown to have acute effects on locomotor activity, body temperature and corticosterone output (Morin, 2013), we measured both circadian (free-running) and diurnal (light-entrained) rhythms of these functions in constant darkness (DD) or a 12:12hour light:dark cycle (LD), respectively. This allowed us to also investigate whether excitatory DMH neurons are a part of the neural circuit by which light directly affects the above functions.

Methods

Animals and housing

All protocols used in this study were approved by the Harvard University or Beth Israel Deaconess Medical Center Animal Care and Use Committees and conform to the regulations detailed in the National Institutes of Health *Guide for the Care and Use of Laboratory Animals*.

We used a line of *VGlut2* conditional knock-out mice (*VGlut2* $^{flox/flox}$) in which exon 2 of the *VGlut2* gene is flanked by loxP sites. The *VGlut2* $^{flox/flox}$ mice were generated and validated by Tong and Lowell. and shown to lose the ability to release glutamate synaptically from *VGlut2*-positive neurons that express

Cre-recombinase (Tong et al., 2007). In our study, homozygous *VGlut2* $^{flox/flox}$ males (n=27) were used for physiological experiments.

Prior to physiological recordings, mice were group housed, up to 5 per cage, in a 12:12h light:dark cycle, with *ad libitum* access to food (Purina formulab chow diet, irradiated, 5008C33) and water. For physiological experiments mice were singly housed and exposed to 12:12h light:dark cycle for some portions of the study and in constant darkness for others, with *ad libitum* access to chow and water or to a liquid diet (Osmolite 1 Cal/ml isotonic formula, Ross Nutrition). Exclusively male mice were used for both tracing and physiological experiments.

Viral vectors and experimental design

Several different adeno-associated viral vectors (AAVs) were used to drive expression of *Cre*-recombinase, green fluorescent protein (GFP) or both in transduced cells.

In one cohort, *VGlut2* $^{flox/flox}$ mice (n=5) received injections into the DMH of an AAV containing the gene for *Cre*-recombinase on a cytomegalovirus promoter (AAV-*Cre*),(serotype 10, titer: 1.13 x 10^{13} genome copies (GC)/ml, with yield of 7.11 x 10^{12} GC/ml). The effectiveness and specificity of *VGlut2* exon 2 deletion by injecting this AAV into *VGlut2* $^{flox/flox}$ mice has been demonstrated previously (Krenzer et al., 2011). For the control experiment, age-matched *VGlut2* $^{flox/flox}$ mice (n=5) had injections of an AAV containing the gene for Aquaphora GFP (humanized UF5 form) on a cytomegalovirus promoter (AAV-GFP), (serotype 8, titer: 6x10^{6} GC/ml) containing the same cassette as described in (Chamberlin et al., 1998).

In a second cohort, *VGlut2* deletion from the DMH was achieved via injection of an AAV containing both the genes for Cre recombinase and GFP (AAV-GFP-ires-Cre) into *VGlut2* $^{flox/flox}$ mice (n=7). This vector was produced by the Harvard Gene Therapy Initiative, Boston by Dr. Jeng-Shin Lee (serotype 8, titer: 8.1 x 10^{12} GC/ml). Effectiveness and specificity of *VGlut2* exon 2 deletion by injecting this AAV into *VGlut2* $^{flox/flox}$ mice has also been demonstrated previously by our group (Kaur et al., 2013). Again, the control group consisted of age-matched *VGlut2* $^{flox/flox}$ mice (n=10) with injections of AAV-GFP into the DMH.

As a control to ensure that effects on physiology seen with Cre expression in *VGlut2* $^{flox/flox}$ mice are indeed due to *VGlut2* exon2 excision and not nonspecific effects of transduction by the vector, a cohort of wild-type mice (n=6) received AAV-GFP-ires-Cre injections into the DMH.

Brain injections

Mice were anesthetized with an intraperitoneal injection of ketamine-xylazine (100mg/kg ketamine, 10mg/kg xylazine) and placed in a stereotaxic apparatus (David Kopf Instruments, Tujunga, CA). Under aseptic conditions the brain was exposed and an injection of viral vector delivered through a glass pipette using an air pressure injection system. The incision was closed with suture and the animals given subcutaneous injections of the analgesic meloxicam (0.2 mg, daily for two days). To delete *VGlut2* exon 2 for physiological experiments, bilateral injections of 50-60 nl of AAV-Cre or 170-200 nl of AAV-GFP-ires-Cre were placed into the DMH (AP -1.75; DV -5.0; RL ±0.4) of *VGlut2* $^{flox/flox}$ mice. For control experiments, 50-70 nl of AAV-GFP were injected bilaterally into the same location in *VGlut2* $^{flox/flox}$ mice, or 170-200 nl of AAV-GFP-ires-Cre were injected bilaterally using the same coordinates in wild type mice. Three to four weeks were allowed for postoperative recovery and for expression of the Cre and/or GFP genes encoded in the viral vectors.

Telemetric recording

Body temperature and spontaneous home cage locomotor activity were measured using radiofrequency biotelemetry transmitters (TA10TA-F20; Data Sciences International). These were implanted intraperitoneally using aseptic technique in the same session of anesthesia during which brain injections were performed. Animals were allowed 3-4 weeks of time for postoperative recovery and for the viral vectors to deliver and express Cre and or GFP genes within neurons. Spontaneous home cage locomotor activity and body temperature were then recorded from mice entrained to a 12:12h light:dark cycle (LD) for at least 5 days and from mice free-running in constant darkness (DD) for at least 10 days. During recordings, mice remained in their home cages with *ad libitum* access to chow and water. Their cages were housed atop DSI telemetry receivers connected to a microcomputer acquisition system. Cages and receivers were inside light-tight, fully ventilated cabinets for the duration of the recordings.

Ambient temperature inside the recording cabinets was maintained at 22±1ºC, and light:dark cycles were controlled via programmable switch timers. Core body temperature was measured every 5 minutes and locomotor activity was recorded in 5 minute bins.

Rotarod test

To check for motor control deficits in mice with VGlu2 deletion in the DMH, these animals and AAV-GFP-injected controls from the same cohort were trained and tested for performance on an accelerating rotarod (Ugo Basile, mouse rota-rod). Training consisted of sessions where each animal was given 5 trials on a rotating beam 6 inches above a platform which accelerated from 2-40 rpm over 4min., with 5min. rest periods in between trials. Testing sessions consisted of 7 such trials, where performance was the average amount of time a given mouse was able to able to run on the beam before falling to the platform below per trial. To control for circadian effects on performance, mice had three training sessions from 4-6pm on three consecutive days, followed by two testing sessions from 4-6pm on the following two days. All mice were fully entrained to a 12:12 light:dark cycle with lights-off at 7pm during training and testing.

Measurement for liquid diet intake and corticosterone rhythm

Since corticosterone levels respond rapidly to stress, repeated measurement of this hormone must be done using a minimally invasive approach which is not stressful to the subject. For this reason we opted to measure urinary corticosterone from samples collected every 4 hours over the course of a day with the aid of metabolic cages (Tecniplast, West Chester, PA), starting after 24 hours of habituation to the metabolic cages. This was done both in mice that were entrained to a 12:12h LD cycle and in mice that were free-running in constant darkness (DD) for at least 10 days prior to urine sample collection. To ensure that a large enough volume of urine could be collected at each time point, mice were maintained on a liquid diet (Osmolite 1 Cal/ml isotonic formula, Ross Nutrition) for the duration of this experiment. This diet is isotonic, and mice do not lose weight after one week of access to exclusively this diet. Bottles of liquid diet were changed every 12 hours to minimize bacterial growth. Liquid diet intake was measured by recording drinking bottle weight every 4 hours as urine samples were being collected. To allow for

habituation, mice in their home cages were switched from a chow and water diet to liquid diet 4 days prior to the start of urine sample collection and were then transferred from their home cages to metabolic cages 24 hours prior to the start of sample collection. To measure phase of free-running animals reliably, body temperature and locomotor activity rhythms were recorded for at least 8 days before habituation to metabolic cages. All mice run together in DD showed a sharp rise in body temperature within 15 minutes of one another, just before the onset of the subjective dark period. Corticosterone concentration was measured using an ELISA assay kit (Enzo Life Sciences), and for each sample, concentration measured was multiplied by the volume of sample collected to calculate amount excreted per 4-hour interval.

Tissue Preparation

After physiological and behavioral experiments were completed mice were anesthetized with chloral hydrate (10 mg/kg) and underwent transcardial perfusion with 0.9% saline followed by 10% neutral buffered formalin (Sigma). Brains were removed and postfixed for approximately 3 hours in formalin then allowed to equilibrate for at least 12 hours in a 20% sucrose solution in phosphate buffered saline with 0.01% sodium azide. Brains were subsequently sectioned at 30 µm on a freezing microtome into four series.

Immunohistochemistry

Immunohistochemistry was performed on floating sections following a protocol described in previous publications (Bruinstroop et al., 2011), and as described in thesis chapter 2. Sections were rinsed at least three times for 5-10 minutes in 0.1M phosphate buffered saline (PBS), pH 7.4, for 1 hour, then were incubated in 0.3% hydrogen peroxide to block endogenous peroxidase activity. Following at least three more rinses in PBS, sections were incubated for at least 16 hours in a solution containing the appropriate primary antibody (see below) in PBS containing 0.3% Triton X-100 and 0.01% sodium azide. Sections were then rinsed at least three more times in PBS before a one-hour incubation in a corresponding secondary antibody (see below for specific information), rinsed three more times in PBS, and then incubated for 60-90 minutes in an avidin-biotin complex solution (Elite ABC, Vector Laboratories). After three more PBS rinses, the tissue was moved to a solution containing 1% 3,3'-

diaminobenzidine (DAB) and reacted with 0.01% hydrogen peroxide to visualize the sites containing antigen in the tissue. Once the desired staining intensity was reached, this reaction was quenched with several rinses of the tissue in a PBS solution containing 0.01% sodium azide. Sections were then mounted onto gelatin coated glass slides and allowed to dry overnight at room temperature. This was followed in some cases by silver-gold enhancement and/or counterstaining with thionin. Silver-gold enhancement consisted of a 30 - 45 minute incubation of desalinated slides in 1% silver nitrate solution at 56 °C, followed by three rinses with water, a 10-20 minute incubation in 0.1% gold chloride, three more rinses and a brief treatment with 5% sodium thiosulfate solution until the tissue reaches the desired background level. All slides were rinsed in distilled water before they were dehydrated in graded alcohols then cleared in xylene for at least 2 hours and cover-slipped with Permaslip medium (Alban Scientific, St. Louis, MO). Counterstained sections were incubated briefly in thionin solution and differentiated in acid alcohol prior to dehydration.

Neurons labeled with the AAV-GFP or AAV-GFP-ires-Cre vectors were visualized with a primary antibody against GFP raised in rabbit against Aquaphora GFP protein (Molecular probes/Invitrogen ca# A6455 Lot# 771568), used at a concentration of 1:20,000. This was followed by rinses and incubation with a biotinylated donkey anti-rabbit secondary (Jackson Immunoresearch Laboratories) used at a 1:1,000 dilution. This antibody did not label any neurons above background level in tissue from uninjected animals or AAV-Cre-injected animals.

Neurons transduced with the AAV-Cre vector were identified via immunolabeling for Cre protein with a monoclonal primary antibody raised in mouse against the Cre recombinase (aa 77 and 343) fusion protein (clone 2D8), (Millipore/Chemicon cat# MAB3120 Lot# LV1414478) used at a dilution of 1:20,000. This antibody does not label any neurons above background level in tissue from un-injected animals or AAV-GFP-injected animals.

Microscopy and photography

Slides were examined and photomicrographs were acquired with a Zeiss Axioplan 2 microscope with a 1.5 megapixel color Evolution MP camera (MediaCybernetics, Bethesda, MD) using Axiovision

software. The images were then processed with Adobe Photoshop software to optimize the brightness/contrast.

Data analysis

Lesion assessment

For each case, whether a *VGlut2* $^{flox/flox}$ mouse injected with AAV-Cre (whose brain tissue was subsequently immunolabeled for Cre recombinase) or a *VGlut2* $^{flox/flox}$ mouse injected with AAV-GFP-ires-Cre (whose brain tissue was subsequently immunolabeled for GFP), lesion extent was quantified by mapping the area of transduced neurons within the DMH (at two rostrocaudal levels: AP – 1.7 and AP – 1.9) and DMH/DHA (at AP – 1.7). Locomotor activity and corticosterone data were analyzed using area of the two DMH levels covered as the criterion for a successful lesion case, while temperature data was analyzed using area of DMH/DHA at AP – 1.7 covered as the criterion. This approach was used because staining for Cre in AAV-Cre-injected mouse brains labels only transduced cell nuclei in a clearly distinguishable way (see Fig 3.1 A-C). However, the AAV-GFP-ires-Cre does not produce Cre recombinase at sufficiently high levels to cause reliable dense staining. (This is not a problem, as it takes only one Cre molecule per cell to cause the recombination event, so even very low levels of expression are sufficient to cause the deletion of the Vglut2 exon 2, as shown in Kaur et al., 2013). In these cases, we instead stained for GFP, which labels cell bodies and processes creating much more spatial overlap of labeled structures, and making it more difficult to distinguish individual GFP-labeled neurons and hence to quantify the actual number of transduced neurons (see Fig. 3.1 D-C), (see Technical Considerations in Discussion). However, assessment at high magnification suggested that the two viral vectors had similar infection efficiency within the DMH. Thus in order to apply identical techniques for quantification of the extent of the genetic deletions across the two cohorts, each injection site (i.e. the region of transduced cells) was mapped onto a brain template at the appropriate rostrocaudal level using a camera lucida (Leitz Wetzlar). These drawings were digitized using a Wacom Intuos PTK-1240 tablet and Adobe Illustrator Software, and the percentage of DMH area covered by transduced cells was quantified using ImageJ software (NIH). Only cases in which at least 50% of the DMH area (across the two rostrocaudal levels) was covered on each side of the brain were considered successful bilateral injections and used for

Figure 3.1 A series of photomicrographs to illustrate two injection sites in the brain of (A-C) one AAV-Cre injected case (NV42, with approximately 96% coverage), stained for Cre-recombinase, and (D-F) one AAV-GFP-ires-Cre injected case (NV138 with approximately76% coverage), stained for GFP. Panels G-I show reference sections at corresponding rostro-caudal levels from the Allen Mouse Brain Atlas (Lein et al., 2007). The DMH at each level is outlined in black.

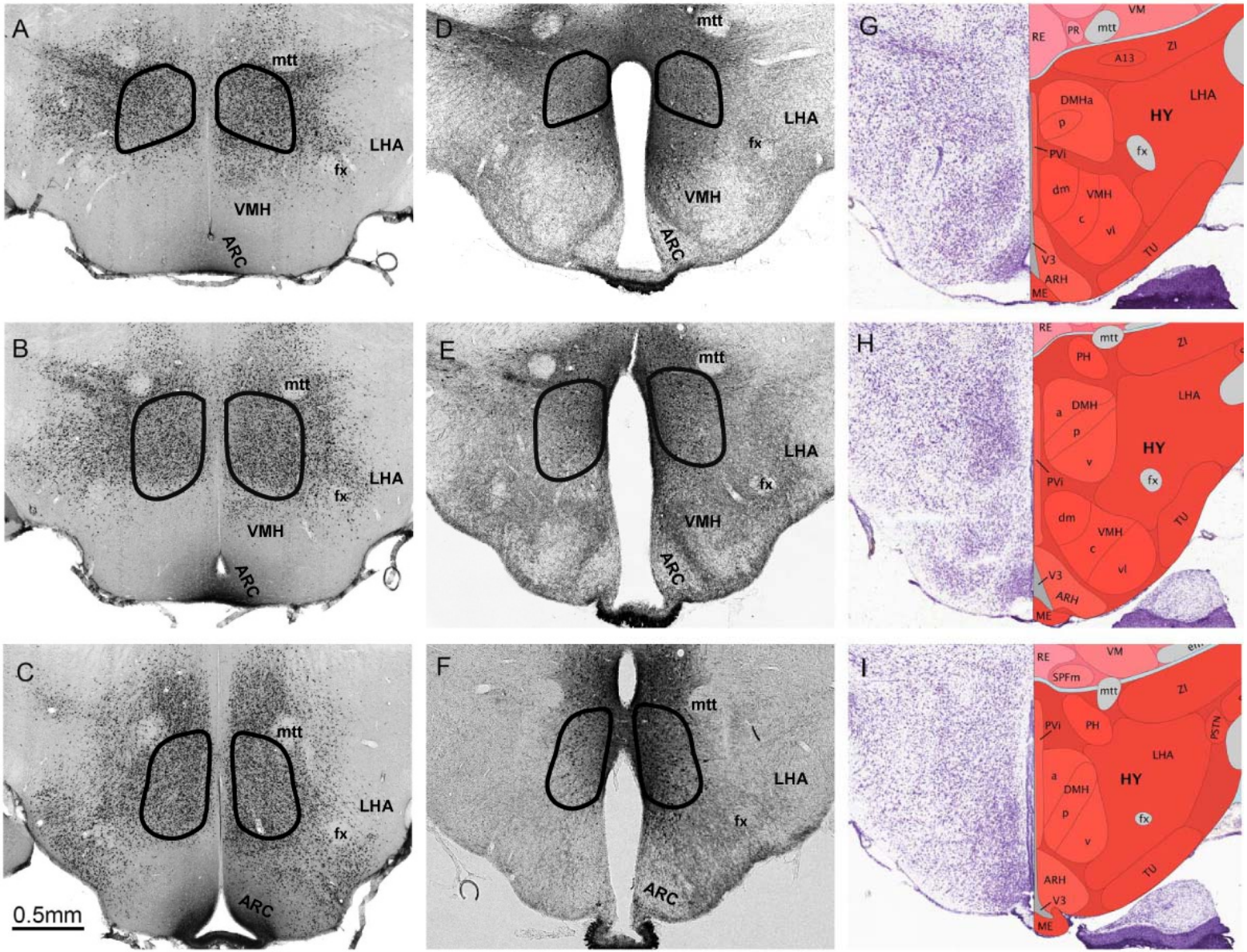

Figure 3.1 (continued)

physiological analysis. This 50% minimum cutoff was employed to avoid potential confounding effects of highly asymmetrical injections, and average coverage per side in successful cases was well above 50% (see results). All injection mapping was done blind with respect to case number or physiology of the animal in question. Calculation of the phase, amplitude or baseline of each rhythm was done blind to the case number or lesion extent of each animal.

Analysis of behavioral and physiological output measures

For all output measures, amplitude of circadian or diurnal oscillation was calculated as circadian index (CI), using the following formula: $CI = (mean_{night} - mean_{day})/mean_{24h}$, normalized to 100% for the control group, where $mean_{night}$ is the average over the subjective dark period, $mean_{day}$ is the average over the subjective light period, and $mean_{24h}$ is the average over the entire subjective day. For mice in DD, the free-running period was calculated using a chi-squared periodogram, and timing of subjective night and day were assessed visually on raster plots, using Clocklab software (Actimetrics, Wilmette, IL). Telemetric recordings of body temperature required special consideration, as there were occasionally spurious readings due to electrical noise (usually with a single out of range reading) and in some cases progressive shifts in the baseline of temperature readings representing loss of proper temperature calibration approaching the end of the battery life of the transmitter. Temperature recordings from five animals were discarded from analysis for the latter reason. To correct for the former, we created a filtering application which identified temperature readings above 40ºC, below 30ºC, or readings that were more than 2ºC different from immediately flanking readings (taken only 5 minutes before/after), and replaced them with NaN placeholders. This was done prior to any other analysis of body temperature recordings.

Statistics

Data is graphed and reported as mean±SEM. Linear mixed models were used to assess the effects of *VGlut2* loss in the DMH on the CI and absolute levels of various physiological and behavioral parameters measured (locomotor activity, body temperature, urinary corticosterone levels, urine volume, and liquid diet intake). For these tests, light cycle (entrained vs. free-running conditions), lesion condition (control

vs. *VGlut2* loss in the DMH) and the interaction between the two were treated as fixed factors, while the effect of individual subject was treated as random. Linear mixed models were also used to check for differences in body temperature and activity level between the active and inactive period in mice with *VGlut2* deletion in the DMH and controls in both free-running and entrained conditions. Here, (subjective) light vs. dark and lesion condition were treated as fixed factors and the effect of individual subject was treated as random. Paired t-tests were used to check for differences in the CI and absolute levels of locomotor activity and body temperature in wild type controls before and after they were injected with Cre-expressing viral vector. The effect of VGlut2 loss in the DMH on rotarod performance was estimated using an unpaired student's t-test (with equal variances not assumed). All statistical tests were performed using SPSS 21 (IBM, SPSS, Chicago, IL, USA). The alpha value was set to $P < 0.05$ (two tailed) for main effects, and $P < 0.10$ (two tailed) for interaction effects.

Results

Twelve *VGlut2*$^{flox/flox}$ mice had injections of Cre-expressing vectors placed successfully, bilaterally in the DMH, and fifteen *VGlut2*$^{flox/flox}$ mice served as controls, with bilateral injections of vector expressing only GFP into the same site. These mice came from two cohorts, with two different Cre-expressing vectors used: n=5 mice had AAV-Cre injected into the DMH (see Fig. 3.1A) and these had locomotor activity and body temperature measured in parallel with n=5 AAV-GFP control mice; n=7 mice had AAV-GFP-ires-Cre injected into the DMH (see Fig. 3.1B) and these mice had locomotor activity, body temperature, urinary corticosterone output and liquid diet intake measured in parallel with n=10 AAV-GFP-injected control mice. Here we show data from the two cohorts pooled (with locomotor activity counts and circadian indices of activity and temperature normalized to the appropriate controls). Effects seen within each cohort independently are extremely similar. Among the n=12 mice with bilateral VGlut2 deletion in the DMH whose activity data was compared to controls, average DMH area covered by Cre-transduced cells was 77% per side. Temperature recordings from n=13 controls and n=9 mice with *VGlut2* deletion in the DMH were usable for analysis. These 9 mice had on average 90% DMH/DHA coverage per side. Reliable, phase-aligned liquid diet intake and corticosterone output data was available

from n=5 control mice and n=5 mice with *VGlut2* deletion in the DMH (all from the AAV-GFP-ires-Cre cohort) with on average 72% DMH coverage per side.

Loss of *VGlut2* expression in the DMH disrupts daily locomotor activity rhythms and levels and lowers body temperature

Raster plots showing double-plotted temperature and activity in a representative control mouse (KR18) (Fig. 3.2A, C respectively) and representative mouse with *VGlut2* deletion from the DMH (NV143) (Fig 3.2B, D), reveal that the latter had a disruption in daily locomotor activity patterns in both entrained (LD, days 1-10) and free-running (DD, day 11 on) conditions. There is a significant effect of lesion condition (control vs. *VGlut2* gene deletion) on CI (our estimate for circadian amplitude, see methods) of locomotor activity for the LD and DD measures combined (p=0.001). Univariate tests done on the LD and DD measures separately indicate that locomotor activity rhythm CI in mice with *VGlut2* deletion from the DMH is significantly lower than in controls in both LD (p=0.001) and DD (p=0.001), see Fig. 3.2E, Table 3.1. There is also a significant effect of lesion condition on average levels of locomotor activity over the whole (subjective) day, with pooled LD and DD data (p=0.013). Univariate tests show these were significantly lower in mice with *VGlut2* deletion from the DMH than controls in both LD (p=0.010) and DD (p=0.025), see Fig. 3.2F. The CI of body temperature rhythms was not significantly affected by lesion condition, or its interaction with light cycle (p=0.088 and 0.711, respectively), see Fig. 3.2A, B, G. There was, however a significant effect of lesion condition on body temperature average over the whole (subjective) day seen with combined LD and DD data (p=0.002). Univariate tests confirmed lowered body temperature (by about 0.2^{o}C in LD and 0.3^{o}C in DD) in mice with *VGlut2* deletion in the DMH compared to controls in both LD (p=0.014) and DD (p=0.001).

To investigate whether decreases in locomotor activity and body temperature occurred throughout the subjective day or were confined to the (subjective) light or dark period, linear mixed models were used to test for the effect of lesion condition, subjective light vs. dark, and the interaction of the two on locomotor activity (normalized to 100% of corresponding control animal levels to account for possible variation in factors affecting activity levels from one run of the experiment to the next) and body temperature (this variable was not normalized as it showed remarkable consistency across cohorts), see

Figure 3.2 Panels A-D: Raster plots (double plotted) showing body temperature (A, B) and locomotor activity (C, D) rhythms in a representative control mouse (A, C) and mouse with VGlut2 deletion in the DMH (B, D). The first 10 days of the recordings shown are in a 12:12 light:dark cycle (LD), with dark grey bars on top indicating the dark phase, the remaining days below are in constant darkness (DD). Panels E-H: Graphs showing circadian index (E, G) and daily averages (F, H) of locomotor activity (E, F) and body temperature (G, H).

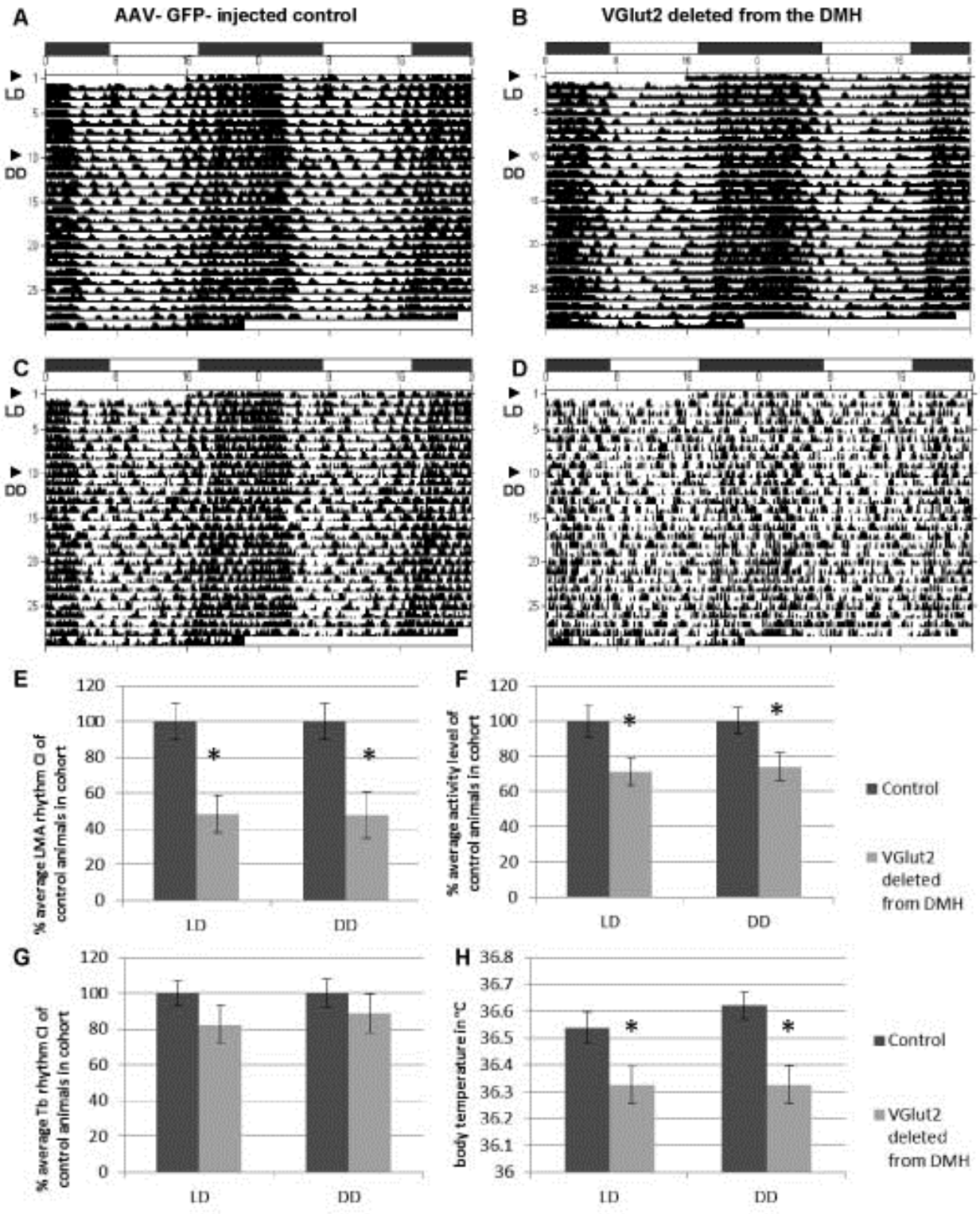

Figure 3.2 (continued)

Table 3.1 Locomotor activity and body temperature averages for the subjective dark phase, subjective light phase, and whole subjective day, as well as circadian index, calculated in both entrained and free-running conditions

	AAV-GFP control	VGlut2 deletion in DMH
entrained (LD) locomotor activity		
daily average	100.00 ± 9.20%	71.01 ± 7.87%*
light phase	100.00 ± 7.97%	94.09 ± 15.84%
dark phase	100.00 ± 9.34%	60.85 ± 7.45%*
circadian index	100.00 ± 10.26%	48.16 ± 10.47%*
free-running (DD) locomotor activity		
daily average	100.00 ± 7.40%	73.96 ± 7.84%*
subjective light phase	100.00 ± 9.56%	93.52 ± 13.31%
subjective dark phase	100.00 ± 10.95%	65.95 ± 7.00%*
circadian index	100.00 ± 10.00%	47.62 ± 12.81%*
entrained (LD) body temperature		
daily average	36.54 ±0.06	36.33 ±0.07
light phase	35.96 ± 0.08	35.87 ± 0.12
dark phase	37.09 ± 0.08	36.78 ± 0.05*
circadian index	100.00 ± 6.81%	82.32 ±10.65%
free-running (DD) body temperature		
daily average	36.62 ±0.05	36.33 ±0.07*
subjective light phase	36.15 ± 0.11	35.86 ± 0.11*
subjective dark phase	37.09 ± 0.12	36.79 ±0.07*
circadian index	100.00 ± 7.42%	88.54 ±10.96%

Fig. 3.3. In mice entrained to the LD cycle, there was a significant effect of lesion condition (p=0.038), light v. dark phase (p=0.023) and the interaction between the two factors (p=0.023) on locomotor activity levels (with type III tests of fixed effects). Univariate tests revealed a significant difference between activity levels in control mice and those with *VGlut2* loss in the DMH in the dark phase (p=0.003) but not in the light phase (p=0.631). In free-running mice, type III tests of fixed effects revealed a significant effect of both lesion condition (p=0.047) and the interaction between lesion condition and subjective light v. dark phase (p=0.099) on locomotor activity levels. Univariate tests again showed a significant difference between activity levels in control mice and those with *VGlut2* loss in the DMH in the dark phase (p=0.009) but not in the light phase (p=0.605). Taken together, these results indicate that the decrease in locomotor activity levels over the whole subjective day seen in mice with *VGlut2* loss in the DMH is attributable exclusively to a decrease in activity levels during the (subjective) dark phase, and that this decrease also accounts for the drop in CI of activity rhythms observed. A very similar pattern was seen when these tests were performed for body temperature in mice entrained to the LD cycle. There was a significant effect of lesion condition (p=0.024), light v. dark phase (p<0.000) and the interaction between the two factors (p=0.071) on average body temperature readings seen with type II tests of fixed effects. Body temperature was significantly lower in mice with *VGlut2* loss in the DMH than in controls in the dark phase (p=0.004) but not the light phase (p=0.337). However, in free-running mice, the interaction between lesion condition and subjective light v. dark phase had no significant influence on body temperature (p=0.915), whereas lesion condition (p=0.024) and subjective light v. dark phase (p<0.000) did on their own. In free-running conditions, mice with *VGlut2* expression loss in the DMH had significantly lower average body temperature readings both during the subjective dark phase (p=0.023) and the subjective light phase (p=0.023) relative to controls. A further type III test was run to ensure that the effect of the interaction between lesion condition and light cycle on (subjective) daytime body temperature was significant, and this proved to be the case (p=0.095). Univariate tests following this analysis confirmed that (subjective) light phase body temperature is significantly lower in mice with *VGlut2* loss in the DMH than in controls under free-running (DD) conditions (p=0.025) but not under light-entrained (LD) conditions (p=0.427). It is worth noting that there was no significant difference between LD light phase body temperature and DD subjective light phase body temperature of mice with *VGlut2*

Figure 3.3 Phase plots showing body temperature (A) and locomotor activity (B) rhythms averaged for n=7 mice with loss of VGlut2 in the DMH and n=9 controls that were all recorded in the same cohort, accompanied by plots showing average body temperature (C, E) and average locomotor activity counts normalized to controls (D, F) during the (subjective) light and dark phase in both entrained (LD) (panels C, D) and free-running (DD) (panels E, F) conditions, for n=9 mice with loss of VGlut2 in the DMH and n=13 controls (all mice with reliable body temperature recordings).

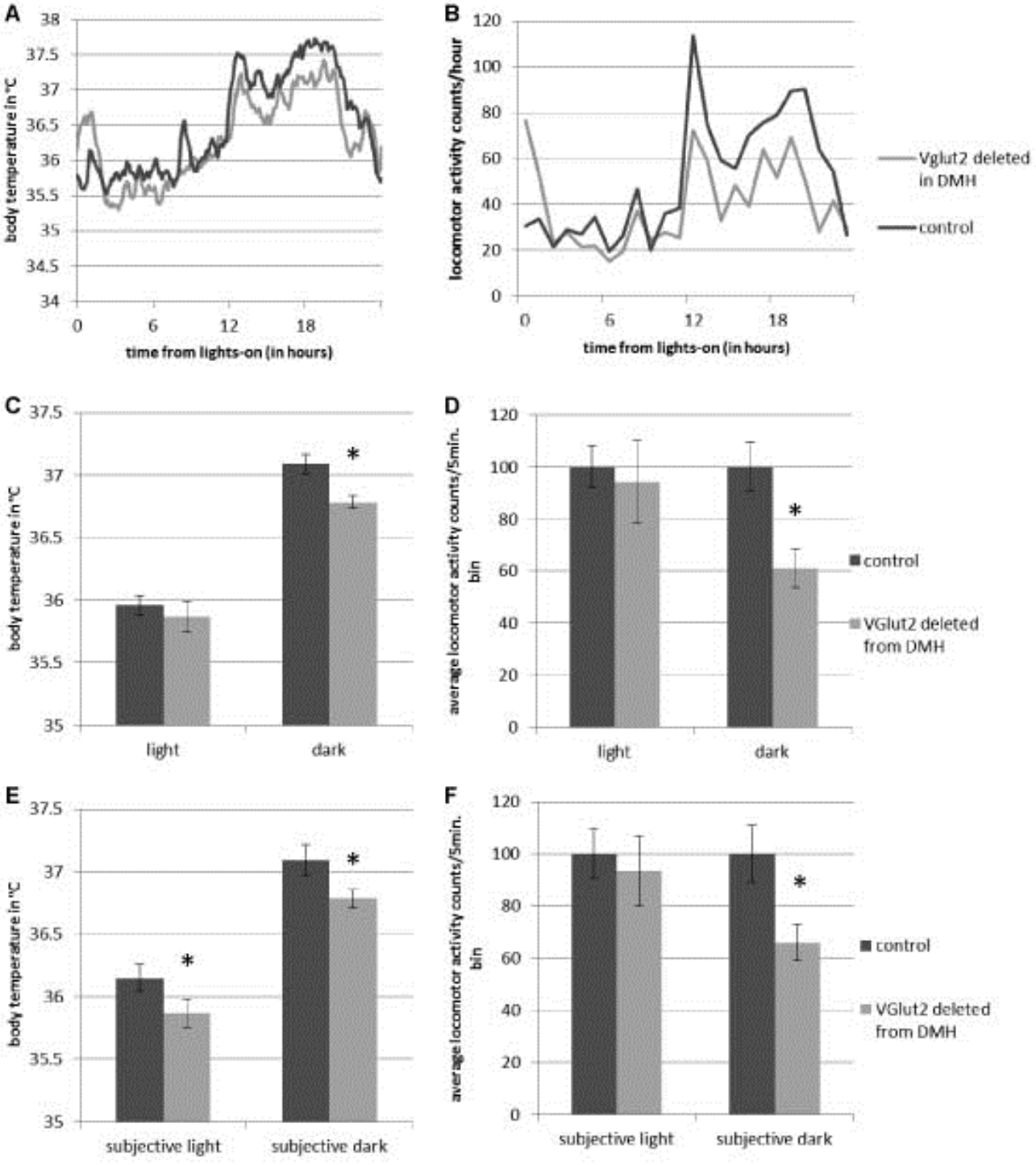

Figure 3.3 (continued)

deletion in the DMH (p=0.960). However, light phase body temperature in entrained control mice was significantly lower than subjective light phase body temperature in free-running control mice (p=0.014) suggesting that light is unable to lower body temperature in mice with *VGlut2* loss in the DMH the way it does in controls.

To determine whether injection of the AAV-GFP-ires-Cre vector itself could account for these findings, we examined wildtype animals receiving this vector before and after the injection. Paired t-tests showed no significant change in average locomotor activity (p=0.909), its CI (p=0.991), average body temperature (p=0.263), or its CI (p=0.142) (n=6) (see Table 3.2), indicating that transduction by the viral vector alone does not explain these findings, but that the effects are due to the excision of the second exon of the *VGlut2* gene by Cre recombinase in DMH neurons. To determine whether the lower activity levels in the animals with DMH deletions was due to motor impairment, we also measured their ability to maintain their balance on a rotating rod There was also no significant change in performance on thise test between controls (n=7) 208.02 ± 25.63 sec. and mice with *VGlut2* deletion from the DMH (n=4) 162.04 ± 24.46 sec., (p = 0.310), suggesting that the decrease in locomotor activity levels seen with loss of *VGlut2* in the DMH is not secondary to a deficit in mobility or motor control.

Loss of *VGlut2* expression in the DMH does not significantly affect rhythms or total daily levels of liquid diet intake

Plots of liquid diet intake rhythms under entrained (see Fig. 3.4A, C, D) and free running (see Fig. 3.4B, C, D) conditions suggest there is no difference in total daily liquid diet intake between control mice and mice with *VGlut2* deletion in the DMH (in either light cycle). This was confirmed by a linear mixed models analysis. Mice with *VGlut2* loss in the DMH showed a trend toward a decrease in the CI of their liquid diet intake rhythm under free-running (but not under entrained) conditions, but this effect was not statistically significant (effect of interaction between lesion condition and light cycle on CI of liquid diet intake rhythm p=0.182, type III test of fixed effects).

Table 3.2 Circadian index and average daily locomotor activity and body temperature in wild type control mice before and after injections of Cre-expressing vector (AAV-GFP-ires-Cre) into their DMH

	WT control pre-Cre	WT control post-Cre
free-running (DD) locomotor activity		
average for whole subjective day (raw counts)	4.90 ± 0.75	4.93 ± 0.78
average for whole subjective day (expressed as % pre-Cre average)	100.00 ± 15.39%	100.53 ± 15.92%
circadian index	100.00 ± 19.48%	99.87 ± 12.44%
free-running (DD) body temperature		
average for whole subjective day	36.47 ± 0.08	36.43 ± 0.05
circadian index	100.00 ± 11.95%	110.21 ± 9.33%

Figure 3.4 Phase plots showing liquid diet intake volumes (A, B) and urinary corticosterone amounts (E, F) measured at each of six time points in both entrained (LD) (panels A, E) and free-running (DD) (panels B, F) conditions, along with graphs showing circadian index (C,G) and daily averages (D, H) of liquid diet intake volumes (C, D) and urinary corticosterone amounts (G, H).

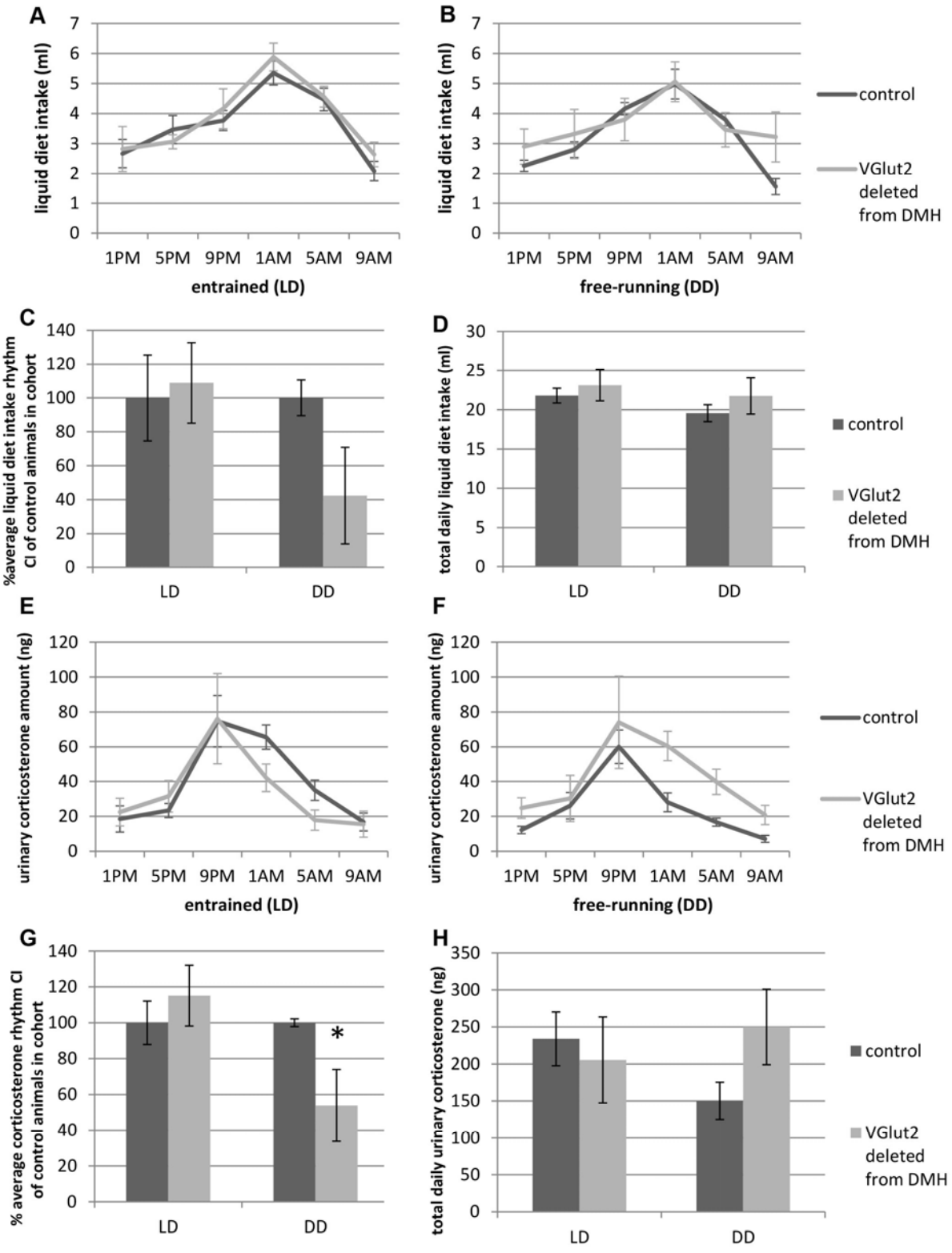

Figure 3.4 (continued)

Loss of *VGlut2* expression in the DMH blunts circadian but not diurnal rhythms in urinary corticosterone

Prior to analysis of rhythms in urinary corticosterone, we tested for potential significant effects of *VGlut2* deletion in the DMH, light cycle, or their interaction on urine output volumes or the CI of urine output volumes and found none. We also tested for effects of the above factors on the total daily amount of corticosterone excreted in the urine and found a significant effect of interaction between lesion condition and light cycle on this parameter ($p=0.065$). However, univariate tests showed no significant difference between total daily urinary corticosterone amount in control mice and mice with loss of *VGlut2* in the DMH under light-cycle entrained conditions ($p=0.827$), and fell just short of significance under free-running conditions ($p=0.053$). Testing for the effect of the same factors on the CI of urinary corticosterone, we also found a significant effect of the interaction between lesion condition and light cycle on this parameter ($p=0.049$). The CI of urinary corticosterone was significantly decreased in free-running mice with *VGlut2* loss in the DMH compared to free-running controls ($p=0.012$), but there was no significant difference between these two groups under light-cycle entrained conditions ($p=0.805$).

Discussion

In this study, we selectively deleted the expression of *VGlut2* from neurons in the DMH, to study the role of glutamatergic DMH neurons in organizing circadian rhythms. Loss of *VGlut2* from DMH neurons produced phenotypes similar to the nonspecific lesions of DMH neurons, with respect to locomotor activity and body temperature. The circadian index of locomotor activity was decreased, as was the overall level of locomotor activity, while the circadian index of body temperature was unaffected, but the mean body temperature was lowered by approximately 0.2-0.3^{o}C relative to controls. Deleting glutamatergic transmission from DMH neurons also reduced the circadian index of corticosteroid secretion, although this effect was not as great as when DMH neurons were non-selectively killed. On the other hand, unlike nonspecific lesions, which almost eliminated the circadian rhythms of food intake, we found that deletion of *VGlut2* expression from DMH neurons did not significantly affect this function.

Technical considerations

To delete the second exon of the *VGlut2* gene in DMH neurons, we stereotaxically injected adeno-associated viral vectors expressing Cre recombinase. To ensure that any effects seen were not a result of transduction with viral vectors in our *VGlut2* $^{flox/flox}$ mice, controls for these experiments were *VGlut2* $^{flox/flox}$ mice injected with AAVs that expressed only GFP. We also controlled for the possibility that Cre-expression on its own could affect function of neurons in the DMH, by injecting Cre-expressing vectors into wildtype mice as well, and saw no resultant effects on locomotor activity or body temperature. Because it is difficult to make symmetric injections of AAVs that involve the bulk of the targeted structure, we first examined the histology in our animals, and chose cases in which the deletions included the bulk of the DMH bilaterally, avoiding any cases with robust bilateral hits to other nearby structures.

Because the AAV-Cre vector expresses Cre recombinase at a higher level than the AAV-GFP-ires-Cre vector, but only one molecule of Cre is required for recombination to occur, we could not compare the completeness of the deletion by counting the absolute number of Cre-immunoreactive neurons, which was low and variable in the animals injected with AAV-GFP-ires-Cre. (In many Cre-expressor mouse lines, the levels of Cre expression are too low to stain them immunohistochemically at all, yet crosses with reporter lines demonstrate extensive Cre recombination.) Because Cre immunolabeling was not an effective way to reveal the spatial extent of viral infection in our cases with AAV-GFP-ires-Cre, immunolabeling for GFP was performed instead. While staining for Cre in AAV-Cre-injected mouse brains labels only transduced cell nuclei in a clearly distinguishable way (see Fig. 3.1 A-C), staining for GFP in AAV-GFP-ires-Cre-injected mouse brains labeled cell bodies and processes creating much more spatial overlap of labeled structures, and making it more difficult to distinguish individual GFP-labeled neurons from each other and from the plexus of labeled axonal/dendritic fibers surrounding them (see Fig. 3.1 D-F), resulting in probable undercounting of transduced DMH neurons. To compensate for these differences in quantification of the number of transduced neurons across the two cohorts, we relied on spatial mapping of the percent of the DMH (or DMH/DHA) covered by the injection sites as a quantitative measure.

We selected the two DMH levels (AP -1.7 and -1.9) based on the level at which cell-specific lesions in the DMH had strongest effects on activity and corticosterone and the levels at which cells

projecting to the LHA and VLPO are concentrated, as determined by retrograde tracing from these two DMH targets (Chou et al., 2003). The DMH/DHA subregion used corresponds to the subregion projecting robustly to the RPa, determined by retrograde tracing from the RPa (Yoshida et al., 2009).

Both of these viral vectors have previously been shown to reliably and effectively excise exon 2 of the VGlut2 gene in transduced VGlut2-expressing neurons of *VGlut2* $^{flox/flox}$ mice both via in situ hybridization for *VGlut2* exon 2 and by immunostaining for VGlut2 protein in synaptic terminals of transduced neurons (Krenzer et al., 2011; Kaur et al., 2013). Electrophysiological recordings on autapses cultured from *VGlut2* $^{flox/flox}$ mice also demonstrate that Cre-expressing neurons from these animals do not show glutamatergic excitatory post-synaptic currents in vitro (i.e. no excitatory post-synaptic currents that could be recorded from Cre-positive neurons are blocked by glutamate receptor antagonists) (Tong et al., 2007). Tong and colleagues also showed that *VGlut2* $^{flox/flox}$ mice crossed to a Cre-expressing line fail to show an increase immediate early gene expression in synaptic targets of the Cre-expressing neurons after stimuli known to drive the Cre-positive cells.

Glutamatergic neurotransmission by DMH neurons is necessary for reaching normal levels of locomotor activity during the (subjective) dark phase

VGlut2 deletion in the DMH decreased the amplitude of locomotor activity rhythm to roughly half that of controls in both free-running and entrained conditions. This came from a significant drop in (subjective) night-time (i.e. dark phase) activity levels, as there was no significant change to (subjective) daytime (i.e. light phase) activity amounts. In both free-running and entrained conditions, the average daily locomotor activity was reduced to approximately 75% of that seen in controls. Since mice with these genetic deletions did not show impaired performance on a rotarod task, we believe the decreased nocturnal activity was not secondary to any kind of motor outflow impairment, but may be related to changes in motivation, wakefulness, consolidation of wakefulness, or some interaction thereof.

By comparison, cell-specific lesions in the DMH lower the amplitude of locomotor activity rhythms to approximately 10% that of controls and decrease total daily locomotor activity levels to roughly one third of levels seen in controls (Chou et al., 2003). Activity counts are lowered both during the subjective light and dark phase, though there is a larger decrease for the subjective dark phase.

Taken together this suggests that glutamatergic neurotransmission in DMH neurons is certainly involved in driving activity rhythms during the dark phase, but cannot account for the full role of the DMH in determining the amount of locomotor activity over the course of the day on its own. It appears most likely that non-glutamatergic DMH efferents (such as its GABAergic projection to the VLPO) are also critically involved in driving normal daily patterns in locomotor activity. That said it is possible that differences in the effect of cell specific lesions vs. *VGlut2* deletions on activity levels across the day are also in part accounted for by species differences between rats and mice, and/or that we saw milder effects with *VGlut2* deletions because they involved a smaller fraction of DMH neurons than excitotoic lesions.

Glutamatergic neurotransmission by DMH/DHA neurons is necessary for maintenance of normal core body temperature throughout the day

Loss of *VGlut2* expression in our experiments decreased core body temperature by approximately 0.3ºC, thus lowering it to the same extent as complete cell-specific DMH lesions in rat (Chou et al., 2003). Hence it is likely that the effect of the neurons in the DMH region on supporting baseline core body temperature is chiefly, if not completely, dependent on its glutamatergic efferents. Studies in rats have shown that a specialized population of glutamatergic neurons, in the DMH/DHA along the dorsal border of the DMH, has direct projections to the raphe pallidus nucleus. The raphe pallidus innervates sympathetic preganglionic neurons in the spinal cord that drive brown adipose tissue thermogenesis and cutaneous vasoconstriction that conserves heat (Zaretskaia et al., 2003; Zaretsky et al., 2003a; Zaretsky et al., 2003b). Thus the input from the DMH/DHA to the raphe pallidus is likely to play a major role in maintaining Tb.

Conditional tracing using injections of a viral vector with a loxP-flanked stop codon upstream of the GFP gene (Gautron et al., 2010) into a *VGlut2*-Cre mouse line (Vong et al., 2011) reveals a robust glutamatergic projection from the DMH/DA to RPa (Vujovic, unpublished results). Furthermore we observe GFP-labeled fibers in the RPa in AAV-GFP-ires-Cre-injected *VGlut2*$^{flox/flox}$ mice showing a decreased body temperature.

The decrease seen in body temperature may also to some extent be secondary to the decrease in locomotor activity seen with this manipulation, however, this cannot account for the full magnitude of the effect. The selective decrease in activity levels during the subjective (and objective) dark phase accounts for both the reduction in total daily activity counts and the amplitude of activity rhythms, whereas there is no significant reduction in the amplitude of body temperature rhythms. Furthermore, during the subjective light period in free-running conditions, we saw a significant decrease in body temperature but not locomotor activity of mice with *VGlut2* loss in the DMH relative to controls.

The fact that body temperature in mice with *VGlut2* loss in the DMH is equally low in the subjective light phase during free running conditions and the objective light phase of entrained conditions, whereas control mice show a lowered temperature in objective light, suggests that *VGlut2* loss in the DMH also prevents normal lowering of body temperature in response to light.

Glutamatergic neurotransmission in DMH neurons is necessary for normal circadian rhythms in corticosterone excretion

Deletion of *VGlut2* from the DMH causes a change in the circadian but not diurnal rhythm in corticosterone excretion. In free-running conditions, the amplitude of the circadian rhythm of corticosterone excretion is lowered to roughly half that seen in controls. In this, VGlut2 deletion resembles the effects of complete excitotoxic (Chou et al., 2003) or electrolytic (Bellinger et al., 1976) DMH lesions in rat, which dramatically lower the amplitude of circadian rhythms in corticosteroids. However, with complete DMH lesions in the rat, this decrease in amplitude comes from a reduction in corticosteroid levels during the subjective dark phase (the phase during which they peak in controls), whereas in mice with *VGlut2* deletion in the DMH the peak is retained and it is the trough that appears altered. While complete DMH lesions in rat lower average daily plasma corticosteroid levels nearly in half, deletion of *VGlut2* in the DMH of mice does not cause a significant decrease in daily corticosterone levels. There is instead an upward trend in total corticosterone levels excreted over the course of a day in free-running conditions, which falls just short of reaching statistical significance ($p=0.053$, see results). Thus while glutamatergic neurons in the DMH do appear involved in mediating normal circadian oscillation in corticosterone, there may be other cell groups playing equally important roles.

However, several important caveats must factor into a comparison between the results reported here and those found following excitotoxic lesions of the DMH in rat. Not only were the studies performed on two different species, but they also used two different techniques to measure two different indicators of corticosteroid levels in the body. Chou et al. report levels of corticosteroids in blood plasma, sampled throughout the day with the aid of an indwelling intravenous catheter. We measured amounts of corticosterone in urine sampled throughout the day with the aid of metabolic cages. The peak of urinary corticosterone lags that of plasma corticosterone by several hours. Levels of plasma corticosteroids can be influenced by the hypothalamo-pituitary adrenal axis, sympathetic input to the adrenal gland and the molecular clock in the adrenal gland, as well as interaction of three (please see Chapter 1 "How does the circadian timing system communicate with brain regions regulating autonomic and neuroendocrine functions?"). In addition, levels of urinary corticosteroids can be influenced by factors affecting the rate at which corticosteroids are metabolized or filtered into urine, including circadian clocks in the kidney and liver, sympathetic or parasympathetic input to these organs, or any other factor that can influence renal and hepatic handling of glucocorticoids.

The above considerations make pinpointing the neural pathway by which glutamatergic neurons in the DMH influence corticosteroid rhythms extremely difficult, although there are certain possibilities that can be eliminated. The significant decrease in the amplitude of circadian rhythms of corticosterone observed in mice with *VGlut2* gene loss in the DMH is unlikely to depend on a direct glutamatergic projection from the DMH to corticotropin-releasing hormone (CRH) neurons in the parvicellular PVH. CRH neurons actively drive corticosterone production and release from the adrenal gland, hence, it is to be expected that withdrawing direct excitatory input to them would lead to a decrease (not an increase) in plasma and urine levels of corticosteroids. The observed effect could be caused by an indirect (multisynaptic) projection in to CRH neurons, which would have a net inhibitory effect on them, and normally function to suppress corticosterone production during the subjective day. It is also possible that glutamatergic projections from the DMH modulate renal, adrenal or hepatic sympathetic nerve input in a way that would alter levels of corticosterone excreted in the urine at various times of day. Finally, peripheral molecular clocks in the adrenal gland have been shown to influence rates of glucocorticoid release into central circulation (Son et al., 2011; Ota et al., 2012) and the amplitude and synchrony of

their oscillations could be affected by a number of factors, notably by timing of food intake or locomotor activity, that may depend on the DMH.

Glutamatergic neurotransmission in DMH neurons is not critical for circadian or diurnal rhythms in nutrient intake

Unlike rats with excitotoxic (Chou et al., 2003) or electrolytic (Bernardis, 1973; Bellinger et al., 1976) lesions in the DMH, which showed a dramatic reduction in the amplitude of circadian rhythms in feeding, mice with *VGlut2* loss in the DMH did not show a consistent reduction in circadian rhythms of nutrient intake (see Fig. 3.4B, C). Importantly, in addition to species differences between these experiments, there was also a critical methodological difference: the mice were sustained on a liquid diet during the experiment measuring caloric intake across the day, to some extent conflating the feeding and drinking rhythms, while the rats were simply fed a chow diet, so a comparison is not straightforward. In our study, the use of liquid diet was necessary for two reasons: (a) mice on chow diet did not excrete a high enough urine volume at a high enough frequency to allow for measurement of urinary corticosterone at six time points and (b) because mice consume very small volumes of solid food or water in a 4-hour time interval, sustaining them on a liquid diet meant each mouse consumed a larger volume between each of the six time points and provided a means to quantify the amount of nutrients consumed at different times of day with reduced measurement error.

It is certainly possible that deletion of *VGlut2* in the DMH does not significantly lower the amplitude of nutrient intake in mice because other, DMH neurotransmitters are responsible for driving this rhythm. However, it is also possible that glutamatergic neurons in the DMH are involved in circadian regulation of food intake but that this experiment was not sufficiently powered in terms of animal numbers to reveal this effect.

Light cycle effects on body temperature and corticosterone excretion rhythms

The light cycle significantly affects the difference between control animals and those with *VGlut2* loss from the DMH with respect to their daytime body temperature and the amplitude of their corticosterone rhythm. Mice with *VGlut2* deletion in the DMH only show a lowered daytime body

temperature and lower amplitude corticosterone excretion rhythm (relative to controls) in free-running conditions.

In the case of body temperature, this difference appears to be caused a by a reduction of daytime (i.e. light phase) temperature in entrained as opposed to free-running control mice, as there is no significant difference in daytime temperature between free-running and entrained mice with loss of *VGlut2* in the DMH. This is consistent with previous reports in the literature of light acutely lowering body temperature in nocturnal rodents (Morin, 2013; Muindi et al., 2013; Studholme et al., 2013). The fact that light does not seem to have this effect in mice with *VGlut2* deletion in the DMH suggests either that acute effects of light on body temperature are dependent on glutamatergic signaling from the DMH (i.e. happen upstream of or at the level of the DMH in the context of outflow circuitry), or that the genetic lesion creates a floor effect on baseline temperature, where light cannot suppress it further without activating homeostatic systems which keep it no lower than 35.8±0.15ºC.

In the case of corticosterone excretion rhythms, the difference seems to be accounted for by an increased daytime corticosterone excretion in free-running compared to entrained mice with *VGlut2* deletion from the DMH. This suggests that light could act to lower daytime corticosterone production or release in LD-entrained mice with *VGlut2* loss in the DMH. It thus suggests that (direct or indirect) input from the retina must act on structures affecting corticosterone release which are further downstream in the outflow circuit than excitatory neurons in the DMH. However, light effects on urinary corticosterone levels in these mice may not be, and indeed do not seem to be the same as acute light effects on corticosterone in intact rodents (Ishida et al., 2005; Mohawk et al., 2007).

Conclusions

Taken together, the results of selective *VGlut2* deletion from the DMH suggest that glutamatergic neurotransmission from DMH neurons may be single-handedly responsible for its role in thermoregulation, and may be necessary for normal lowering of body temperature in response to light. Together with other neurotransmitters in the DMH, glutamate in this region plays a significant role in establishment of circadian and diurnal rhythms in locomotor activity and maintenance of normal daily activity levels. Glutamatergic DMH neurons seem to impact urinary corticosterone levels in a light-

dependent manner, such that loss of VGut2 in the DMH blunts free-running but not entrained rhythms of urinary corticosterone.

Acknowledgments

We would like to thank Quan Ha and Sathyajit Bandaru for superb technical assistance, Vetrivelan Ramalingam for thoughtful input on result interpretation, and Janet Mullington and Monika Haack for assistance with statistical methods. This work was supported by USPHS grants NS072337, AG09975 awarded to C. Saper and the F31 NS071890-03 and NSFGRFP fellowships awarded to N. Vujovic.

References

Abrahamson EE, Moore RY (2001) Suprachiasmatic nucleus in the mouse: retinal innervation, intrinsic organization and efferent projections. Brain research 916:172-191.

Bellinger LL, Bernardis LL, Mendel VE (1976) Effect of ventromedial and dorsomedial hypothalamic lesions on circadian corticosterone rhythms. Neuroendocrinology 22:216-225.

Bernardis LL (1973) Disruption of diurnal feeding and weight gain cycles in weanling rats by ventromedial and dorsomedial hypothalamic lesions. Physiology & behavior 10:855-861.

Bruinstroop E, Cano G, Vanderhorst VG, Cavalcante JC, Wirth J, Sena-Esteves M, Saper CB (2011) Spinal projections of the A5, A6 (locus coeruleus), and A7 noradrenergic cell groups in rats. The Journal of comparative neurology.

Chamberlin NL, Du B, de Lacalle S, Saper CB (1998) Recombinant adeno-associated virus vector: use for transgene expression and anterograde tract tracing in the CNS. Brain research 793:169-175.

Chou TC, Scammell TE, Gooley JJ, Gaus SE, Saper CB, Lu J (2003) Critical role of dorsomedial hypothalamic nucleus in a wide range of behavioral circadian rhythms. The Journal of neuroscience : the official journal of the Society for Neuroscience 23:10691-10702.

Cline HT (2001) Dendritic arbor development and synaptogenesis. Current opinion in neurobiology 11:118-126.

Dimicco JA, Zaretsky DV (2007) The dorsomedial hypothalamus: a new player in thermoregulation. American journal of physiology Regulatory, integrative and comparative physiology 292:R47-63.

Elmquist JK, Ahima RS, Elias CF, Flier JS, Saper CB (1998) Leptin activates distinct projections from the dorsomedial and ventromedial hypothalamic nuclei. Proceedings of the National Academy of Sciences of the United States of America 95:741-746.

Elmquist JK, Coppari R, Balthasar N, Ichinose M, Lowell BB (2005) Identifying hypothalamic pathways controlling food intake, body weight, and glucose homeostasis. The Journal of comparative neurology 493:63-71.

Gautron L, Lazarus M, Scott MM, Saper CB, Elmquist JK (2010) Identifying the efferent projections of leptin-responsive neurons in the dorsomedial hypothalamus using a novel conditional tracing approach. The Journal of comparative neurology 518:2090-2108.

Ishida A, Mutoh T, Ueyama T, Bando H, Masubuchi S, Nakahara D, Tsujimoto G, Okamura H (2005) Light activates the adrenal gland: timing of gene expression and glucocorticoid release. Cell metabolism 2:297-307.

Kaur S, Pedersen NP, Yokota S, Hur EE, Fuller PM, Lazarus M, Chamberlin NL, Saper CB (2013) Glutamatergic signaling from the parabrachial nucleus plays a critical role in hypercapnic arousal. The Journal of neuroscience : the official journal of the Society for Neuroscience 33:7627-7640.

Krenzer M, Anaclet C, Vetrivelan R, Wang N, Vong L, Lowell BB, Fuller PM, Lu J (2011) Brainstem and spinal cord circuitry regulating REM sleep and muscle atonia. PloS one 6:e24998.

Mohawk JA, Pargament JM, Lee TM (2007) Circadian dependence of corticosterone release to light exposure in the rat. Physiology & behavior 92:800-806.

Morin LP (2013) Nocturnal light and nocturnal rodents: similar regulation of disparate functions? Journal of biological rhythms 28:95-106.

Morrison SF, Madden CJ, Tupone D (2012) Central control of brown adipose tissue thermogenesis. Frontiers in endocrinology 3.

Muindi F, Zeitzer JM, Colas D, Heller HC (2013) The acute effects of light on murine sleep during the dark phase: importance of melanopsin for maintenance of light-induced sleep. The European journal of neuroscience 37:1727-1736.

Ota T, Fustin JM, Yamada H, Doi M, Okamura H (2012) Circadian clock signals in the adrenal cortex. Molecular and cellular endocrinology 349:30-37.

Son GH, Chung S, Kim K (2011) The adrenal peripheral clock: glucocorticoid and the circadian timing system. Frontiers in neuroendocrinology 32:451-465.

Studholme KM, Gompf HS, Morin LP (2013) Brief light stimulation during the mouse nocturnal activity phase simultaneously induces a decline in core temperature and locomotor activity followed by EEG-determined sleep. American journal of physiology Regulatory, integrative and comparative physiology 304:R459-471.

Thompson RH, Swanson LW (1998) Organization of inputs to the dorsomedial nucleus of the hypothalamus: a reexamination with Fluorogold and PHAL in the rat. Brain research Brain research reviews 27:89-118.

Tong Q, Ye C, McCrimmon RJ, Dhillon H, Choi B, Kramer MD, Yu J, Yang Z, Christiansen LM, Lee CE, Choi CS, Zigman JM, Shulman GI, Sherwin RS, Elmquist JK, Lowell BB (2007) Synaptic glutamate release by ventromedial hypothalamic neurons is part of the neurocircuitry that prevents hypoglycemia. Cell metabolism 5:383-393.

Vong L, Ye C, Yang Z, Choi B, Chua S, Jr., Lowell BB (2011) Leptin action on GABAergic neurons prevents obesity and reduces inhibitory tone to POMC neurons. Neuron 71:142-154.

Watts AG, Swanson LW (1987) Efferent projections of the suprachiasmatic nucleus: II. Studies using retrograde transport of fluorescent dyes and simultaneous peptide immunohistochemistry in the rat. The Journal of comparative neurology 258:230-252.

Watts AG, Swanson LW, Sanchez-Watts G (1987) Efferent projections of the suprachiasmatic nucleus: I. Studies using anterograde transport of Phaseolus vulgaris leucoagglutinin in the rat. The Journal of comparative neurology 258:204-229.

Yoshida K, Li X, Cano G, Lazarus M, Saper CB (2009) Parallel preoptic pathways for thermoregulation. The Journal of neuroscience : the official journal of the Society for Neuroscience 29:11954-11964.

Zaretskaia MV, Zaretsky DV, DiMicco JA (2003) Role of the dorsomedial hypothalamus in thermogenesis and tachycardia caused by microinjection of prostaglandin E2 into the preoptic area in anesthetized rats. Neuroscience letters 340:1-4.

Zaretsky DV, Zaretskaia MV, DiMicco JA (2003a) Stimulation and blockade of GABA(A) receptors in the raphe pallidus: effects on body temperature, heart rate, and blood pressure in conscious rats. American journal of physiology Regulatory, integrative and comparative physiology 285:R110-116.

Zaretsky DV, Zaretskaia MV, Samuels BC, Cluxton LK, DiMicco JA (2003b) Microinjection of muscimol into raphe pallidus suppresses tachycardia associated with air stress in conscious rats. The Journal of physiology 546:243-250.

Chapter 4: Conclusions and future directions

The work described here focuses on elucidating neural circuits that drive circadian and diurnal rhythms in behavior and physiology in mammals and keep these functions synchronized. As described in Chapter 1, there is evidence that disruption of the synchrony between these functions can substantially impair sleep quality, diminish cognitive performance, and be a risk factor for mental health/affect disorders, hypertension, diabetes and metabolic deficits, cancer, and significantly elevated mortality rate.

The main pacemaker in mammals that drives and synchronizes these rhythms is the SCN. This nucleus has robust circadian molecular oscillators in every neuron, which are well-coupled to each other. The SCN also shows daily patterns in neuronal firing rate and (in younger animals) in the release of paracrine signaling factors, and relies on such outputs to communicate timing signals to the rest of the brain and body.

Several lines of evidence reveal the importance of neural efferents from the SCN in driving circadian rhythms throughout the body at their maximum amplitude (see Chapter 1). SCN transplants cannot restore systemic rhythms to their full amplitude, and cannot restore certain kinds of rhythms at all. Lesions to SCN efferent targets and/or knife cuts between the SCN and its efferent targets result in severe disruption of many circadian rhythms. In particular, lesion studies show that the SPZ and DMH are both critical for normal expression of circadian rhythms in activity, sleep-wake, and body temperature, and in the case of the DMH also corticosteroid release and feeding. These two structures both receive input from the SCN: robust direct neural input in the case of the SPZ and more sparse direct input coupled with indirect (multisynaptic) input via the SPZ in the case of the DMH. Thus, they are thought to act as relay nuclei in the outflow circuit by which the SCN communicates with the rest of the brain and body. The experimental work presented in chapters 2 and 3 furthers our understanding of how the SPZ and DMH, respectively, act to relay signals from the SCN to the rest of the brain and body, and how they may integrate non-circadian inputs and outputs into this neural circuit.

Connectivity of the subparaventricular zone and its subdivisions: findings and future directions

The SPZ is mainly GABA-ergic and cytoarchitecturally indistinguishable from the neighboring AHA. It is chiefly defined as the area dorsal to the SCN, receiving a dense input from the SCN. That said, the inputs received by the medial vs. lateral SPZ differ, with the medial SPZ receiving more input from AVP-ergic neurons in the SCN shell, and the lateral SPZ receiving more input from the SCN's VIP-ergic core as well as from the retina. Furthermore, the physiological functions of the dorsal vs. ventral SPZ seem to be different as well, with the dorsal subdivision implicated in the regulation of rhythms in body temperature and the ventral in regulation of locomotor activity and sleep-wake rhythms. This suggests that there may be four relevant SPZ subdivisions. As described in Chapter 2, we studied the efferents of the four SPZ subdivisions and of the SPZ as a whole and made several significant observations. First, in addition to its previously reported efferent targets, the SPZ also innervates the dorsal raphe, locus coeruleus, pre-coeruleus region, lateral parabrachial nucleus and Barrington's nucleus, which may play a role in circadian modulation of behavioral state. We also observed that the four SPZ subdivisions project to each other and to the suprachiasmatic nucleus. This connectivity allows for local circuits to share information within the SPZ and suggests circadian outflow through it could be considerably more complex than previously described. Finally the four SPZ subdivisions, dorsomedial (dmSPZ), ventromedial (vmSPZ), dorsolateral (dlSPZ), and ventrolateral (vlSPZ), differ slightly in the density of their inputs to certain targets, as summarized in Fig. 3.1. Taken together with differences in their inputs, this suggests the four SPZ subdivisions may have functionally distinct roles (See Fig. 4.1).

The functional consequences of these differences in anatomical connectivity remain to be tested. For instance, though it is implicated in determining diurnal vs. nocturnal preference in developing rodents, does the vlSPZ play a role in light entrainment in adult animals or in mediating acute effects of light on downstream measures? Does it perhaps only do so in animals with a damaged or non-functional SCN? Given its projections to the IGL and PVT, is the vlSPZ involved in non-photic entrainment? Does the remarkably robust projection from the dlSPZ to the VMH mediate rhythms of feeding, metabolic regulation, or aggression? Given its efferents to the AVPe, is the vmSPZ necessary for normal rhythms in leutenizing hormone in females? Testing the above questions by lesioning, stimulating or inhibiting the

Figure 4.1 Diagram summarizing inputs to the four different SPZ subregions [dorsomedial (dmSPZ), ventromedial (vmSPZ), dorsolateral (dlSPZ) and ventrolateral (vlSPZ)], the targets preferentially innervated by each subdivision, and the functional role this may suggest for each subdivision (based on data from Chapter 2).

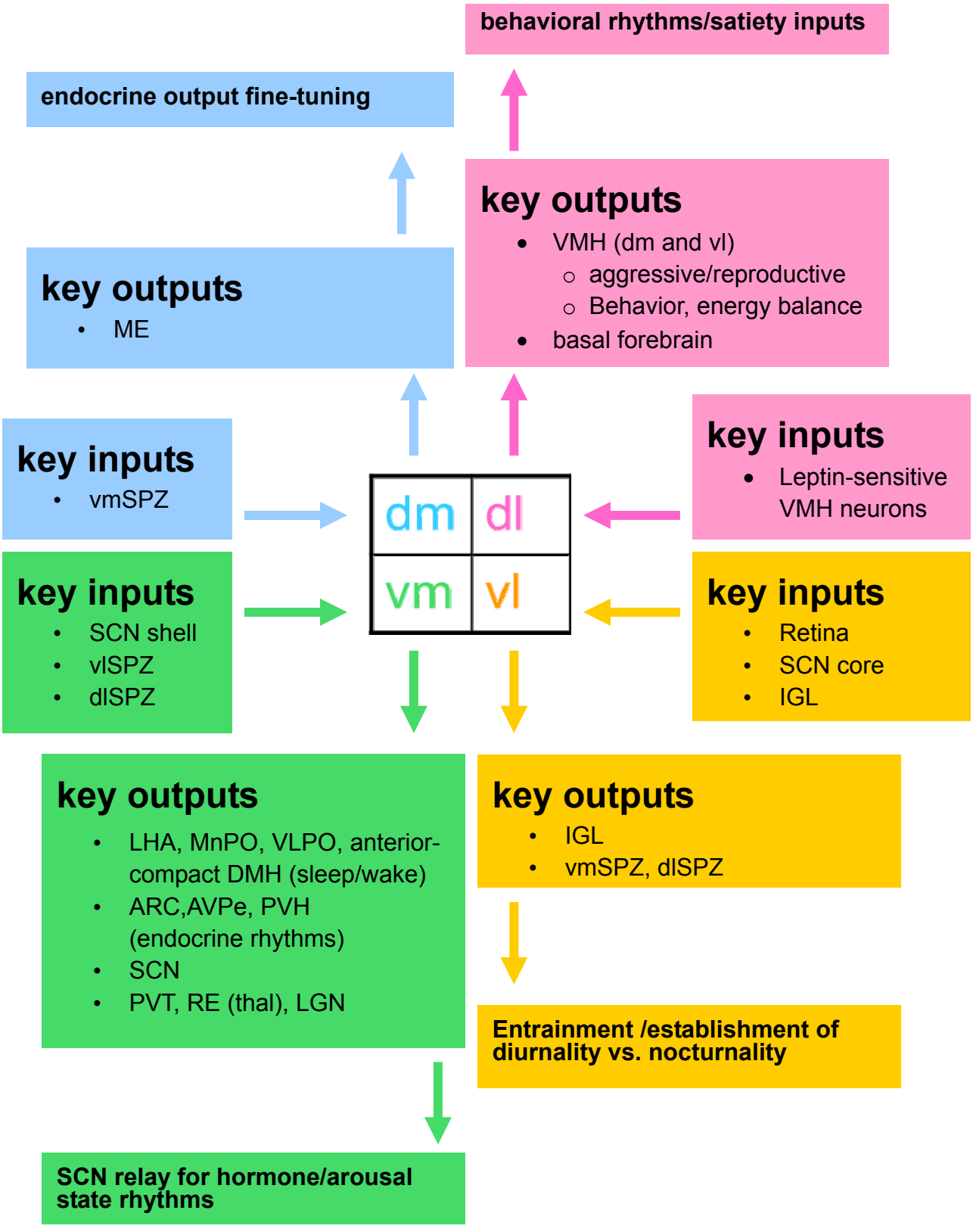

Figure 4.1 (continued)

four SPZ subdivisions would yield valuable information on how outflow from the clock drives circadian patterns.

There are a number of relatively new methodologies which could facilitate testing these hypotheses in a functional manner in the future. For example, using genetic markers such as receptors for pituitary adenylate cyclase activating peptide (PACAP), which is co-released with glutamate by retinal fibers innervating the SPZ, could potentially help restrict a lesion to the vlSPZ. Similarly, expression of receptors for arginine vasopressin (AVP) a neurotransmitter expressed in the SCNshell, which preferentially innervates the medial SPZ, could be exploited to achieve a more selective lesion of the vmSPZ and dmSPZ.

There is also an interesting consideration of the overall circuit that could explain the function of intra-SPZ projections. SCN lesions, SPZ lesions and DMH lesions all blunt the amplitude of rhythms in activity/wake in nocturnal rodents by decreasing overall levels throughout the day. There is evidence to suggest that the main SCN output to the SPZ would be inhibitory, as would SPZ input to the DMH. If this rhythm really does depend on two inhibitory projections, one could expect that disruption of the circuit at the level of the SPZ would lead to increased activity/wakefulness (since this lesion would be disinhibiting downstream neurons in the DMH and elsewhere that drive wakefulness and activity). However, the opposite is true, but could easily be explained by acknowledging the presence of an extra inhibitory synapse in the SPZ as part of the circuit (see Fig. 4.2). It is important to remember that provides excitatory retinal input to the SCN, vlSPZ, and many other sites in the brain simultaneously, and the circuits proposed in fig. 4.2 are only predictive in a free-running or stably entrained context (as opposed to a phase-shifting and/or light masking situation). Much work remains to be done be done before we truly understand the neural circuits mediating the acute effects of light on physiology.

The role of excitatory DMH neurons in circadian and homeostatic regulation: findings and future directions

The DMH is a considerably more heterogeneous nucleus than the SPZ, having both cytoarchitecturally and neurochemically defined subdivisions. We chose to test the role of glutamatergic

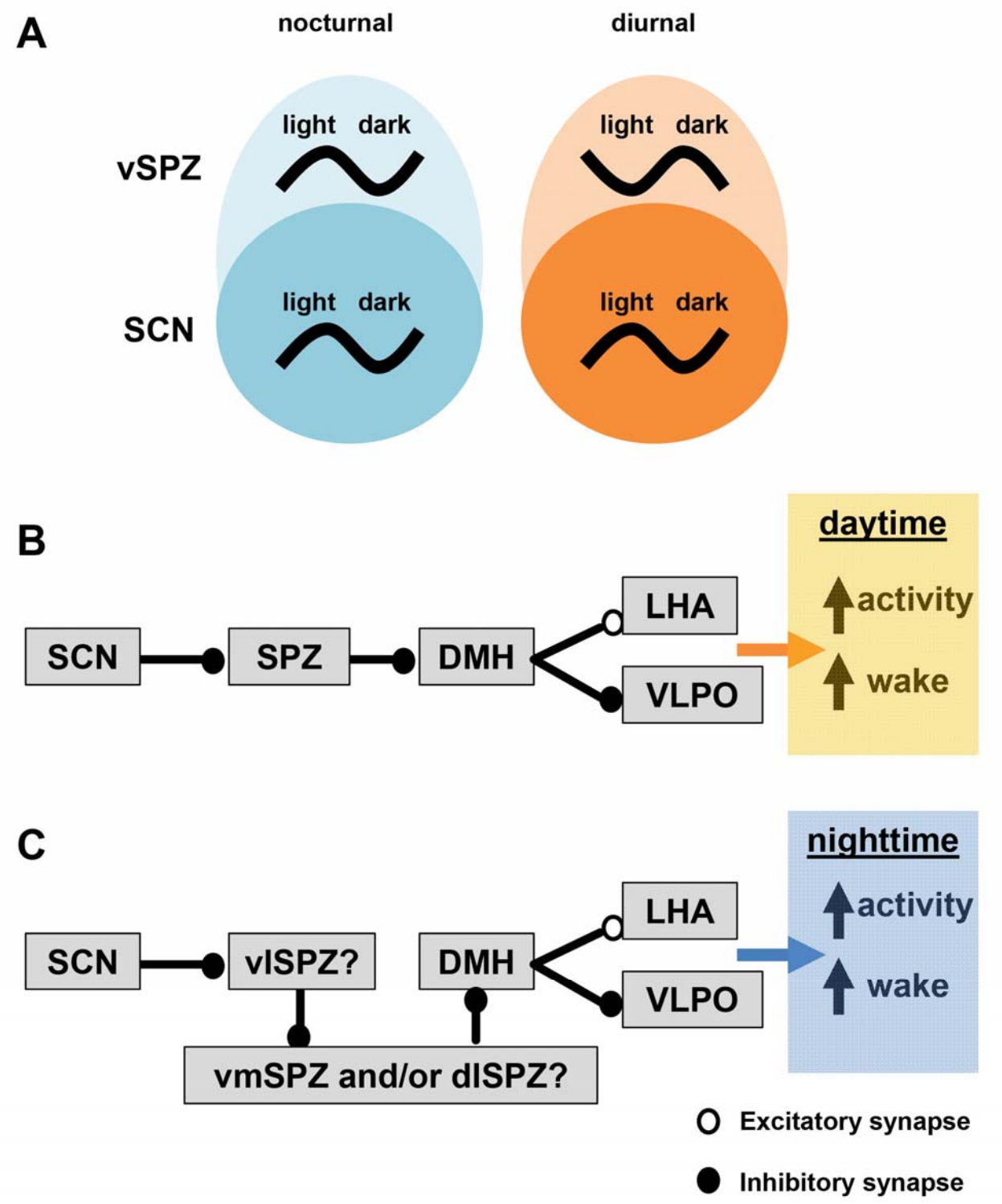

Figure 4.2 Schematic diagrams illustrating (A) rhythms of immediate early gene activity and presumably also maximum neuronal firing in the SCN and vSPZ of nocturnal vs diurnal rodents: in nocturnal rodents, both the SCN and vSPZ fire most during the (subjective) light phase, in alignment with each other, but in diurnal rodents they appear to be in antiphase patterns [with the SCN peak still during (subjective) light, but the vSPZ peak occurring during the (subjective) dark]. (B) schematic depiction of how a neural circuit with only one synaptic contact going from the SCN to SPZ and SPZ to DMH gives rise to diurnal behavior (C) and how adding an intra-SPZ connection would instead give rise to nocturnal behavior.

efferents from this nucleus in part because of their largely accepted role in thermoregulation (i.e. projection to RPa) and hypothesized role in wake consolidation (i.e. projection to LHA).

We found that selective loss of glutamatergic signaling was enough to disrupt many of the physiological outputs disrupted by whole DMH lesions. The amplitude of the circadian rhythm in locomotor activity was significantly decreased, as were average activity levels over the course of the whole subjective day, but neither was decreased to the same extent seen with cell-specific DMH lesions. The amplitude of circadian rhythms in corticosteroid release is also reduced by loss of *VGlut2* expression in the DMH, but again to a lesser extent than by cell-specific DMH lesions. Loss of *VGlut2* expression in the DMH lowered the baseline body temperature by approximately the same amount as excitotoxic DMH lesions.

It is not yet clear whether the above results were obtained because glutamatergic signaling from the DMH is necessary and sufficient to drive the effects of this nucleus on body temperature, but other neurotransmitters are involved in mediating DMH effects on activity and corticosteroid release. This interpretation is highly consistent with the literature. However, the results may also be explained by differences in lesion extent. In the experiment reported in Chapter 3, there was on average 90% DMH/DHA coverage per side for the mice in which body temperature was successfully measured, 77% coverage per side of the relevant DMH levels for mice with successful locomotor activity recordings, and 72% DMH coverage per side for mice in which reliable, phase-aligned corticosterone output data was available.

This leaves open the question of which other neurotransmitters in the DMH may play a significant role in the regulation of activity and corticosteroid rhythms. Histological evidence implicates GABA (see Chapter 1), a hypothesis testable by using conditional knockout mice to prevent release of this neurotransmitter from DMH neurons. The role of many other neurotransmitter candidates can be studied using methods similar to those described in Chapter 3.

Although previous work (see Chapter 1) suggests that the DMH sends a predominantly glutamatergic projection to LHA and predominantly GABAergic projection to VLPO, it also suggests that neither VLPO lesions nor LHA lesions reduce the amplitude of circadian rhythms in activity (and probably wakefulness) to the extent that DMH lesions do, or even to the extent that *VGlut2* deletion in this region

does. Are there other projections from the DMH, perhaps to other sleep or wake promoting regions in the brain that are also involved? Conditional tracing studies from genetically defined subpopulations of DMH neurons could begin to answer this question. In the case of body temperature regulation, both previous literature and unpublished conditional tracing experiments from our own lab (using a Cre-driven tracer injected into the DMH *VGlut2*-Cre mice) strongly implicate a glutamatergic projection from the DMH to the raphe pallidus.

Finally, it bears mention that, *in vivo*, many of the parameters we typically attempt to study independently may interact with each other. There are well documented interactions between sleep, activity, circulating corticosteroids and body temperature (see Chapter 3). Can we clarify which of these functions are perturbed secondarily to disruption of another function? Can extrinsically driving one rhythm, perhaps via light-cycle or feeding schedule, restore other, secondary rhythms, even in an animal or person with circadian disruption? The fact that mice with *VGlut2* loss in the DMH show normal urinary corticosterone rhythms in a 12:12 light:dark cycle, even though they do not under free-running conditions (see Chapter 3), is encouraging in that regard. We have much to learn from doing physiological experiments in both free-running and entrained conditions in tandem.